Alexey Dudkov

Chip and Signature Interleaving in DS CDMA Systems

Turku Centre *for* Computer Science

TUCS Dissertations
No 118, May 2009

Chip and Signature Interleaving in DS CDMA Systems

Alexey Dudkov

University of Turku
Department of Information Technology
FI-20014 TURKU

2009

Supervisors

Adjunct professor Valery Ipatov
Department of Information Technology
University of Turku
FI-20014 Turku
Finland

Professor Jouni Isoaho
Department of Information Technology
University of Turku
FI-20014 Turku
Finland

Reviewers

Professor Victor N. Malyshev
Faculty of Radio Engineering and Telecommunications
Saint-Petersburg Electrotechnical University "LETI"
Professor Popov str. 5, 197376, St. Petersburg
Russia

Adjunct professor Yevgeni Koucheryavy
Department of Communication Engineering
Tampere University of Technology
Korkeakoulunkatu 10, 33720, Tampere
Finland

ISBN 978-952-12-2300-6
ISSN 1239-1883

Abstract

This Thesis considers aspects of chip and signature interleaving in direct sequence code division multiple access (DS CDMA) communication systems. In DS CDMA each user is assigned a user-specific code sequence called signature, and one of the dominating issues in designing DS CDMA air interface is an adequate choice of signature ensemble securing necessary quality of service for any individual user despite a potential presence of multiple access interference (MAI) created by signals of other (side) users. Designing optimal signature ensemble is easiest in the case of entirely synchronous CDMA, which is possible only if the number of users K is no greater than the spreading factor (signature length) N. In this case the conventional (single-user) reception algorithm applied to any set of $K \leq N$ orthogonal sequences of length N provides separation of all users' signals with no MAI and best possible processing against the background thermal noise.

Practically, however, this idealistic scenario is rather unlikely even in the systems initially based on a "pure" synchronous philosophy, such as mobile radio downlink. Actually, multipath replicas accompanying users' signals are inevitable, multipath "tail" of the l-th user being a probable source of MAI for the receiver of the k-th user ($l \neq k$). The effect becomes even more dramatic considering data modulation of signatures typical of DS CDMA and involving along with even also odd – much less controllable – correlations.

In this Thesis the efficiency of signature-interleaved (SI) DS CDMA is analyzed in comparison with conventional DS CDMA. It is demonstrated that for SI DS CDMA the average MAI power at the output of a single user correlator and RAKE receiver depends only on correlations of either non-shifted at all or just one-chip-shifted signatures *independently* of the multipath delay value. These correlations can be easily retained under predictably low bound, and as a result, SI DS CDMA provides markedly better performance in terms of bit error rate. A procedure of designing signature ensembles for SI DS CDMA is considered in a separate chapter, where the obtained ensembles are then compared using average MAI power, average squared correlation and average bit error rate (BER) criteria. All analytical results are confirmed with simulations.

Acknowledgements

It is with tremendous pleasure that I would like to now express my sincere gratitude to the people and institutions that have provided me with both support and assistance during my work on this thesis.

First and foremost, I am extremely grateful to my supervisor, Professor Valery Ipatov, for his attentive and patient guidance over the years; it has truly been an honour and a privilege to have him as a mentor and teacher.

I would like to thank the University of Turku and the Turku Centre for Computer Science (TUCS) for providing me with the opportunity to conduct my study therein. I am also extremely grateful to the Dtv group and Mikko Jalonen for the financial support over recent years. It was a delight to work in such a stimulating environment, which bestowed upon me everything I required to succeed in my research. I would particularly like to acknowledge the assistance I received from Jarkko Paavola, the extent of whose help and support cannot be overestimated; I am deeply indebted to him for his contributions of both time and effort.

My sincere thanks must also go to Jussi Poikonen, Tero Hurnanen, Eero Lehtonen, Piritta Hakala and all of my colleagues and friends from the Department of Information Technology. I am, likewise, much obliged to Luka and Riia Milovanov.

A very special thank-you must be extended to Kristian and Sonja Nybom, whose knowledge of and expertise in oenology ensured that the time I spent working on this thesis was very much more pleasant than it might otherwise have been.

I would also like to acknowledge Sergey Balandin and Alexander Sayenko for the numerous and very interesting discussions we had, including those that went beyond the scope of this work. I am similarly grateful to Vladimir and Alexey Yurin, Sergey Malkov, Alena Kipreeva and all of my other friends from Saint-Petersburg for their constant support and encouragement.

I am grateful to Tomi "bgt" Mäntylä for his assistance with both printing issues and the preparation of the final version of this study.

Finally, it would be remiss of me if I failed to extend my most sincere and humble gratitude to my family, Vladimir and Nina, the people who have given me everything.

Contents

List of Acronyms

2G	Second generation of mobile phones
3G	Third generation of mobile phones
4G	Fourth generation of mobile phones
ACF	Autocorrelation function
APSK	Amplitude-phase shift keying
AWGN	Additive white Gaussian noise
BER	Bit error rate
BPSK	Binary phase shift keying
CCF	Crosscorrelation function
CDMA	Code division multiple access
CP	Cyclic prefix
DS CDMA	Direct sequence CDMA
DSSS	Direct sequence spread spectrum
EGC	Equal gain combining
FDMA	Frequency division multiple access
FHSS	Frequency hopping spread spectrum
GF	Galois field
GO-CDMA	Group-orthogonal CDMA
GSM	Global system for mobile communications
LCZ	Low-correlation zone signatures/sets
LFM	Linear frequency modulation
LFSR	Linear feedback shift register
MAI	Multiple access interference
MF	Matched filter
MRC	Maximal ratio combining
ML	Maximal likelihood
MMSE	Minimum mean square error
OFDM	Orthogonal frequency division multiplexing
PACF	Periodic autocorrelation function
PN	Pseudonoise
PSK	Phase shift keying
SINR	Signal-to-interference-plus-noise ratio

SIR	Signal-to-interference ratio
SNR	Signal-to-noise ratio
TDMA	Time division multiple access
UMTS	Universal mobile telecommunication system
UWB	Ultra wide-band
WBE	Welch bound equality
WCDMA	Wideband CDMA
ZCZ	Zero-correlation zone signatures/sets

List of Symbols

$\mathbf{0}_{P\times M}$	Zero matrix of size $P \times M$
A_k	k-th user amplitude
A_r	Amplitude of the r-th multipath ray
$\mathbf{A}$	Diagonal matrix of users' amplitudes
$\mathbf{b}$	Transmitted bit vector
b_k	Transmitted information bit of the k-th user
$\hat{b}_k$	Estimation of the transmitted information bit of the k-th user
$\mathbf{C}$	Signature correlation matrix
Δ	Chip repetition interval
E	Signal energy
E_0	Chip energy
f_0	Carrier frequency
φ_r	Phase of the r-th multipath ray
γ_k	Energy (SNR) loss
$\mathbf{H}$	Hadamard matrix
$\mathbf{I}_M$	Identity matrix of size M
K	Number of users
L	Maximal delay in number of chips
$\mathrm{LCZ}(P, Z, N)$	Low-correlation zone ensemble for P signatures of length N for zone Z
M	Length of the interleaving block
m_k	k-th user delay in number of chips
m_{kl}	Relative delay of the k-th and l-th users
$\mathbf{n}$	Noise vector
$n(t)$	Noise signal
n_k	Noise sample at the output of the k-th user receiver
N	Spreading factor, length of a code sequence
P_i	Power of multiple access interference
P_n	Noise power
P_s	Power of useful signal
$\overline{P_{\mathrm{MAI},k}}$	Average MAI power for the k-th user
$Q(\cdot)$	Complementary error function
R	Number rays in multipath channel

$R(\tau)$	Correlation function
$\rho(\tau)$	Correlation coefficient
$R_{a,kl}(m)$	Aperiodic crosscorrelation of shift m of the k-th and l-th users' signals
$R_{p,kl}(m)$	Periodic crosscorrelation of shift m of the k-th and l-th users' signals
$R_{p,kl}^{\text{odd}}(m)$	Odd periodic crosscorrelation of shift m of the k-th and l-th users' signals
$\rho_{a,\max}$	Maximal level of sidelobe of aperiodic ACF
$\rho_{p,\max}$	Maximal level of sidelobe of periodic ACF
$\mathbf{s}_k(t)$	k-th user signature
$\mathbf{s}_k$	k-th user code vector (signature)
$s_k(i)$	i-th chip of the k-th user signature $\mathbf{s}_k$
$\mathbf{S}$	Signature matrix
$\mathbf{s}(\mathbf{b};t)$	Group signal
$\|\mathbf{s}\|^2$	Squared geometrical length (Euclidean norm) of the code vector $\mathbf{s}$
$\dot{S}(t)$	Complex envelope of the signal
$\dot{S}_0(t)$	Complex envelope of the chip
σ^2	Noise power at the chip matched filter output
T_t	Total available time resource
τ	Signal delay
$\mathbf{u}_k$	k-th user mismatched signature
W_t	Total available frequency resource
$y(t)$	Observation
z_k	Matched filer output for the k-th user
$\text{ZCZ}(P,Z,N)$	Zero-correlation zone ensemble for P signatures of length N for zone Z

Chapter 1

Introduction

1.1 Multiple Access Technologies in Mobile Networks

During the recent years we have witnessed an exponential growth of the number of mobile networks' subscribers, first of all, users of mobile phones. A device that just a decade ago was a luxury, has now become an integral part of the everyday life; it was repeatedly reported that in many countries the number of subscribers of mobile networks exceeded the population size. In addition to that, nowadays the term "mobile network" is not limited to cellular networks only, that were designed originally to the voice transmission, but also includes networks primarily oriented for data transmission, like WiMAX [43], for example. During the last years several other trends in network construction appeared, which are not associated with a mobile phone at all, like car-to-car communications [89], sensor networks and others.

All these networks rely on the principle of multiple access, where services must be provided to several users simultaneously. This can be achieved, for example, by *dividing* the available resource between all the users, and this is exactly how it was done historically. If the time resource is somehow divided between users, this approach is called time division multiple access (TDMA). This idea is utilized, for example, in the well-known Global System for Mobile communications (GSM) standard [39, 57] and in IEEE 802.16 wireless MAN standards. If, on the other hand, the available frequency resource is shared, it is called frequency division multiple access (FDMA). This method was used in Advanced Mobile Phone System (AMPS) and Nordic Mobile Telephone (NMT) [116]. Postponing the detailed description for Section 2.3, it is enough to say that both these approaches have several disadvantages.

There does exist another method how several users can be serviced si-

multaneously. In this approach every user utilizes *the whole* available time-frequency resource; neither time nor frequency is divided between users. Instead, every user is assigned a unique *code* or signature, and the distinction between different users is performed by these user codes, which gives this approach the name code division multiple access (CDMA). Naturally, the manner in which the codes are constructed and distributed among users is of utmost importance since it directly affects the system performance.

From a history perspective we can say that the basic ideas of CDMA were introduced as early as 1949 by Claude Shannon and Robert Pierce [3], and in 1950 De Rosa-Rogoff proposed a direct sequence (DS) CDMA [22], the one that is used in this Thesis. However, it was not until 1993 that CDMA was introduced in cellular mobile systems for the first time in IS-95 standard [103]. Since then the CDMA approach has become an integral part of almost every modern mobile network standard (cdma2000 [68], WCDMA [87], LTE [43] etc).

1.2 Objectives of the Thesis

Since all user signals in CDMA completely overlap in time and frequency, in a general case they will cause interference to each other, which, due to its multiple access nature is called *multiple access interference* (MAI). As will be demonstrated later, MAI level directly affects the system performance, and it is not an overestimation to say that decreasing MAI level is among the most critical issues in CDMA systems.

CDMA systems can be divided into synchronous and asynchronous ones. For the former all user signals are strictly synchronized; no delay between them is possible. An example of such a system is a "downlink" radio channel in mobile systems, that is, the signal transmission from a base station to mobile stations. For asynchronous CDMA, on the other hand, user signals can be shifted in time relatively to each other. This is a typical situation in an "uplink" channel, when mobile stations send their signals to the base station. Since mobile stations can be located at arbitrary distances from the base station, their signals can arrive to the base station with arbitrary delays even for the situation when all the signals were synchronized at the transmission. In addition to that, even for synchronous CDMA system asynchronism can appear due to multipath propagation, when a signal is received accompanied by its time shifted reflections from the surrounding objects.

While for synchronous CDMA MAI can occur only from the initial user signals themselves, for asynchronous CDMA, on the other hand, time-shifted copies of users' signals can also be source of MAI and should be taken into account. In this Thesis the usage of *chip-interleaving* and its modifications

will be considered and analyzed in order to decrease MAI level and enhance the system performance.

To the best of the author's knowledge, chip interleaving, traditionally used to disperse burst errors in error correction coding [110], in DS CDMA was first introduced in [21] in order to simplify the channel estimation task, and since then has become a topic for several research directions.

A synchronous DS CDMA system based on block spreading in the presence of frequency-selective fading was analyzed in [74, 75], where a receiver that completely removes MAI without using any channel information was proposed and investigated. In [132,133] chip-interleaving was combined with zero-padding, which allowed to remove MAI in multipath channels deterministically and independently of the multipath delay profile in exchange for the reduction of the information transmission rate.

Coexistence in practical systems and retaining orthogonality between chip-interleaved signals and conventional ones are considered in [58]. A big number of works was dedicated to the analysis of DS CDMA systems with chip-interleaving under some form of jamming [56, 117, 118].

In this Thesis the main emphasis is given to the approach called *sequence interleaving*. The main distinctive feature of such an approach is utilization of *several* signatures per user, whereas in conventional DS CDMA only one signature is used. It is shown that usage of multiple signatures combined with chip interleaving is very promising against MAI level increase caused by users' asynchronism due to multipath propagation and allows to achieve smaller bit error rate and accommodate more users.

1.3 Overview of the Thesis

This Thesis is organized in seven chapters. Chapter 2 provides general overview of spread spectrum philosophy, discrete signals, correlation functions and multiple access systems, all of which are used in the following chapters. All definitions, concepts and notations that are used throughout the Thesis are presented. A special emphasis is given to the signature ensembles used in conventional DS CDMA systems, including the selection criteria and practical examples. Various user receivers are also considered, including the single-user (matched-filter) receiver, decorrelator and MMSE receiver.

Chapter 3 concentrates on single-path asynchronous systems, where an arbitrary delay is possible between user signals. Negative effects of asynchronism to the system performance are considered, and it is demonstrated that due to uncontrollable level of odd correlations, MAI can also be dangerously increased leading to unacceptable bit error rate. A concept of chip interleaving is introduced in this Chapter; although this idea is relatively

known, we will present several new applications of this approach. In particular, implementation of the chip interleaving to the decorrelation receiver and to oversaturated systems is considered. It is shown that chip interleaving transforms *arbitrary* asynchronous delays between user signals into delays of shift no greater than one chip, which are much more controllable than odd correlations of big shifts. All theoretical results are supported by computer simulations, demonstrating the superiority of the proposed systems in terms of bit error rate. Finally, in the end of the chapter one more method is presented aimed at neutralizing harmful effects of odd correlations. The method is based on the cyclic prefix redundancy traditionally used in orthogonal frequency division multiplexing (OFDM), but here we will draw attention to another potential merit of the cyclic prefix related to the removal of odd correlations of signatures.

In Chapter 4 the cornerstone of the Thesis is presented, the approach called signature-interleaved DS CDMA. The main focus in this Chapter is on asynchronism created by multipath propagation, the negative effects it might cause to the system performance and possible ways how to neutralize them. In this Chapter it is suggested, in addition to chip interleaving, to utilize more than one signature per user in comparison to the conventional DS CDMA where only one signature per user is employed. It is shown that this approach allows to keep maximal values of odd crosscorrelation functions – the main reason of MAI increase – under the predictable low bound, improving thus the system performance. Expressions for average MAI power for a single-user receiver for conventional DS CDMA and for signature interleaved DS CDMA are obtained and compared.

Chapter 5 focuses on construction of signature ensembles for signature-interleaved CDMA. First, criteria for such ensembles are considered, and the bound connecting the number of users and the maximal value of correlation functions is obtained. Then, based on this bound, several cases are considered, and for each of them some practical ensemble designs are suggested. Finally, a comparison in terms of bit error rate for a single-user receiver is performed between conventional DS CDMA and signature interleaved DS CDMA employing the created signature ensembles, showing the superiority of the latter.

In Chapter 6 efficiency of an equal gain combining RAKE receiver is analyzed for signature-interleaved DS CDMA. Results for MAI power as well as comparison in terms of bit error rate with conventional DS CDMA are presented. It is demonstrated, for example, that for a constant bit error rate level signature interleaved DS CDMA is able to accommodate up to five more users.

Finally, conclusions to the Thesis are drawn in Chapter 7.

1.4 Author's Contribution

This Thesis is partially based on extended versions of the previously published publications. The list of the publications is given below, with indication of the author's contribution to the each of them.

- [32] Alexey Dudkov and Valery Ipatov. Asymptotic Optimality of Random PSK Signature Ensembles. In *Proceedings of the IEEE 6th International Symposium on Electromagnetic Compatibility and Electromagnetic Ecology*, Saint-Petersburg, Russia, 2005.

  Author's contributions: the author performed the theoretical analysis of the signature ensembles and performed the computer simulations. Professor Valery Ipatov helped with the paper structuring and theoretical analysis and provided the general supervision of the paper.

- [34] Alexey Dudkov and Valery Ipatov. Chip-Interleaved Decorrelation in Asynchronous DS CDMA. In *Proceedings of the VIII IEEE Workshop on Signal Processing Advances in Wireless Communications (SPAWC 2007)*, Helsinki, Finland, 2007.

  Author's contributions: the author performed computer simulations and minor part of the theoretical analysis, the major part of which as well as the general supervision were performed by Professor Ipatov.

- [33] Alexey Dudkov and Valery Ipatov. Eliminating Odd Correlations in Asynchronous DS CDMA Employing Cyclic Prefix. In *Proceedings of the IEEE Mediterranean Electrotechnical Conference (MELECON 2006)*, Malaga, Spain, 2006.

  Author's contributions: the author performed minor theoretical analysis and computer simulations.

- [35] Alexey Dudkov and Valery Ipatov. Signature-Interleaved DS CDMA: Controlling Odd Correlation Peaks. In *Proceedings of the 16th Annual IEEE International Symposium on Personal Indoor and Mobile Radio Communications (PIMRC'05)*, Berlin, Germany, 2005.

  Author's contributions: the author performed minor theoretical analysis and computer simulations.

- [31] Alexey Dudkov. Signature-Interleaved DS CDMA In Rayleigh Multipath Channel. *Proceedings of the IEEE International Symposium on Wireless Communication Systems (ISWCS'07)*, Trondheim, Norway, 2007

  Author's contributions: this paper is an independent contribution of the author. A general model of multipath propagation was considered,

and theoretical analysis of SI DS CDMA system in such a model was performed. The paper contains main results of the comparison of DS CDMA and SI DS CDMA in terms of bit error rate.

- [29] Alexey Dudkov. RAKE Reception For Signature-Interleaved DS CDMA In Rayleigh Multipath Channel. In *Proceedings of the 6th International Workshop on Multi-Carrier Spread Spectrum (MC-SS 2007)*, Herrsching, Germany, 2007.

  Author's contributions: Analysis of signature-interleaved DS CDMA was extended to RAKE receiver in this paper.

- [30] Alexey Dudkov. Signature Ensembles for Signature-Interleaved DS CDMA. In *Proceedings of the Signal Processing for Wireless Communications Workshop (SPWC 2007)*, London, United Kingdom, 2007.

  Author's contributions: Independent contribution of the author. In this paper demands to signature ensembles for SI DS CDMA were established and several ensembles specifically tailored for SI DS CDMA were constructed. Existing signature ensembles and their applicability to SI DS CDMA were considered, as well as the performance comparison.

- [28] Alexey Dudkov. Optimization of Signature Ensembles for SI DS CDMA Using Random Search. In *Proceedings of the IEEE VIIth International Symposium on Electromagnetic Compatibility and Electromagnetic Ecology*, Saint-Petersburg, Russia, 2007.

- [37] Alexey Dudkov, Jarkko Paavola and Valery Ipatov. Oversaturated Group Orthogonal CDMA in Multipath Channels Using Chip Interleaving with Zero Padding. In *Proceedings of the 18th Annual IEEE International Symposium on Personal Indoor and Mobile Radio Communications (PIMRC'07)*, Athens, Greece, 2007

  Author's contributions: in this paper the author suggested to implement chip interleaving with zero padding to the oversaturated systems in multipath channels, which allowed to significantly increase the system performance. The author also performed all the simulations and summarized the results. Doctor Jarkko Paavola provided the expertise of oversaturated systems, and professor Valery Ipatov helped with theoretical analysis and provided general supervision of the paper.

- [36] Alexey Dudkov and Jarkko Paavola. Asynchronous Oversaturated Group Orthogonal CDMA Using Chip Interleaving with Zero Padding. *Proceedings of the IEEE International Symposium on Wireless Communication Systems (ISWCS'07)*, Trondheim, Norway, 2007

Author's contributions: comments of the previous article apply. The author suggested usage of chip interleaving with zero padding for oversaturated systems in asynchronous channels, where they can not be normally used. Theoretical work and simulations were also the author's responsibilities.

Chapter 2

Spread Spectrum Signals and CDMA

This Chapter gives an overview of spread spectrum concept and CDMA systems, introducing all the notations, concepts and definitions that will be used throughout the Thesis.

The chapter starts with Section 2.1, where an overview of the spread spectrum concept and the discussion on potential benefits of spread spectrum signals in comparison with the "conventional" ones are given. Section 2.2 concentrates on discrete signals, given their predominant role nowadays, and in Section 2.3 an idea of synchronous code division multiple access is presented.

Section 2.4 provides definitions and notations of correlation functions, the cornerstone of this Thesis. Section 2.5 gives description of several receiver structures for synchronous CDMA, and Section 2.6 introduces asynchronous DS CDMA.

Section 2.7 opens the subject of signature ensemble design, discussing the necessary requirements for the signatures and presenting signatures with good autocorrelation properties. In Section 2.8 the discussion on the criteria for signature ensemble design for asynchronous DS CDMA is presented, and an overview of several signature ensembles that will be used in the following chapters is given.

2.1 Spread Spectrum Concept

This Thesis is largely based on the concept of spread spectrum signals. Although this term nowadays has become one of the most popular in engineering and communication community, its definition is sometimes formulated equivocally. Some sources [17,26,59,114] define a system or a signal as spread spectrum if its bandwidth significantly exceeds minimum bandwidth neces-

sary for the information transmission, which can be misleading. According to this definition, GSM mobile system operating with data rate about 9.6 kbps and occupying at the same time bandwidth around 200 kHz [39] should be evidently classified as spread spectrum. This system, however, does not possess genuine features of a spread spectrum one, having wider then transmission rate bandwidth only because of implementation of time division multiple access [57, 101].

After [62], we will call a signal spread spectrum if the product of its duration T and bandwidth W (*time-frequency product*, *processing gain*) is significantly bigger than one:

$$WT \gg 1. \tag{2.1}$$

On the contrary, conventional, non-spread spectrum signals are called *plain* and have time-frequency product around one, $WT \approx 1$. The product WT is also called the *spreading factor*, since it shows how many times signal bandwidth is expanded as compared to the bandwidth of an ordinary plain-signal data transmission.

Let us underline that 'wide band' and 'spread spectrum' are not synonyms. By shortening the signal duration its bandwidth can be made as wide as one wishes; bandwidth of the ultra wide-band systems, which are based on exactly this approach, is around several gigahertz [8, 49, 113]. This idea is also used, for example, in industrial standards such as IEEE 802.15.3*a* (high data rate) [1] and IEEE 802.15.4*a* (very low data rate) [2, 5] (later adopted for ZigBee standard [10, 14, 50]). What is important is that spectrum widening thus achieved by no means changes the time frequency product and the signal remains plain, $WT \approx 1$.

In strong contrast with this, a spread spectrum signal can have arbitrary wide spectrum *without* changing the signal duration. This is illustrated by Figure 2.1, where two signals of identical duration are presented. One of them is plain (upper row) with constant carrier frequency f_0 and no internal modulation, and the other one is spread spectrum with linear frequency modulation (LFM) [119] (lower row). It is seen that the bandwidth of the spread spectrum signal is significantly bigger, although its duration is exactly the same.

Simultaneously, Figure 2.1 illustrates that the *spreading* of the signal spectrum can be achieved by an appropriate modulation, angle modulation usually playing the major role. This is due to the fact that the amplitude modulation alone can spread spectrum only at the cost of concentrating the signal energy within short signal duration, which may lead to unacceptable increase of the signal peak power [62].

Big value of time-frequency product WT, in turn, can be quite beneficial, providing spread spectrum system with numerous merits. The latters

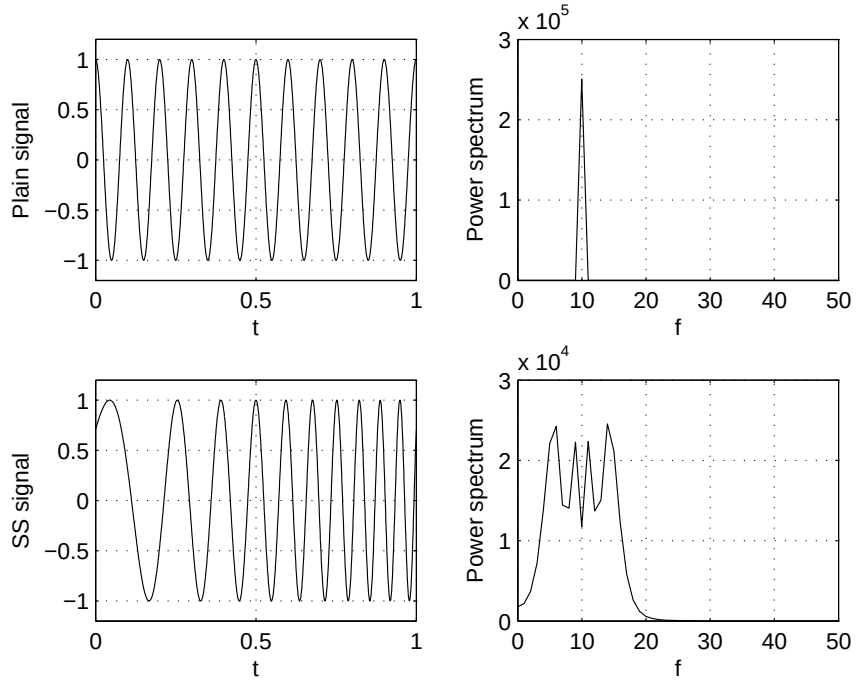

Figure 2.1: Power spectra of plain and spread spectrum signals

include high accuracy in time and frequency measurement and resolution, immunity to jamming, low probability of detection and others [62, 98, 112]. Consider as just one example signal resolution problem, that is, the ability to distinguish time-shifted replicas of the original signal between themselves [121]. Scenarios of this type, caused by multipath propagation, are very typical throughout communication systems. Certainly, if signal replicas do not overlap in time, telling them apart is a trivial task, but is they do overlap it might be very complicated for the case of conventional (plain) signals. The evident solution – shortening signal duration – is not always possible, since most systems have some limitations on the signal peak power, and in order to keep the signal energy the same, while shortening the signal duration its power should be proportionally increased.

Spread spectrum signals, on the other hand, provide markedly better results when multipath signal replicas overlap in time, which is achieved due to the property of *time compression*, meaning significant reduction of signal duration at the output of the matched filter (MF) [62, 97].

Figure 2.2 illustrates the difference between signal resolution of a plain signal (first column) and a spread spectrum one (second column) of the same energy and duration. Figure 2.2 (a) demonstrates the initial signals, plain

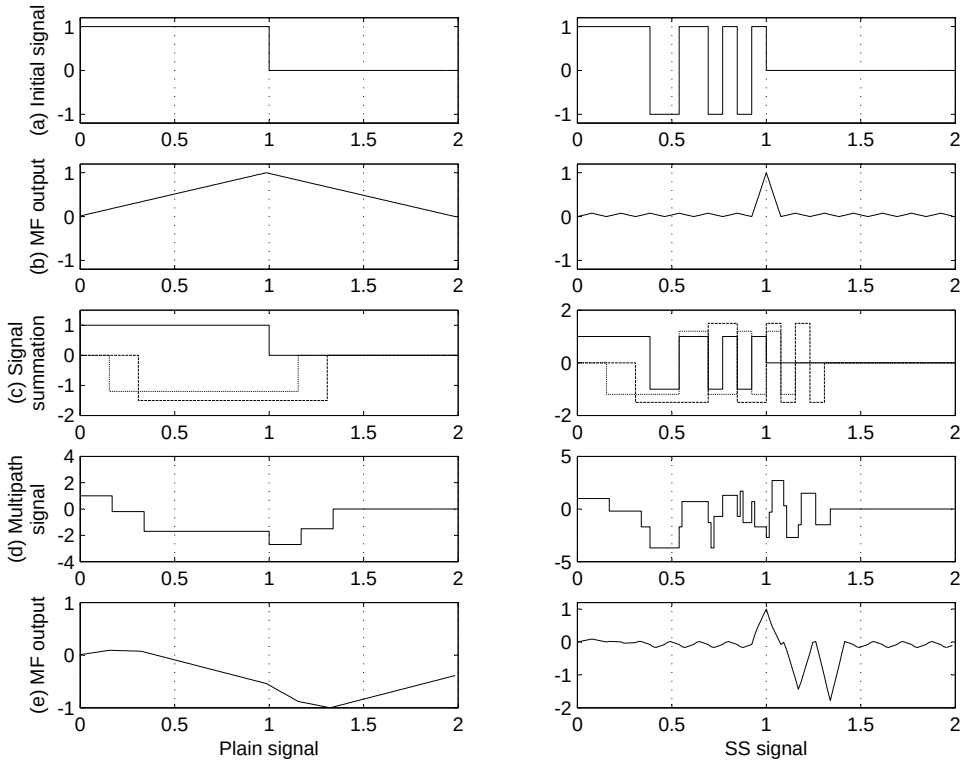

Figure 2.2: Multipath resolution for plain and spread spectrum signals

(a rectangle of unity duration and amplitude) and spread spectrum one (the same rectangle with internal modulation), and Figure 2.2 (b) presents the output of the MF for both of them. The time compression property for the spread spectrum signal is clearly seen – the MF output is much sharper.

Figure 2.2 (c) shows the initial signal (solid line) and two delayed replicas with amplitudes -1.2 (dotted line) and -1.5 (dashed line), and Figure 2.2 (d) shows the superposition of these three replicas. Figure 2.2 (e) provides the MF response to the latter. It is seen that while for the case of plain signal replicas are indistinguishable, usage of spread spectrum signal allows to fully separate them, the three peaks are clearly seen.

2.2 Discrete Signals

A significant part of this Thesis is based on the idea of a discrete signal, which is defined in this Section. We will call a signal discrete if parameters of its modulation law are changed by hops at discrete moments of time [62, 98, 112, 114]. A complex envelope $\dot{S}(t)$ of such a signal can thus be defined

as

$$\dot{S}(t) = \sum_{i=-\infty}^{\infty} s(i)\dot{c}_0(t - i\Delta)\exp(j2\pi f_i t), \tag{2.2}$$

where $s(i)$ and f_i are, correspondingly, a complex amplitude and the frequency of the i-th chip, $\dot{c}_0(t)$ is complex envelope of the chip, describing its amplitude and internal angle modulation, and Δ is a chip repetition interval. In this work attention is concentrated on chips for which the waveform $c_0(t)$ is a rectangle of duration Δ. Sequence $\{|s(i)|, i = \ldots, -1, 0, 1, \ldots\}$ defines real amplitudes of the chips, that is, their amplitudes modulation law while sequence $\{\phi_i = \arg s(i), i = \ldots, -1, 0, 1, \ldots\}$ defines the modulation law of chip phases. Sequence $\{s(i)\}$ is called a *code sequence* or just a *code*. The real signal $\mathtt{s}(t)$ is then obtained from the complex envelope as

$$\mathtt{s}(t) = \mathrm{Re}\left[\dot{S}(t)\exp(j2\pi f_0 t)\right], \tag{2.3}$$

where f_0 is the carrier frequency.

Spread spectrum systems operating with discrete signals can be divided into two main categories. In frequency hopping spread spectrum (FHSS) systems, the spreading is achieved by the modulation of f_i in (2.2) according to some predefined law; these systems can further be divided into fast and slow hopping ones [26, 112]. This kind of spreading technique is used, for example, in Bluetooth standard [18], which among other things allows to increase network security [66, 86].

The different approach is used in a direct sequence spread spectrum (DSSS) system. In this case only complex amplitudes $s(i)$ are modulated and chip frequencies are assumed as zeros ($f_i = 0$), so (2.2) can be simplified to

$$\dot{S}(t) = \sum_{i=-\infty}^{\infty} s(i)\dot{c}_0(t - i\Delta). \tag{2.4}$$

Sometimes a combination of FHSS and DSSS is used, but this Thesis is limited to DSSS case only.

Suppose now that in the model (2.4) real amplitudes $|s(i)|$ are zeros outside window $[0, N-1]$: $|s(i)| = 0 \quad \forall i < 0, i > N-1$. In this case a signal consists of N chips and is called *pulse* or *aperiodic*. If, on the other hand, the code sequence repeats itself with a period of N chips $s(i + N) = s(i)$, $i = \ldots, -1, 0, 1, \ldots$, the signal is called *periodic*. In both cases parameter N is called the *length* of the code, while the code itself can be fully defined by the vector of dimension N

$$\mathbf{s} = [s(0), s(1), \ldots, s(N-1)]. \tag{2.5}$$

Any periodic signal can be constructed by repetitions with period $N\Delta$ of aperiodic one containing N chips:

$$\dot{S}(t) = \sum_{r=-\infty}^{\infty} \sum_{i=0}^{N-1} s(i)\dot{c}_0\left(t - (i + rN)\Delta\right) = \sum_{i=-\infty}^{\infty} s((i))\dot{c}_0(t - i\Delta), \qquad (2.6)$$

where $((i))$ means that the index operation is performed modulo N: $((i)) = i \bmod N$, $0 \le ((i)) \le N - 1$.

In the most general case of the considered model, when both amplitudes and phases of the chips can be different, a discrete signal is called *amplitude-phase shift keying* (APSK) one. We will call a discrete signal *phase shift keying* (PSK) one if real amplitudes of all chips are equal, $|s(i)| = \text{const}$, $i = 0, 1, \ldots, N-1$, and chips can differ by phase values only. Finally, if code elements can take on only two values ± 1, $s(i) \in \{\pm 1\}$, $i = 0, 1, \ldots, N-1$, a discrete signal is called *binary phase shift keying* (BPSK) one.

Note that the signal thus constructed is a spread spectrum one. Indeed, since the chip waveform is taken as a rectangle of duration Δ, it is, certainly, a plain signal with bandwidth $W \approx 1/\Delta$. On the other hand, an APSK signal consists of N such chips, but its bandwidth is defined by the bandwidth of the chip, so that its time-frequency product (spreading factor, processing gain) is the length of the code: $(N\Delta)W = N$.

Continuous spread spectrum signals are also possible, but nowadays they are used mostly in radar and sonar applications [76, 82, 119].

2.3 Synchronous Code Division Multiple Access

In many communication systems, called *multiuser* ones, it is required to provide service to more than one user simultaneously, meaning the necessity of sharing the available total time-frequency resource. Historically, first methods allowing to arrange such independent transmission and reception of user data were time- and frequency division multiple access (TDMA and FDMA).

In TDMA the total available time resource T_t is divided between K users, so that each one operates within time interval K times smaller $T = T_t/K$ (Figure 2.3). At the same time total frequency resource W_t is the same for all users, $W = W_t \approx 1/T$. Due to non-overlapping in time domain, signals are *orthogonal* [62], which makes their separation a relatively simple task. Every user signal is plain, since its time-frequency product is one: $WT = 1$.

Analogously to TDMA, in FDMA the frequency resource is distributed between K users, $W = W_t/K$, while time resource is the same for all of them, $T = T_t$. In this scenario user signals are, certainly, also plain, $WT = 1$.

In strong contrast with that, in *code division multiple access* (CDMA) every user occupies the whole time interval $T = T_t$ and bandwidth $W = W_t$

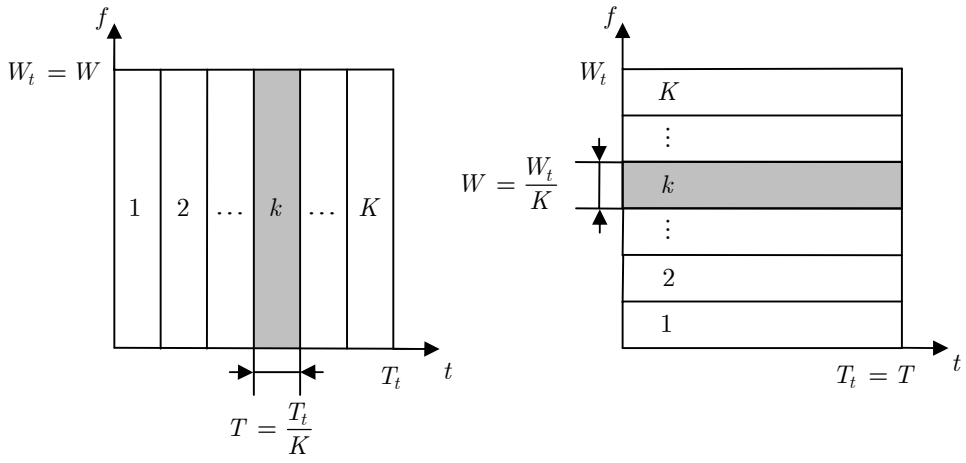

Figure 2.3: Time- and frequency division multiple access

(Figure 2.4). With a large number of users, signals in this case are spread spectrum: $WT = W_t T_t = K \gg 1$.

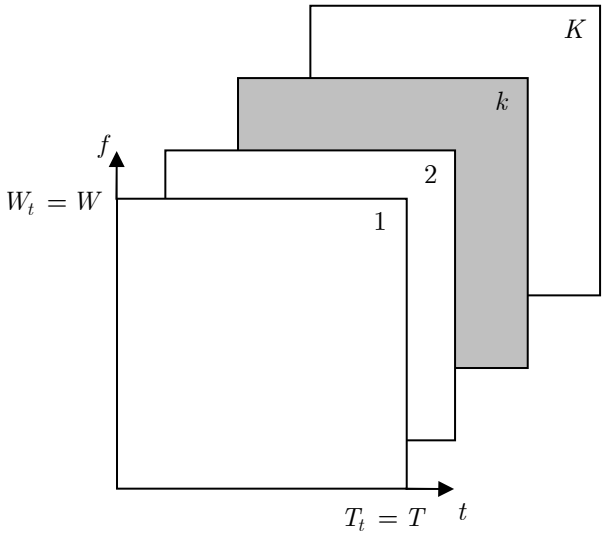

Figure 2.4: Code division multiple access

Data transmission in CDMA is organized as follows. Every user is assigned its own specific *signature* $\mathbf{s}_k$, $1 \leq k \leq K$ of unity norm, $\|\mathbf{s}_k\|^2 = 1$:

$$\mathbf{s}_k = [s_k(0), s_k(1), \ldots, s_k(N-1)]. \tag{2.7}$$

In *direct sequence* CDMA (DS CDMA) user signatures are modulated by user information bits b_k, $1 \leq k \leq K$, which for the BPSK transmission can take on only two values $b_k \in \{\pm 1\}$ (Figure 2.5).

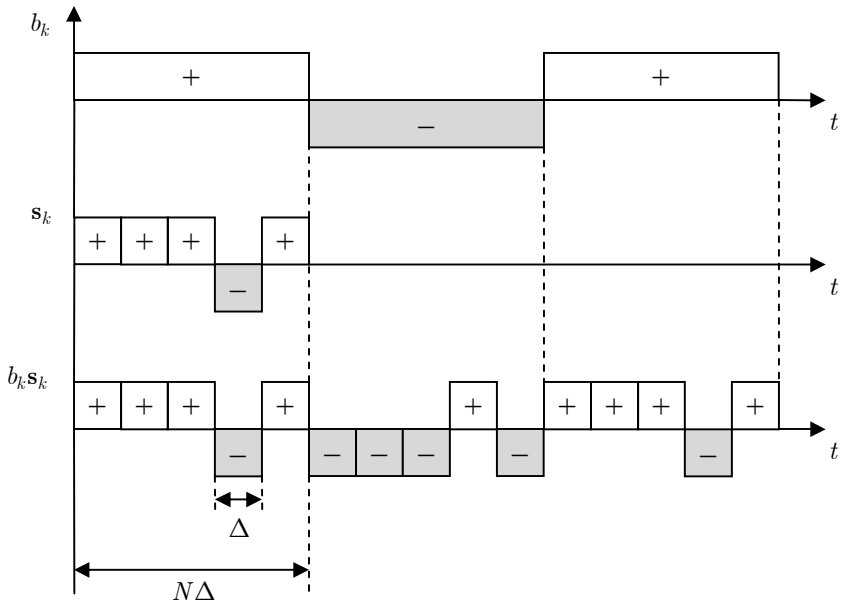

Figure 2.5: Example of DS CDMA, k-th user signature $\mathbf{s}_k$ is modulated by the information bit b_k

When all user signals in DS CDMA are synchronized and no mutual delay between them is possible the system is called *synchronous* DS CDMA. This transmission scheme is used, for example, in the downlink channel from a base station to mobile stations in cellular systems (cdmaOne, WCDMA, cdma2000 [44,51,68,88,128]). In these systems data-modulated user signals are summed before the transmission, forming the *group signal*

$$\mathbf{s}(\mathbf{b}) = \sum_{k=1}^{K} b_k \mathbf{s}_k = \mathbf{S}\mathbf{b}, \tag{2.8}$$

where $\mathbf{S}$ is the *signature matrix* defined as

$$\mathbf{S} = [\mathbf{s}_1^T, \mathbf{s}_2^T, \ldots, \mathbf{s}_K^T], \tag{2.9}$$

where superscript T means transpose, and $\mathbf{b}$ is the data vector denoted as $\mathbf{b} = [b_1, b_2, \ldots, b_K]^T$.

The inverse procedure of the data extraction is considered in Section 2.5, where several receiver schemes are discussed and compared.

2.4 Correlation Functions

One of the most important role in communication systems belongs to signal correlation functions. They are of critical significance, for example, in prob-

lems of time measurement and resolution [62, 121]. More than that, the art of communication system design is in many aspects tantamount to finding signals with adequate correlation properties [98, 112].

An *autocorrelation* function (ACF) is defined as the inner product of two copies of the same signal, time-shifted to each other by τ seconds:

$$\dot{R}(\tau) = \int_{-\infty}^{\infty} \dot{S}(t)\dot{S}^*(t-\tau)dt, \tag{2.10}$$

where superscript '$*$' symbolizes complex conjugation. Scaling (2.10) by inverse signal energy produces normalized ACF, which is a *correlation coefficient* of time-shifted signal copies:

$$\dot{\rho}(\tau) = \frac{1}{2E}\int_{0}^{T} \dot{S}(t)\dot{S}^*(t-\tau)dt, \tag{2.11}$$

where the energy is defined as $E = \|\mathbf{s}\|^2 E_0$ and integration limits are changed with assumption that the signal duration is $T = N\Delta$. Here E_0 is the chip energy and $\|\mathbf{s}\|^2$ is a squared geometrical length (Euclidean norm) of the code vector (2.5), $\|\mathbf{s}\|^2 = \sum_{i=0}^{N-1} |s(i)|^2$.

Consider now correlation functions of APSK signals. It is known [62] that ACF of an APSK signal is, in turn, an APSK signal itself:

$$\dot{\rho}(\tau) = \sum_{m=-\infty}^{\infty} \rho(m)\dot{\rho}_c(\tau - m\Delta), \tag{2.12}$$

where

$$\rho(m) = \frac{1}{\|\mathbf{s}\|^2}\sum_{i=0}^{N-1} s(i)s^*(i-m) \tag{2.13}$$

is the ACF of the code sequence $\{s(0), s(1), \ldots, s(N-1)\}$ and

$$\dot{\rho}_c(\tau) = \frac{1}{2E_0}\int_{-\infty}^{\infty} \dot{c}_0(t)\dot{c}_0^*(t-\tau)dt \tag{2.14}$$

is the ACF of a single chip.

Analogously, a *crosscorrelation* function (CCF) of two different (k-th and l-th) APSK signals is defined as

$$\dot{\rho}_{kl}(\tau) = \sum_{m=-\infty}^{\infty} \rho_{kl}(m)\dot{\rho}_c(\tau - m\Delta), \tag{2.15}$$

where

$$\rho_{kl}(m) = \frac{1}{\|\mathbf{s}_k\|\|\mathbf{s}_l\|} \sum_{i=0}^{N-1} s_k(i) s_l^*(i-m) \tag{2.16}$$

is the CCF of the signal code sequences $\{s_k(0), s_k(1), \ldots, s_k(N-1)\}$ and $\{s_l(0), s_l(1), \ldots, s_l(N-1)\}$.

Along with (2.13) and (2.16), non-normalized correlation functions of code sequences are also used:

$$R(m) = \sum_{i=0}^{N-1} s(i) s^*(i-m), \qquad R_{kl}(m) = \sum_{i=0}^{N-1} s_k(i) s_l^*(i-m). \tag{2.17}$$

If the code sequence $\{s(0), s(1), \ldots, s(N-1)\}$ is used to generate a pulse signal, in (2.2) $|s(i)| = 0$ for $\forall i < 0, i \geq N$, so we can define *aperiodic* or *pulse* ACF as

$$R_a(m) = \begin{cases} \sum\limits_{i=m}^{N-1} s(i) s^*(i-m), & m \geq 0 \\ \sum\limits_{i=0}^{N-1+m} s(i) s^*(i-m), & m < 0 \end{cases} \tag{2.18}$$

If, on the other hand, the signal is periodic, i.e. $s(i+N) = s(i)$, $i = \ldots, -1, 0, 1, \ldots$ then (2.13) turns to the *periodic* ACF (PACF):

$$R_p(m) = \sum_{i=0}^{N-1} s(i) s^*(i-m), \tag{2.19}$$

always containing N summands, since $s(-1) = s(N-1)$, $s(-2) = s(N-2)$ and so on. Periodic and aperiodic ACF are connected by the following equation:

$$R_p(m) = R_a(m) + R_a(m-N), \quad m = 0, 1, \ldots, N-1. \tag{2.20}$$

We will also define aperiodic and periodic CCF as

$$R_{a,kl}(m) = \begin{cases} \sum\limits_{i=m}^{N-1} s_k(i) s_l^*(i-m), & m \geq 0 \\ \sum\limits_{i=0}^{N-1+m} s_k(i) s_l^*(i-m), & m < 0 \end{cases} \tag{2.21}$$

and

$$R_{p,kl}(m) = \sum_{i=0}^{N-1} s_k(i) s_l^*(i-m). \tag{2.22}$$

Equation (2.20) remains true for CCF, as well:

$$R_{p,kl}(m) = R_{a,kl}(m) + R_{a,kl}(m-N), \quad m = 0, 1, \ldots, N-1. \tag{2.23}$$

2.5 Receivers for Synchronous CDMA

To simplify the notation assume within this Section that the BPSK data modulation is used, generalization to other modes being straightforward, and that all user signatures $\mathtt{s}_k(t)$, $1 \leq k \leq K$ are normalized to have unit energy.

An equivalent form of the group signal (2.8) is

$$\mathtt{s}(\mathbf{b}; t) = \sum_{k=1}^{K} A_k b_k \mathtt{s}_k(t) \tag{2.24}$$

where we also introduced A_k as the k-th user amplitude. Suppose that after passing through the channel the group signal is corrupted by the additive white Gaussian noise (AWGN), so the received observation is

$$\mathtt{y}(t) = \mathtt{s}(\mathbf{b}; t) + n(t) = \sum_{k=1}^{K} A_k b_k \mathtt{s}_k(t) + n(t), \tag{2.25}$$

where $n(t)$ symbolizes the noise component. The *maximal likelihood* (ML) joint estimate $\hat{\mathbf{b}}$ of the transmitted bits of all K users may be obtained at the receiver on the basis of minimum distance rule [121]:

$$\hat{\mathbf{b}} = \arg\min_{\mathbf{b}} d^2(\mathbf{b}), \tag{2.26}$$

making the decision in favour of the binary data vector $\mathbf{b}$ for which the group signal $\mathtt{s}(\mathbf{b}; t)$ appears to be the closest to the observation $\mathtt{y}(t)$ in terms of the Euclidian distance

$$d^2(\mathbf{b}) = \int_0^T [\mathtt{y}(t) - \mathtt{s}(\mathbf{b}; t)]^2 \, dt. \tag{2.27}$$

An equivalent form of this ML rule is

$$\hat{\mathbf{b}} = \arg\max_{\mathbf{b}} \left\{ z(\mathbf{b}) - \frac{E(\mathbf{b})}{2} \right\}, \tag{2.28}$$

where

$$z(\mathbf{b}) = \int_0^T \mathtt{y}(t) \mathtt{s}(t; \mathbf{b}) dt \tag{2.29}$$

is the correlation between the observation and the group signal and

$$E(\mathbf{b}) = \int_0^T \mathtt{s}^2(t; \mathbf{b}) dt \tag{2.30}$$

is the group signal energy, both in dependence on the binary data vector $\mathbf{b}$.

Substitution of (2.24) into the statistics (2.28) produces

$$z(\mathbf{b}) - \frac{E(\mathbf{b})}{2} = \sum_{k=1}^{K} A_k b_k z_k - \frac{1}{2} \sum_{k=1}^{K} \sum_{l=1}^{K} A_k A_l b_k b_l R_{kl}, \tag{2.31}$$

where

$$z_k = \int_0^T \mathtt{y}(t)\mathtt{s}_k(t)dt \tag{2.32}$$

is the correlation of the observation and the k-th signature, and

$$R_{kl} = \int_0^T \mathtt{s}_l(t)\mathtt{s}_k(t)dt \tag{2.33}$$

is the correlation of the k-th and l-th signatures.

If we neglect dependence of the group signal energy $E(\mathbf{b})$ on users' bit vector $\mathbf{b}$, the decision rule is reduced to just maximizing $z(\mathbf{b})$ over all binary data vectors $\mathbf{b}$, producing estimate of a current bit of the k-th user by the polarity of z_k:

$$\hat{b}_k = \operatorname{sgn} z_k = \begin{cases} 1, & z_k \geqslant 0, \\ -1, & z_k < 0. \end{cases} \tag{2.34}$$

This simplest algorithm operates as if only the k-th user signal is received and it fully ignores presence of signals of other users. Due to this fact it is called the *single-user* (or *conventional*) detection, which usually is realized as a correlator or matched filter. Obviously, a single-user receiver is optimal if and only if the assumption above is true, i.e. the signature set $\{\mathtt{s}_1(t), \mathtt{s}_2(t), \ldots, \mathtt{s}_K(t)\}$ is designed in a way making $\mathbf{b}$ a *non-energy* parameter, so that $E(\mathbf{b})$ is really independent of users' data $\mathbf{b}$. It is easy to make sure [62] that this condition holds if and only if all signatures are *orthogonal*: $R_{kl} = 0, k \neq l$.

With non-orthogonal signatures single-user receiver yields to the ML one, which may be called *optimal multiuser receiver* [85,125]. A big trouble with the latter is its implementation complexity. In a general case it should calculate values of the test statistics for all 2^K possible realizations of binary data vector $\mathbf{b}$, meaning exponential growth of complexity with number of users K. For example for $K = 60$ the optimal multiuser receiver will have to compute and compare $2^{60} > 10^{18}$ values of test statistics during one bit interval.

In the light of the aforesaid it seems natural to use orthogonal signatures wherever possible. However, the largest number of orthogonal signals is upper bordered by the signal space dimension, i.e. by the spreading factor. In DS CDMA this is just the number of chips per one bit N, i.e. the length

of signature code sequence. Rate given, N is limited by the bandwidth W allocated to the system, making available number of orthogonal signatures $K \leq N$. Chasing greater system capacity K within the fixed bandwidth, one of the nowadays trends is to operate in an *oversaturated* (or *overloaded*) mode, i.e. with the number of users K exceeding the spreading factor N [90]. Then prohibitive complexity of optimal multiuser receiver pushes towards seeking for *quasi-optimal* multiuser algorithms, though yielding to the optimal one, but beating the single-user receiver.

2.5.1 Decorrelating Receiver

As will be repeatedly mentioned in this Thesis, non-orthogonality of users' signatures will inevitably produce *multiple access interference* at the correlator output of the k-th user's conventional receiver. Indeed, substituting $\mathtt{s}(t, \mathbf{b})$ into (2.32) gives

$$z_k = A_k b_k + \sum_{\substack{l=1 \\ l \neq k}}^{K} A_l b_l R_{kl} + n_k, \tag{2.35}$$

where the first term represents the useful effect carrying information about the k-th user's current bit, the last one is a sample of Gaussian noise, and the middle one is MAI, which turns into zero independently of amplitudes and data of side users if and only if $R_{kl} = 0$ for all pairs of different k, l. One simplest intuitive way to reduce a harm of MAI is mismatching correlator reference, i.e. calculation of z_k as

$$z_k = \int_0^T \mathtt{y}(t)\mathtt{u}_k(t)dt, \tag{2.36}$$

where mismatched reference $\mathtt{u}_k(t)$ replacing the matched one $\mathtt{s}_k(t)$ is designed in a way providing reduction or even a complete suppression of MAI [79]. If $\mathtt{u}_k(t)$, like signatures, is normalized to have unit energy, then the new version of the correlation (2.35) is

$$z_k = A_k b_k R'_{kk} + \sum_{\substack{l=1 \\ l \neq k}}^{K} A_l b_l R'_{kl} + n_k, \tag{2.37}$$

with the last term being as before a sample of Gaussian noise and

$$R'_{kl} = \int_{-\infty}^{\infty} \mathtt{s}_l(t)\mathtt{u}_k(t)dt \tag{2.38}$$

being correlation coefficient between the l-th signature $\mathtt{s}_l(t)$ and the k-th reference $\mathtt{u}_k(t)$. Let us recall from Section 2.3 that in DS CDMA the k-th signature $\mathtt{s}_k(t)$ is fully determined by a code sequence of length N or N-dimensional row vector $\mathbf{s}_k = \{s_k(0), s_k(1), \ldots, s_k(N-1)\}$ whose elements $s_k(i)$, $i = 0, 1, \ldots, N-1$ are complex amplitudes manipulating chips of a given shape $c_0(t)$. The same way every reference may be represented by its code sequence or row vector $\mathbf{u}_k = \{u_k(0), u_k(1), \ldots, u_k(N-1)\}$, $k = 1, 2, \ldots, K$, where $u_k(i)$ defines complex amplitude of the i-th chip in the k-th reference. In what follows we (to simplify notation) limit ourselves to the case of real signatures (e.g. BPSK), generalization presenting no difficulties. Then, preserving unit-energy normalization for all signature and reference vectors, we have

$$R_{kl} = \mathbf{s}_k \mathbf{s}_l^T, \quad R'_{kl} = \mathbf{u}_k \mathbf{s}_l^T, \quad k, l = 1, 2, \ldots, K. \tag{2.39}$$

Let us now introduce the *signature correlation* (Gram) matrix $\mathbf{C} = [R_{kl}]$ as $\mathbf{C} = \mathbf{S}^T\mathbf{S}$, where $\mathbf{S}$ is the signature matrix (2.9). Find now the reference vector $\mathbf{u}_k$ corresponding to the so-called *decorrelating receiver* completely eliminating MAI [19, 38]. Obviously, for the k-th user receiver MAI will be completely removed if and only if $R'_{kl} = 0$ for all $l \neq k$, but $R'_{kk} \neq 0$, the last condition necessary for preserving nonzero useful effect of the k-th user. Therefore, the following set of linear equations determines the decorrelating reference $\mathbf{u}_k$:

$$\mathbf{u}_k \mathbf{S} = R'_{kk} \mathbf{e}_k, \tag{2.40}$$

where $\mathbf{e}_k$ denotes row vector whose k-th element equals one, the rest being zeros.

If the signature correlation matrix $\mathbf{C} = \mathbf{S}^T\mathbf{S}$ is nonsingular, the k-th user decorrelating reference is just the k-th row of (pseudoinverse to $\mathbf{S}$) matrix $\mathbf{C}^{-1}\mathbf{S}^T = (\mathbf{S}^T\mathbf{S})^{-1}\mathbf{S}^T$ [62]. Physically, the decorrelating reference is simply orthogonal to all signatures but the k-th one. Regretfully, decorrelation is only available when $\mathbf{C}$ is nonsingular, i.e. all signatures are linearly independent, excluding thereby at once any oversaturation scenario $K > N$. In the case of orthogonal signatures matched reference is orthogonal to all interfering signals, performing decorrelation (suppressing MAI) automatically. When $K \leq N$ but signatures are not best (orthogonal) the price of decorrelation is loss in signal to noise ratio (SNR) against matched filtering γ_k, growing as signatures become 'less' orthogonal:

$$\gamma_k = q^2_{k,mf} / q^2_{k,dc} = \mathbf{C}^{-1}{}_{kk} \tag{2.41}$$

where $q_{k,mf}$ and $q_{k,dc}$ are, respectively, matched filter and decorrelator SNR and $\mathbf{C}^{-1}_{kk}$ is the k-th diagonal element of inverse signature correlation matrix $\mathbf{C}^{-1}$.

2.5.2 Maximum SINR (MMSE) Receiver

Let us now try to find the reference $\mathbf{u}_k$ removing MAI only partially but providing the optimal balance between the residual MAI and noise [80, 95], under which the SINR (signal-to-interference-plus-noise ratio), defined as

$$q_i^2 = \frac{P_s}{P_i + P_n}, \tag{2.42}$$

where P_s, P_i, and P_n are, respectively, powers of useful signal, MAI and noise at the correlator output, achieves its maximum. Analytically it is more convenient to maximize the following ratio

$$\xi = \frac{P_s}{P_s + P_i + P_n} = \frac{q_i^2}{1 + q_i^2} \in [0, 1]. \tag{2.43}$$

Obviously, q_i^2 grows monotonically with ξ, so that maximizing the second maximizes the first. Let us define the symmetric matrix $\mathbf{R}$ as

$$\mathbf{R} = \mathbf{S}\mathbf{A}^2\mathbf{S}^T + \sigma^2\mathbf{I}_N, \tag{2.44}$$

where $\mathbf{A} = \mathrm{diag}(A_1, A_2, \ldots, A_K)$ is a diagonal matrix of users' amplitudes, while $\mathbf{S}$ and $\mathbf{b}$ are, as before, signature matrix and users' bit vector, respectively.

Leaving some calculations aside [62], ratio ξ to be maximized is

$$\xi = \frac{P_s}{P_s + P_i + P_n} = \frac{A_k^2 \left|\mathbf{u}_k \mathbf{s}_k^T\right|^2}{\mathbf{u}_k \mathbf{R} \mathbf{u}_k^T}. \tag{2.45}$$

The matrix $\mathbf{R}$, being positive definite, has positive definite inverse $\mathbf{R}^{-1}$, and the latter in turn has the positive definite square root [55, 129]:

$$\mathbf{R}^{-1} = \mathbf{R}^{-\frac{1}{2}} \mathbf{R}^{-\frac{1}{2}}. \tag{2.46}$$

Then we can write, again skipping some calculations for the sake of brevity, that the optimal reference vector is

$$\mathbf{u}_k = \mathbf{s}_k \mathbf{R}^{-1} = \mathbf{s}_k (\mathbf{S}\mathbf{A}^2\mathbf{S}^T + \sigma^2\mathbf{I}_N)^{-1}.$$

The reference just obtained is typically derived in literature on the basis of the criterion of minimum mean-square error (MMSE) of reproducing interference-plus-noise-free useful effect [108]. Thus, *maximum SINR* and *MMSE* receivers are identical.

It is readily seen that if noise goes to zero ($\sigma^2 \to 0$) and $\mathbf{C}^{-1}$ exists, the MMSE receiver turns into the decorrelating one. In the opposite extreme case of noise dominating over MAI signature correlation matrix $\mathbf{C}$ may be neglected resulting in the matched (single-user) correlator reference.

2.6 Asynchronous DS CDMA

In strong contrast with Section 2.3, for *asynchronous* CDMA user signals can have arbitrary mutual delays (Figure 2.6). Scenario like this is typical, for example, for an uplink channel in cellular systems, where mismatch of user signal time arrival to the base station is caused by different distances to user terminals [84, 112].

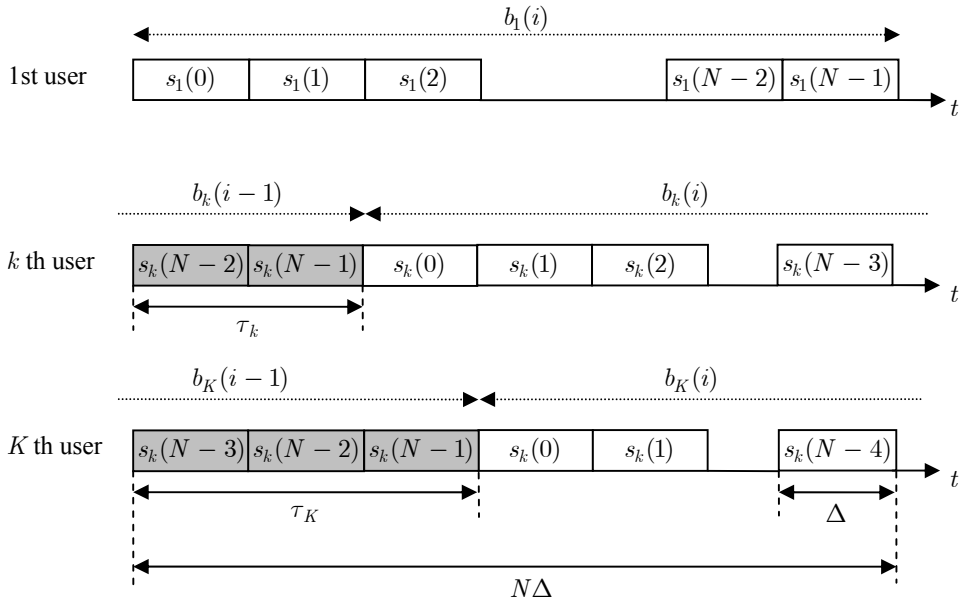

Figure 2.6: Asynchronous CDMA

Let us now describe a model of asynchronous DS CDMA that will be used in this Thesis repeatedly. We will assume that user signal delays are nonnegative multiples of the chip duration Δ, $\tau_k = m_k\Delta$, $1 \le k \le K$, generalization being straightforward, and that users are sorted in order of their delay increase: $0 \le m_1 \le m_2 \le \ldots \le m_K$.

Consider now two arbitrary users number k and l, $1 \le k, l \le K$, $k \ne l$, and suppose that their mutual delay is nonzero: $\tau_k - \tau_l = \tau_{kl} = m_{kl}\Delta \ne 0$. If this mutual delay is positive, the l-th user signal surpasses the k-th one, and during time interval of the i-th bit of the k-th user $b_k(i)$ there will be parts of two bits of the l-th one, $b_l(i)$ and $b_l(i+1)$ (Figure 2.7). On the contrary, if mutual delay is negative $m_{kl} < 0$, the l-th user signal is delayed, and during the time interval of $b_k(i)$ there will be parts of bits $b_l(i)$ and $b_l(i-1)$ (Figure 2.8).

Consider now output of the k-th user correlator (matched filter) corre-

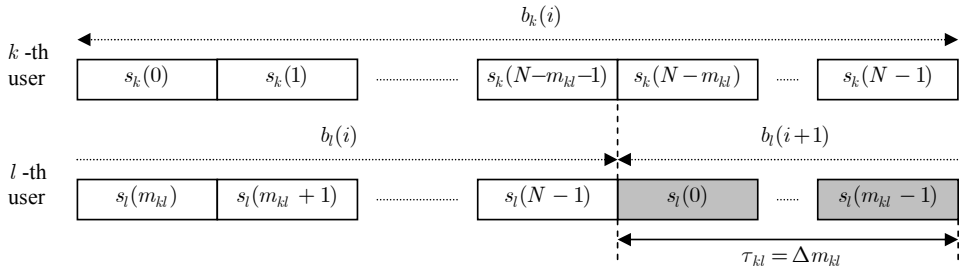

Figure 2.7: Group signal for two users, $m_{kl} = m_k - m_l > 0$

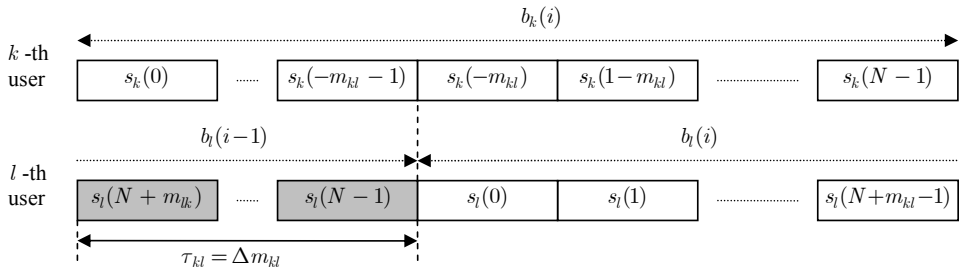

Figure 2.8: Group signal for two users, $m_{kl} = m_k - m_l < 0$

sponding to the data bit $b_k(i)$:

$$z_k = b_k(i) + \begin{cases} b_l(i)R_{a,kl}(-m_{kl}) + b_l(i+1)R_{a,kl}(N-m_{kl}), & m_{kl} \geqslant 0 \\ b_l(i-1)R_{a,kl}(-m_{kl}-N) + b_l(i)R_{a,kl}(-m_{kl}), & m_{kl} < 0 \end{cases} \tag{2.47}$$

When two consecutive bits of the l-th user $b_l(i)$ and $b_l(i+1)$ (or $b_l(i-1)$ and $b_l(i)$) coincide, sum of two aperiodic CCF produces periodic CCF (2.23):

$$R_{p,kl}(m) = R_{a,kl}(m) + R_{a,kl}(m-N), \tag{2.48}$$

which is called *even* CCF. On the contrary, when these bits are not equal, their difference results in *odd* CCF:

$$R^{\text{odd}}_{p,kl}(m) = R_{a,kl}(m) - R_{a,kl}(m-N). \tag{2.49}$$

2.7 Sequences with Good ACF

Among demands to code sequences used in communication systems one of the most important one is demand to their autocorrelation functions [98, 121]. Let us refer to a sequence aperiodic ACF as "good" if its *sidelobes* $R_a(m)$, $0 < m \leq N-1$ are small comparing to the *main lobe* $R_a(0)$ [62]. Sequences of this sort are crucial for time measuring and resolution problems,

but as will be shown later, they are also very widely used in DS CDMA systems.

Denoting the maximal normalized level of aperiodic code ACF sidelobe as

$$\rho_{a,\max} = \max_{m\neq 0} |\rho(m)|\,, \quad \rho(m) = \frac{R_a(m)}{R_a(0)} \tag{2.50}$$

we will call a sequence the *minimax* one if its maximal ACF sidelobe is minimal:

$$\rho_{a,\max} = \min\,. \tag{2.51}$$

Certainly, ideally it would be to have $\rho_{a,\max} = 0$, but for aperiodic discrete signal it is not possible in principle. It is known that for a PSK sequence $\mathbf{s}$, where $|s(i)| = 1$, $0 \leq i \leq N-1$ we have

$$R_a(m) \geq 1, \quad m \neq 0. \tag{2.52}$$

PSK sequences which achieve this bound possess *perfect* aperiodic ACF and are called *Barker codes* [9]. From the practical implementation point of view most attractive are BPSK signals whose code sequence is binary: $s(i) = \pm 1$, $i = 0, 1, \ldots, N-1$. It was as far back as in early 50th that all possible binary sequences with perfect aperiodic ACF were found (binary Barker codes). They exist only for lengths $N = 2, 3, 4, 5, 7, 11, 13$ [41, 122].

Unfortunately, there are no regular rules to construct binary sequences with good aperiodic ACF. The most straightforward solution, an exhaustive search, becomes unrealistic for lengths $N > 50$ considering current computational resource. For this reason the following strategy is popular. From (2.20) we can write

$$\rho_{p,\max} = \max_{m=1,2,\ldots,N-1} \left| \frac{R_p(m)}{R(0)} \right| \leqslant 2\rho_{a,\max}, \tag{2.53}$$

where designation $\rho_{p,\max}$ stands for maximal level of sidelobe of periodic ACF $R_p(m)$ of the code sequence. This leads to the following inequality:

$$\rho_{a,\max} \geqslant \frac{1}{2}\rho_{p,\max}, \tag{2.54}$$

pointing that low level of *periodic* ACF sidelobes is a necessary condition of achieving low level of aperiodic ACF.

Note first of all that unlike the aperiodic ACF, for PACF it is possible in principle to have zero sidelobes, and such PACF is called called the *perfect* PACF:

$$R_p(m) = 0, \quad m = 1, 2, \ldots, N-1. \tag{2.55}$$

Unfortunately, the only binary code with ideal PACF of length $N < 12100$ is a trivial one of length four: $\{+1+1+1-1\}$ [12]. The nonexistence

of such sequences is proved up to the lengths $N < 4 \times 165^2 = 108900$ [107], and their existence beyond that length looks quite improbable.

Stepping aside from binary sequences for a moment, there do exist sequences with perfect PACF for bigger than binary alphabet. Among polyphase codes with PSK alphabet the most well-known ones are Chu codes [20] and Frank codes [48]. However, they are not very practical, as their alphabets' sizes grow with length N as N and $\sqrt{N}$, correspondingly.

Probably the most interesting non-binary sequences with perfect PACF are ternary ones, or Ipatov sequences [63, 64]. Their alphabet consists of three symbols $\{-1, 0, 1\}$, which practically means combining BPSK with pauses and does not pose much practical difficulties in implementation. The most powerful rule of constructing ternary sequences provides sequences with lengths

$$N = \frac{q^n - 1}{q - 1},$$

where $q = p^w$ is a natural power of a prime p and n is odd. At the same time, ternary sequences provide the peak-factor (that is, ratio of peak and average power) as close to unity as necessary, which is also quite attractive from a practical point of view.

Let us now return to binary sequences. Not being able to realize perfect ($\rho_{p,\max} = 0$) PACF it is desirable to discover binary codes with as small PACF sidelobes as possible and the next interesting sidelobe values are $R_p(m) = +1$ or $R_p(m) = -1$ at any $m = 1, 2, \ldots, N-1$ ($\rho_{p,\max} = 1/N$). Sequences with these correlation properties are usually called *minimax* ones. It is proved that sequences with $R_p(m) = +1$ must have length of the form $N = 4t + 1$; only two sequences of lengths $N = 5$ and $N = 13$ of this sort are known. As for sequences with $R_p(m) = -1$, they must have length of the form $N = 4t - 1$, and there are at least five families of sequences with regular rules of construction. The most important one is considered in the following section.

2.7.1 m-sequences

Consider a sequence $\{d_i\}$ of elements 0 and 1 of GF(2) generated according to a *linear recurrent equation*, where GF stands for Galois field [77]:

$$d_i = f_{n-1}d_{i-1} + f_{n-2}d_{i-2} + \ldots + f_0 d_{i-n}, \quad i = n, n+1, \ldots, \tag{2.56}$$

where all f_l, $l = 0, 1, \ldots, n-1$ are constant and also belong to GF(2), additions and multiplications are performed by the GF(2) rules, and n is called the memory of the sequence. It is seen that the current element of sequence $\{d_i\}$ is a linear combination of n previous elements and owing to this $\{d_i\}$ is called the *linear recurrent sequence*.

Any linear recurrent sequence can be generated by a linear feedback shift register (LFSR) [77]. LFSR contains n binary memory cells (flip-flops) and is clocked, each clocking shifts state of any specific (but the last) cell to the next one, while state of the leftmost cell after a current clocking is equal to a current state of the feedback logic (Figure 2.9).

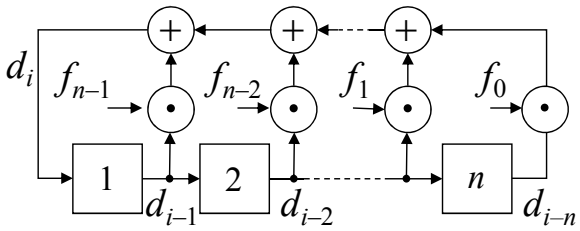

Figure 2.9: Linear feedback shift register

Since number of different states of n-cell register is finite, linear recurrent sequence is always periodic. The maximal possible sequence period N equals the maximal number of different register states, i.e. $2^n - 1$. The linear recurrent sequence having maximal period $N = 2^n - 1$, given memory n, is called a *maximal length* sequence or an m-sequence [53]. Such a sequence possesses a number of marked properties making it somewhat similar to a truly random binary sequence of heads and tails when a fair coin is repeatedly tossed, whereby m-sequences is an example of *pseudorandom* (PN) sequence.

The binary m-sequence, whose elements take on values $\{\pm 1\}$, has a minimax PACF:

$$R_p(m) = \begin{cases} N, & m = 0 \\ -1, & m = 1, 2, \ldots, N-1 \end{cases} \Rightarrow \rho_{p,\max} = 1/N. \tag{2.57}$$

In order to generate an m-sequence with the help of the n-cell shift register it is necessary that the feedback (or recurrent equation) coefficients $f_{n-1}, f_{n-2}, \ldots, f_0$ be equal to coefficients of a special polynomial of degree n

$$f(x) = x^n + f_{n-1}x^{n-1} + f_{n-2}x^{n-2} + \ldots + f_0,$$

called *primitive* one. Primitive polynomials exist for any natural n providing thereby existence of minimax binary codes based on m-sequences for any periods of the form $N = 2^n - 1 = 3, 7, 15, 31, 63, 127, \ldots$. Tables of primitive polynomials are published and readily available [77, 115, 134].

2.8 Signature Ensembles for Asynchronous DS CDMA

Let us now turn to ensemble of signatures that are used in DS CDMA systems. Consider a signature ensemble of K signatures $\mathbf{s}_k$ of length N, and suppose that all signatures are PSK ones. A fundamental measure of the ensemble's correlation properties is the *total squared correlation* (TSC) [104, 124, 126], defined as

$$\mathrm{TSC} = \sum_{k=1}^{K} \sum_{l=1}^{K} |\rho_{kl}|^2, \tag{2.58}$$

where ρ_{kl} is the correlation coefficient (2.16) between the k-th and l-th signatures.

There exists a fundamental Welch bound [62,130], dictating the minimal possible value of TSC:

$$\mathrm{TSC} \geq \begin{cases} K, & K \leqslant N \\ \dfrac{K^2}{N}, & K > N \end{cases} \tag{2.59}$$

Certainly, the set of sequences achieving (2.59) (Welch-bound sequences) is the best possible in minimal MAI criterion. General methods to produce such ensembles are given for example in [102, 123, 131]. But in fact, the significance of these sets goes far beyond only this feature, since Welch-bound sequences maximize the Shannon capacity of CDMA channels with AWGN and Gaussian input, the latter constraint losing its importance whenever a receive symbol SNR becomes small enough [104].

Since TSC includes K squared correlations of signatures with themselves, each being equal to unity, it is natural to consider the difference $\mathrm{TSC} - K$ which corresponds to unwanted CCFs only between distinct signatures. Then introducing the average squared correlation $\overline{\rho^2}$ as

$$\overline{\rho^2} = \frac{\mathrm{TSC} - K}{K(K-1)} \tag{2.60}$$

we can rewrite (2.59) as

$$\overline{\rho^2} \geq \begin{cases} 0, & K \leqslant N \\ \dfrac{K-N}{N(K-1)}, & K > N \end{cases} \tag{2.61}$$

For the asynchronous DS CDMA not only a signature itself, but also all its N cyclic replicas should be taken into account. Substituting KN for N into the (2.61) we obtain

$$\overline{\rho^2} \geqslant \frac{K-1}{KN-1}. \tag{2.62}$$

For big enough number of users K this bound can be approximated as

$$\overline{\rho^2} \geqslant \frac{1}{N}, \quad K \gg 1. \tag{2.63}$$

Let us define the maximal *cross-correlation peak* $\rho^c_{\max}$ and maximal (over all nonzero time shifts of all signatures) *autocorrelation peak* $\rho^a_{\max}$ as

$$\rho^c_{\max} = \max_{\substack{k \neq l \\ m}} \left| \frac{R_{p,kl}(m)}{R(0)} \right|, \qquad \rho^a_{\max} = \max_{\substack{k \\ m \neq 0}} \left| \frac{R_{p,kk}(m)}{R(0)} \right| \tag{2.64}$$

and the *correlation peak* as $\rho = \max\{\rho^c_{\max}, \rho^a_{\max}\}$.

Since the maximal value can never be smaller than its average, $\rho^2_{\max} \geqslant \overline{\rho^2}$, using (2.62) and (2.63) we can write

$$\rho^2_{\max} \geqslant \frac{K-1}{KN-1} \approx \frac{1}{N}. \tag{2.65}$$

With additional limitations on the PSK alphabet, the bound above may appear rather loose, especially when the number of sequences approaches N. In particular, for sufficiently large ensembles of binary $\{\pm 1\}$ sequences the Sidelnikov bound holds [106, 111]:

$$\rho^2_{\max} \geqslant \frac{2}{N}, \quad K \geqslant \frac{N}{2}. \tag{2.66}$$

For the general case of binary antipodal signature sets there exist other tight lower bounds on the TSC of for all possible combinations of K and N [25, 61, 69].

Interestingly enough, for random PSK ensembles (that is, the ones where all signature elements are taken at random from a PSK alphabet), TSC converges to the Welch bound both in the mean and in probability with increasing K/N, which allows treating random ensembles as asymptotically optimal or asymptotically Welch-bound ones [32].

In the following chapters it will be shown that in order to increase the system performance it is desirable to have the correlation peak $\rho^2_{\max}$ as small as possible, which is called the *minimax criterion*. The sequences providing this minimal correlation peak are correspondingly called *minimax sequences* [54]. Many minimax polyphase signature ensembles are known, but the binary ones are traditionally considered more attractive from a hardware point of view. Some of them are briefly discussed in the following sections.

2.8.1 Gold Ensembles

The Gold binary ensembles [52] are most popular and applicable due to a great size (number of signatures, i.e. users K) under a fixed length N. To

generate a Gold ensemble two specially arranged m-sequences of equal length $N = 2^n - 1$ are necessary, where memory n is either odd or equal to 2 modulo 4 ($N = 7, 31, 63, 127, 511, 1023, \ldots$). Both of them may be generated by n-cell LFSRs. The constructing procedure [62] results in $K = N + 2$ binary signatures with the correlation peak

$$\rho_{\max} = \begin{cases} \dfrac{\sqrt{2(N+1)}+1}{N} \xrightarrow[N\to\infty]{} \sqrt{\dfrac{2}{N}}, & n \text{ odd}, \\ \dfrac{2\sqrt{(N+1)}+1}{N} \xrightarrow[N\to\infty]{} \dfrac{2}{\sqrt{N}}, & n \equiv 2 \mod 4, \end{cases} \tag{2.67}$$

and according the bound (2.66) shows asymptotic optimality of Gold ensembles of odd memory n among binary ensembles.

The Gold ensembles of length $N = 1023$ ($n = 10$) are used in the space segment of GPS to organize the standard-positioning service (so called C/A or unprotected code) [40, 60]. Another example of Gold ensemble employment can be found in 3G UMTS standard, where it is used for scrambling in both down- and up-links [4, 24, 87].

2.8.2 Kasami Ensembles

Kasami ensembles (sometimes called small Kasami ensembles [70]) exist for lengths $N = 2^n - 1$ where $n = 2m$ is even ($N = 15, 63, 255, 1023, 4095, \ldots$) and contain $K = \sqrt{(N+1)} + 1 = 2^m$ signatures.

Mechanism of forming Kasami sequences resembles the one for Gold ensembles and consists in modulo-2 addition of two m-sequences of different lengths [45, 62]. The correlation peak of this ensemble is

$$\rho_{\max} = \frac{\sqrt{N+1}+1}{N} \xrightarrow[N\to\infty]{} \frac{1}{\sqrt{N}} \tag{2.68}$$

making these binary signature ensembles asymptotically optimal.

The comparison of the Kasami binary ensemble with the Gold one shows a significant gain (6 dB) of Kasami ensembles in the correlation peak versus Gold ensembles of the same length in exchange for much smaller ($(N+2)/\sqrt{N+1} \approx \sqrt{N}$ times) number of sequences K. However, a Kasami ensemble can be extended almost two times without sacrificing the correlation peak [67].

Let us underline again that the described ensembles provide minimal correlation peak only for *even* correlations, while prediction and control of odd correlations in a wide range of delays is quite problematic [99]. An example is shown in Figure 2.10, where maximal values of odd and even CCFs are given in dependence of the delay value m. The results are shown for Kasami ensemble of length 63 and Gold ensemble of length 127. It is

seen that the maximal value of odd CCFs (dotted line) can be up to three times bigger than that of the even CCFs (solid line).

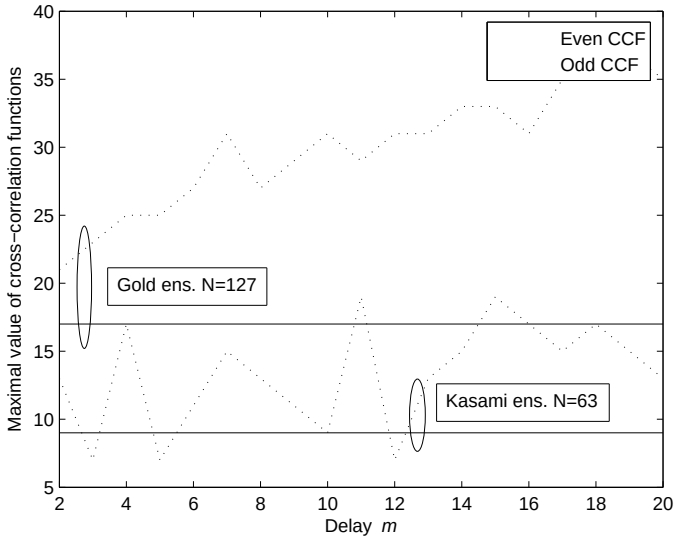

Figure 2.10: Maximal values of odd and even CCFs for different signature ensembles

As will be shown in Section 3.4, big values of CCF will result in high level of average MAI power, which, in turn, will result in system performance degradation in terms of bit error rate. The most part of the rest of the Thesis will be dedicated to controlling maximal odd CCF values and decreasing average MAI power.

Chapter 3

Chip-Interleaved DS CDMA

Having described an asynchronous DS CDMA system and a potential MAI increase due to aperiodic CCF appearance, this Chapter will be dedicated to approaches which allow to mitigate this increase. In this Chapter a well-known idea of chip interleaving [21, 74, 75, 132] will be considered from the point of view of mitigating harmful effect of asynchronism. It will be shown in Section 3.1 that for a chip-interleaved DS CDMA any mutual delay between users will be transformed into the delay of one chip only, and MAI will be only affected by the even or odd periodic CCF of shift one.

Section 3.2 addresses the idea of using a multi-user receiver in an asynchronous channel [65, 79, 81, 94, 109]. The idea of chip-interleaving will be revised and analyzed in application to decorrelating processing. Within this approach the time interval of processing the deinterleaved signal is as short as just one bit duration, and what is more, the proposed technique may provide an energy gain against the referenced "non-interleaved" system with the same signature ensemble and even greater gain under a proper modification of the latter.

In Section 3.3 another modified idea of chip interleaving, chip interleaving with zero padding, is considered in application to oversaturated systems. The latter are by design limited to synchronous channels only, whereas many practical channels are asynchronous. The receiving algorithm of oversaturated systems relies on the fact that user signatures are strictly synchronous, and any asynchronism between them is catastrophic, leading to unacceptable system performance. It will be shown that the proposed approach makes user signals at the receiving end bit-synchronous *independently* of the user delay profile, making thus oversaturated systems applicable in asynchronous transmission conditions as well. Theoretical calculations and computer simulations demonstrate that at high signal-to-noise ratio values the performance of the system is equivalent to the one operating in synchronous channels. In addition to the above, chip interleaving with zero padding can also

improve performance of oversaturated systems in multipath channels [37].

Finally, in Section 3.4 we describe and analyze one more method aimed at neutralizing harmful effects of odd CCFs based on the *cyclic prefix* (CP) redundancy. Typical of OFDM [47], cyclic prefix technique may appear promising in the traditional single carrier DS CDMA applications to instrument simple frequency-domain equalization [11]. Here we draw attention to another potential merit of the cyclic prefix related to the removal of odd correlations of signatures.

3.1 Chip-Interleaving

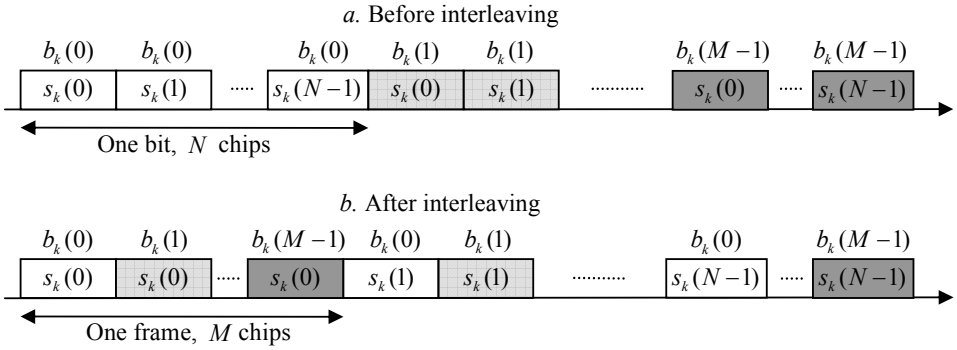

Figure 3.1: Illustration of the interleaving procedure of the k-th user M-block

Let us consider an interleaving procedure that will be used in this Thesis repeatedly. This procedure can be described by writing a user signal into an $M \times N$ matrix row-wise and reading it column-wise, as is performed by conventional block interleavers intended to disperse burst errors in error correction coding [15, 110]. Then the chip pattern of the M-bit data block (further M-block) at the output of the k-th user's interleaver is permuted into a sequence of N M-chip frames: first frame is formed by the first element of the k-th signature $s_k(0)$ repeated M times and modulated by M successive bits of the k-th user $b_k(0), b_k(1), \ldots, b_k(M-1)$, the second is again M-fold repetition of the second signature element $s_k(0)$ modulated by the same M bits, and so forth (see Figure 3.1, chips of consecutive bits differ by shade density). To present this formally, write the M-block of the k-th user before interleaving as

$$\mathrm{v}_k(t) = \sum_{i=0}^{M-1} b_k(i) \sum_{j=0}^{N-1} s_k(j) c_0(t - j\Delta - iN\Delta). \tag{3.1}$$

Then after interleaving this M-block takes the form

$$\mathrm{v}_k(t) = \sum_{i=0}^{M-1} b_k(i) \sum_{j=0}^{N-1} s_k(j) c_0(t - i\Delta - jM\Delta). \tag{3.2}$$

As can be seen, after these rearrangements signature elements modulated by a specific k-th user's bit are spaced from each other by M chip positions. As will be shown later, if the block size M is no smaller than the maximal delay $L = \max\{m_k\}$, the chip-interleaving reduces asynchronism of users at the receiving side from L chips to one chip only. Simultaneously, interleaving brings about delay in bit demodulation, and, being interested in its minimization, it makes sense to put $M = L$ [34].

Let $t = 0, 1, \ldots$ denote discrete time counted in chip intervals and suppose that delay of the first user is zero, $m_1 = 0$. Then the M-block of the first user at the receiving side spans the interval $0 \le t < MN$, while the k-th user M-block, $k = 1, 2, \ldots, K$, spans the interval $m_k \le t < MN + m_k$. Thus, to comprise entirely M-blocks of all users it is enough to run receive processing within the window $0 \le t < MN + L = M(N + 1)$. Let $i = t \mod M$ be the ordinal number of position within one frame of the chip stream released by the interleaver. Then (again since $m_1 = 0$) in order to retrieve the i-th bit of the first user at the receiving end, observed samples at the chip matched filter should be decimated with index M. In other words, the received chips with numbers $t = i, i+M, \ldots, i+(N-1)M$ should be picked out and correlated with the first user signature thereby realizing deinterleaving. In a similar manner for retrieving the k-th user i-th bit, the samples with numbers $t = m_k+i, m_k+i+M, \ldots, m_k+i+(N-1)M$ should be correlated with the k-th signature.

The point of chip-interleaving is in minimizing the depth of intersymbol interference between different users. Consider as an example bit $b_1(i)$ of the first user in a conventional asynchronous DS CDMA. If the k-th user signature is time-shifted by m_k relative to the first user's one, polarity change of the k-th user bit at the moment m_k causes MAI defined by the odd cross-correlation of the first and the k-th signatures, which for arbitrary values of m_k is much less controllable as compared to the even one (see again Figure 2.10 in the previous Chapter).

With chip-interleaving, on the other hand, chips of the same bit of the k-th user are spaced from each other by $M = L$ positions, and therefore with any time shift $m_k \le L$ of the k-th signature, polarity change of the k-th user bit happens only at the position of the initial chip of the first user, not m_k-th one. Therefore, normalized odd and even cross-correlations of the two signatures differ from each other by a quantity within $2/N$ (for PSK signatures) avoiding the troubles of uncontrollable behavior of odd ones for arbitrary time shifts. The same remains true for an arbitrary pair of the

k-th and l-th signatures.

Consider as an example the situation when the l-th user signal is delayed relatively to the k-th one by $m_{kl} = 3$ chips (Figure 3.2). Suppose that we are interested in demodulating the k-th user bit $b_k(0)$, for which we need to pick out from the observation chips

$$\mathbf{u}_k = b_k(0)[s_k(0), s_k(1), \ldots, s_k(N-1)] \tag{3.3}$$

(shown as gray rectangles in the Figure 3.2). But as it is seen from the figure, at time positions of these chips the following chips of the l-th user are located:

$$\mathbf{u}_l = [b_l^{\text{prev}}(M-3)s_l(N-1), b_l(M-3)s_l(0), \ldots, b_l(M-3)s_l(1)], \tag{3.4}$$

where the first chip $s_l(N-1)$ is modulated by the information bit $b_l^{\text{prev}}(M-3)$ from the *previous* M-block, and all the rest chips are modulated by $b_l(M-3)$. Output of the k-th user correlator will thus take the form

$$\begin{aligned} z_k &= (\mathbf{u}_k + \mathbf{u}_l)\mathbf{s}_k^T = b_k(0) + b_l^{\text{prev}}(M-3)R_{a,kl}(1-N) + b_l(M-3)R_{a,kl}(1) \\ &= b_k(0) + \begin{cases} b_l(M-3)R_{p,kl}(1), & b_l^{\text{prev}}(M-3) = b_l(M-3) \\ b_l(M-3)R_{p,kl}^{\text{odd}}(1), & b_l^{\text{prev}}(M-3) \neq b_l(M-3) \end{cases} \end{aligned} \tag{3.5}$$

As it is seen, despite the fact that the mutual delay is $m_{kl} = 3 > 1$, the correlator output of the k-th user is affected by the periodic correlation (even or odd) of the *first* shift only $R_{p,kl}(1)$. For conventional DS CDMA, for example, the same delay would cause appearance of the correlation of shift $m_{kl} = 3$, $R_{p,kl}(3)$, which is less controllable and can increase MAI.

As a second example consider demodulation of the bit $b_k(3)$. Similarly to the previous case, it is necessary to extract from the observation chips of the k-th user

$$\mathbf{u}_k = b_k(3)[s_k(0), s_k(1), \ldots, s_k(N-1)], \tag{3.6}$$

but in this case corresponding chips of the l-th user are

$$\mathbf{u}_l = b_l(0)[s_l(0), s_l(1), \ldots, s_l(N-1)], \tag{3.7}$$

and the output of the k-th user correlator is

$$z_k = (\mathbf{u}_k + \mathbf{u}_l)\mathbf{s}_k^T = b_k(3) + b_l(0)R_{p,kl}(0). \tag{3.8}$$

Equation (3.8) shows that MAI for the k-th user correlator output *does not* contain correlations of non-zero shifts at all. This situation will, certainly, remain the same for all k-th user data bits $b_k(i)$, $m_{kl} \leq i \leq M-1$, whereas for conventional DS CDMA MAI will contain crosscorrelation of shift m_{kl}.

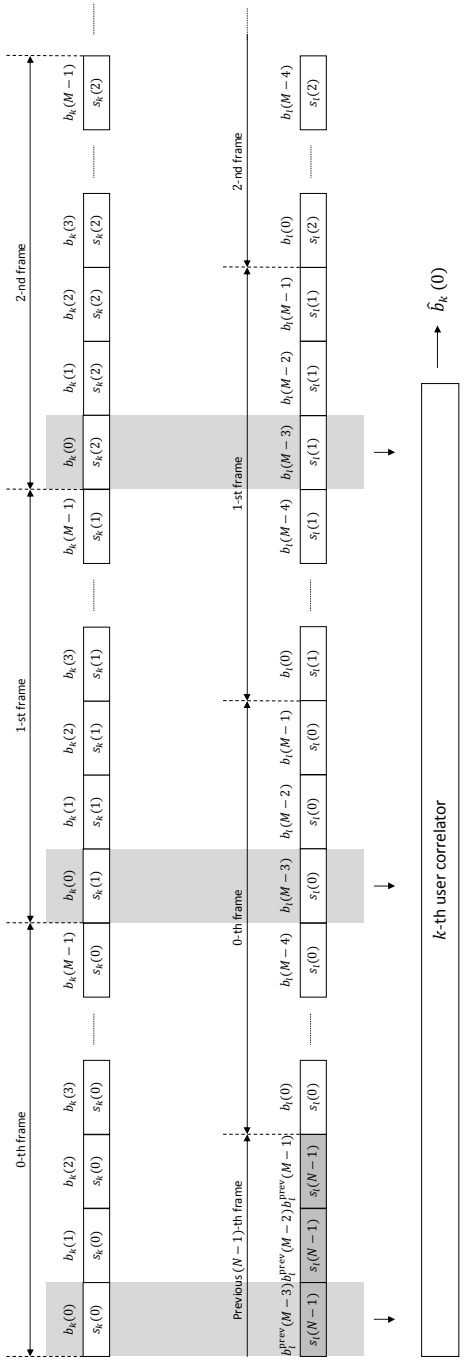

Figure 3.2: Illustration of chip interleaving in asynchronous CDMA (mutual delay is $m_{kl} = 3$ chips); obtaining decision on bit $b_k(0)$

Generalizing (3.5) and (3.8), we can write that for the mutual delay $m_{kl} > 0$ output of the k-th user for the i-th bit, $0 \leq i \leq M-1$ is (for two user case)

$$z_k = b_k(i) + \begin{cases} b_l^{\text{prev}}(M-i)R_{a,kl}(1-N) + b_l(M-i)R_{a,kl}(1), & i < m_{kl} \\ b_l(M-i)R_{p,kl}(0), & i \geq m_{kl} \end{cases} \tag{3.9}$$

3.2 Chip-Interleaved Decorrelation in Asynchronous DS CDMA

As equation (3.9) shows, for the case of chip-interleaving any mutual delay between users will be transformed into the delay of one chip only, and MAI will be affected by the even or odd periodic CCF of shift one. However, it is possible to change the system design so that MAI will contain even CCF only, making MAI level even more controllable.

3.2.1 Synchronous Decorrelator

Let us reproduce for convenience some definitions introduced earlier, still considering a DS CDMA system with BPSK data modulation and K user signatures of length N. Assume first that there are no mutual delays between user signals, i.e. the system is synchronous. Then the group signal of all users can be expressed as $\mathbf{SAb}$, where, as before, $\mathbf{A}$ is diagonal matrix of user amplitudes, $\mathbf{S}$ is a signature matrix and $\mathbf{b}$ is a bit vector. The vector $\mathbf{z}$ of output samples of a bank of K correlators with signature references is then found as

$$\mathbf{z} = \mathbf{CAb} + \mathbf{n} \tag{3.10}$$

where $\mathbf{C}$ is signature correlation matrix and $\mathbf{n}$ is noise vector with correlation matrix $\sigma^2\mathbf{C}$, σ^2 being noise power at the correlator output.

Whenever the signatures are correlated, the k-th component of $\mathbf{z}$ is dependent not only on the k-th user bit b_k but also on bits of other users, which means presence of MAI. A complete removal of MAI is possible if signatures are linearly independent, i.e. $\mathbf{C}$ is nonsingular. Clearly, the necessary condition of nonsingularity of $\mathbf{C}$ (ultimate MAI removal), is the system non-oversaturation, meaning that number of users is no greater than the signature length: $K \leq N$. With linearly independent signatures $\mathbf{C}$ is invertible, and *decorrelation* algorithm, described in Section 2.5.1, is applicable, meaning multiplication of $\mathbf{z}$ by $\mathbf{C}^{-1}$, diagonalizing thereby a matrix factor of the first term in (3.10). The decorrelating detector outputs estimation of transmitted bits as

$$\hat{b}_k = \operatorname{sgn}\left((\mathbf{C}^{-1}\mathbf{z})_k\right), \quad k = 1, 2, \ldots, K, \tag{3.11}$$

where $(\mathbf{C}^{-1}\mathbf{z})_k$ is the k-th element of the vector $\mathbf{C}^{-1}\mathbf{z}$.

For any non-orthogonal signature set decorrelation is accompanied by SNR loss and the latter for the k-th user detector, γ_k, is found as [79, 125]

$$\gamma_k = \frac{q_k^2}{q_{d,k}^2} = \mathbf{C}_{kk}^{-1}, \quad k = 1, 2, \ldots, K, \tag{3.12}$$

where $q_k^2 = A_k^2/\sigma^2$ and $q_{d,k}^2$ are power SNRs at the outputs of the k-th user correlator and decorrelating detector respectively, while $\mathbf{C}_{k,k}^{-1}$ is the k-th diagonal element of $\mathbf{C}^{-1}$.

3.2.2 Asynchronous Decorrelator

Let us now turn to an asynchronous system described in Section 2.6. Let us consider a packet transmission of a block of M consecutive bits and redefine the bit number i, $0 \le i \le M-1$ of k-th user k, $1 \le k \le K$ in the block as a bit of dummy *pseudouser* whose number is $k_i = iK + k$, $1 \le k_i \le KM$. Then there are KM pseudousers altogether, k_i-th one utilizing individual signature of length $N_a = NM + L$ with only N nonzero elements, which reproduce one period of original k-th signature. In more details the k_i-th signature vector thus introduced contains $m_k + iN$ zeros, followed by $\mathbf{s}_k$ and $(M-1-i)N + L - m_k$ more zeros. Now the system can be treated as synchronous and a decorrelating detector can be implemented in the ordinary way. As it was done before, denote $K \times K$ signal cross-correlation matrices $\mathbf{C}(n) = [R_{kl}(n)]$,

$$R_{kl}(n) = \sum_{j=-\infty}^{\infty} s_k(j - m_k) s_l(j + nN - m_l) \tag{3.13}$$

where n is integer and by agreement $s_k(j) = 0$ for $j < 0$ and $j > N-1$. Recalling that users are numbered so that $0 = m_1 \le m_2 \le \ldots \le m_K \le L$, $\mathbf{C}(1)$ is an upper triangular matrix, $\mathbf{C}(-1)$ is a lower triangular matrix, $\mathbf{C}(1) = \mathbf{C}^T(-1)$, and $\mathbf{C}(n) = 0$, $|n| > 1$. Then correlation matrix $\mathbf{C}_a$ of all pseudousers' signatures has size $KM \times KM$ and looks as

$$\mathbf{C}_a = \begin{pmatrix} \mathbf{C}(0) & \mathbf{C}(-1) & 0 & \cdots & 0 \\ \mathbf{C}(1) & \mathbf{C}(0) & \mathbf{C}(-1) & & \vdots \\ 0 & \mathbf{C}(1) & \mathbf{C}(0) & \ddots & 0 \\ \vdots & & \ddots & \ddots & \mathbf{C}(-1) \\ 0 & \cdots & 0 & \mathbf{C}(1) & \mathbf{C}(0) \end{pmatrix} \tag{3.14}$$

Vector of the K-correlator bank output is then

$$\mathbf{z} = \mathbf{C}_a \mathbf{A}_a \mathbf{b}_a + \mathbf{n} \tag{3.15}$$

where $\mathbf{b}_a = [b_1(1), \ldots, b_K(1), \ldots, b_1(M), \ldots, b_K(M)]^T$, $b_k(i)$ being the i-th information bit of the k-th user, $\mathbf{A}_a = \mathrm{diag}(\mathbf{A}, \mathbf{A}, \ldots, \mathbf{A})$ is $KM \times KM$ matrix and $\mathbf{n}$ is Gaussian noise vector with correlation matrix $E[\mathbf{n}\mathbf{n}^T] = \sigma^2 \mathbf{C}_a$. Then a decorrelating detector can be implemented analogously to (3.11), so that the estimation of the i-th bit of the k-th user is

$$\hat{b}_k(i) = \mathrm{sgn}\left((\mathbf{C}_a^{-1}\mathbf{z})_{k_i}\right). \tag{3.16}$$

Suppose now that the transmission is continuous rather than packet. Then truncated last bits of the previous block and first bits of the next block fall within the current block observation window of length $KM + L$ causing the *edge effect*, i.e. non-suppressed residual MAI, whose damaging effect decreases as block size M grows [65]. This additional MAI can be dealt with in several ways. Firstly, the truncated edge bits can be also treated as transmitted ones by additional $2K - 2$ pseudousers, if taken into account in a modified matrix $\mathbf{C}_a$, preserving thereby entire decorrelation [81]. This, however, results in higher error probability for the edge bits in comparison with the inner ones. Alternatively, edge bits can be estimated and their contribution subtracted from the observation [109] before processing the bits in the block. In what follows we describe and analyze a novel efficient asynchronous decorrelation technique based on chip interleaving.

3.2.3 Chip-Interleaved Decorrelator

Developing further the approach described in Section 3.1 we can entirely exclude even the minor effects of bit polarity changes by limiting receiver processing interval to the window $M \le t < NM$, which spans only $N - 1$ frames. Indeed, current received interleaved M-block of the k-th user starts and finishes at the moments m_k and $m_k + MN - 1$, respectively, implying that the last chip belonging to the previous M-block occupies time position $t' = m_k - 1$, while the position of initial chip of the next M-block is $t'' = m_k + MN$. Since $0 \le m_k \le L = M$, these moments fall beyond the processing window $M \le t < NM$, meaning that no interblock interference is present, or, in other words, no edge effect will accompany decorrelation processing. It follows then that whenever decorrelation is realizable in such a system, MAI is suppressed entirely and near-far resistance is ultimate. The penalty for this is energy loss due to omitting front ($0 \le t < M$) and end ($NM \le t < N(M + 1)$) segments of the stream of chip matched filter samples in the course of processing. As is shown below this energy loss versus non-interleaved system in all practical scenarios cannot be significant, since actually just one signature chip is dropped out per one user bit. A complete MAI elimination with no edge effects obtained in return may overpower this SNR loss leading to improvement of resultant performance against noise plus MAI background.

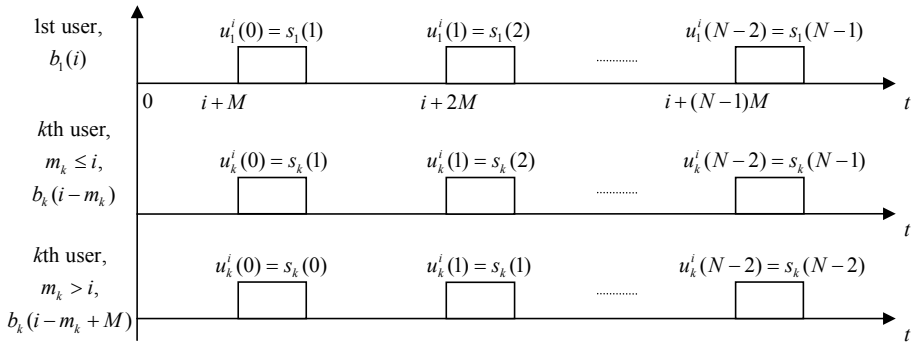

Figure 3.3: Illustration of the signature modification procedure

To clarify details of the chip-interleaving decorrelation consider sequence of chip matched filter samples at the moments

$$t = i + M, i + 2M, \ldots, i + (N-1)M, \tag{3.17}$$

where i as before belongs to the range $0, 1, \ldots, M-1$. Obviously, these samples contain all but initial chips of first user signature modulated by the i-th first user bit $b_1(i)$. Thus, as for the first user, the signature matrix $\mathbf{U}_i = [\mathbf{u}_1^i, \mathbf{u}_2^i, \ldots, \mathbf{u}_K^i]$ involved in the decorrelation processing of the sample stream above should contain the first column $\mathbf{u}_1^i = [s_1(1), s_1(2), \ldots, s_1(N-1)]^T$.

Turn now to an arbitrary (k-th, $1 \le k \le K$) user. It is easy to see that the sample stream specified by (3.17) is entered by chips of the k-th signature modulated by a bit whose number i_k obeys the congruence

$$i_k + m_k \equiv i \mod M.$$

Therefore, for a user number k the bit to be retrieved from samples (3.17) has the number depending on relation between i and the user's delay m_k:

$$i_k = \begin{cases} i - m_k, & m_k \leqslant i, \\ i - m_k + M, & m_k > i, \end{cases} \tag{3.18}$$

Simultaneously, sequence of $N-1$ chips of the k-th user's signature falling within the processing window $[M, MN-1]$ starts with either $s_k(1)$ if $m_k \le i$, or $s_k(0)$ if $m_k > i$, so that the k-th column of $\mathbf{U}_i$ is defined by

$$\mathbf{u}_k^i = \begin{cases} [s_k(1), s_k(2), \ldots, s_k(N-1)]^T, & m_k \leqslant i, \\ [s_k(0), s_k(1), \ldots, s_k(N-2)]^T, & m_k > i, \end{cases} \tag{3.19}$$

$k = 1, 2, \ldots, K$, $i = 0, 1, \ldots, M-1$. Figure 3.3 illustrates signature modification according to (3.19); $u_k^i(j)$, $0 \le j < N-2$ symbolizing the j-th element of the k-th modified signature $\mathbf{u}_k^i$.

Now let $\mathbf{z}_i$ be the vector which is output by a K-correlator bank using as references the modified signatures $\mathbf{u}_k^i$ and $\mathbf{C}_i = [N/(N-1)]\mathbf{U}_i^*\mathbf{U}_i$ be the crosscorrelation matrix of the latters. Then

$$\mathbf{z}_i = \mathbf{C}_i\mathbf{A}\mathbf{b}_i + \mathbf{n}, \tag{3.20}$$

where the vector of users' bits $\mathbf{b}_i$ corresponding to the sample stream defined by (3.17)

$$\mathbf{b}_i = [b_1(i_1), b_2(i_2), \ldots, b_K(i_K)]^T,$$

i_k given by (3.18).

The necessary condition of invertibility of $\mathbf{C}_i$ ($K \leq N-1$) is only slightly more demanding than in the case of synchronous CDMA. It is well expected that with a proper choice of initial signatures $\mathbf{s}_k$ their modified versions (3.19) will remain linearly independent. Therefore, the decorrelating detector (3.11) may be implemented producing estimate of the i_k-th bit of k-th user as

$$\hat{b}_k(i_k) = \operatorname{sgn}\left((\mathbf{C}_i^{-1}\mathbf{z}_i)_k\right), \quad k = 1, 2, \ldots, K.$$

The effect of curtailing signatures discussed above reduces SNR additionally $N/(N-1)$ times, so that the summary decorrelation loss (3.12) becomes

$$\gamma_{k,i} = \frac{N}{N-1}(\mathbf{C}_i^{-1})_{kk} \tag{3.21}$$

$i = 0, 1, \ldots, M-1$.

3.2.4 System Comparison and Numerical Results

Due to the complete removal of MAI, probability of error for the k-th user can be expressed as

$$P_k = Q\left(q_{d,k}\right), \tag{3.22}$$

where $q_{d,k} = q_k/\sqrt{\mathbf{C}_{kk}^{-1}}$ for the conventional asynchronous decorrelator of Section 3.2.2 and $q_{d,k} = q_k\sqrt{N-1}/\sqrt{N\mathbf{C}_{k,k}^{-1}}$ for the chip-interleaved one, and $Q(\cdot)$ is the complementary error function:

$$Q(x) = \frac{1}{\sqrt{2\pi}}\int_x^\infty \exp\left(-\frac{t}{2}\right)dt. \tag{3.23}$$

In the conventional decorrelator correlation matrix $\mathbf{C}_a$ contains aperiodic cross-correlations between user signatures with shifts up to L, whose values are hard to control. On the other hand, after the chip-interleaving all cross-correlations entering $\mathbf{C}_i$ correspond to only zero or one chip shifts between signatures, i.e. may be much more easily retained within the predictably

narrow range. After discarding first or last chip of signatures (see (3.19)), cross-correlation magnitude changes by the value no greater than $1/N$ (for PSK signature ensembles), which has the lower effect the bigger spreading factor N. Therefore, there are convincing reasons to expect better performance of the interleaved decorrelator relative to the conventional one.

Let us now comment on the prospects of increasing an interleaver block size versus maximal delay: $M > L$. Then, as it follows from (3.19), for any position i in the range $L \leq i \leq M-1$ all cross-correlations entering $\mathbf{C}_i$ will be of mutual zero shift. It is of no difficulty to have these cross-correlations minimal, decreasing thereby error probability for corresponding bits. Furthermore, for all such i $\mathbf{C}_i$ remains the same; thus computational complexity per one data bit depending on number of inverted matrices decreases as block size grows. Simultaneously, since at the positions $L \leq i \leq M-1$ interblock interference is not present (position of the last chip of the previous M-block is $t' = m_k - 1 < L < M$), in this case it makes sense to start the processing window at $t = L$ instead of $t = M$, escaping discard of the initial signature chips along with accompanying energy loss for the positions in question.

To compare numerically the decorrelators above, the example was investigated of asynchronous CDMA with spreading factor $N = 31$, $K = 15$ active users, equal user powers and maximal delay $L = 14$. As a reference the ensemble of Gold sequences employed as users' signatures, which is a typical choice in actual practice [62,112] was tested in combination with the conventional decorrelator of Section 3.2.2.

As the first alternative the chip-interleaved decorrelator with block size $M = L = 14$, employing the same ensemble of user signatures was analyzed. In order to uncover the benefits of a chip-interleaving decorrelator even more convincingly, the second option was also checked: the chip-interleaved decorrelator for the system where signature ensemble is formed of even cyclic shifts of a fixed m-sequence of length $N = 31$. This ensemble provides $\lfloor N/2 \rfloor$ signatures, which is enough for the assumed number of users and secures minimal value of signature cross-correlation magnitudes ($1/N$) at zero and one chip shifts possible for binary sequences.

The computer simulation was performed in MATLAB environment to estimate the system performance. Number of iterations was 10^5. For each iteration users were randomly assigned delays from $[0, L]$ interval, their M-block formed, summed and transmitted through a noisy channel with a fixed SNR value. Then a bit error probability (BER) was calculated and averaged over users and M transmitted bits. The procedure was repeated for every fixed value of SNR.

The dependencies of BER on SNR for all three versions of decorrelator described above are shown in Figure 3.4. As is seen, interleaving decorrelation technique exploiting the same initial Gold ensemble provides SNR gain of about 1 dB versus conventional asynchronous decorrelator. This gain be-

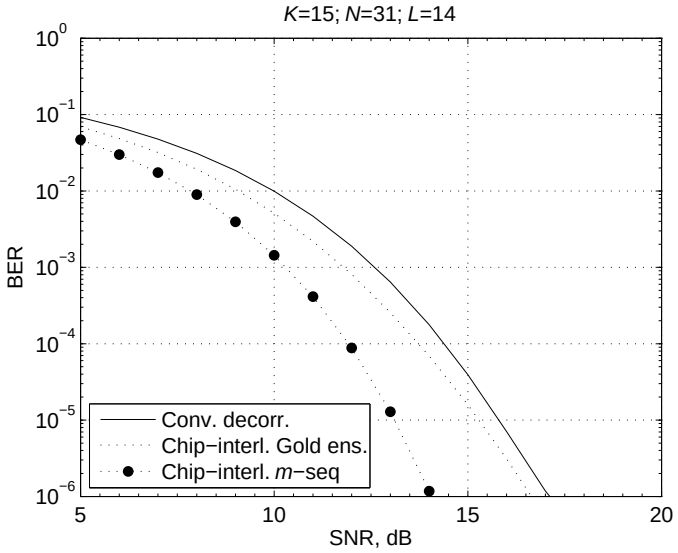

Figure 3.4: Average BER dependence on SNR.

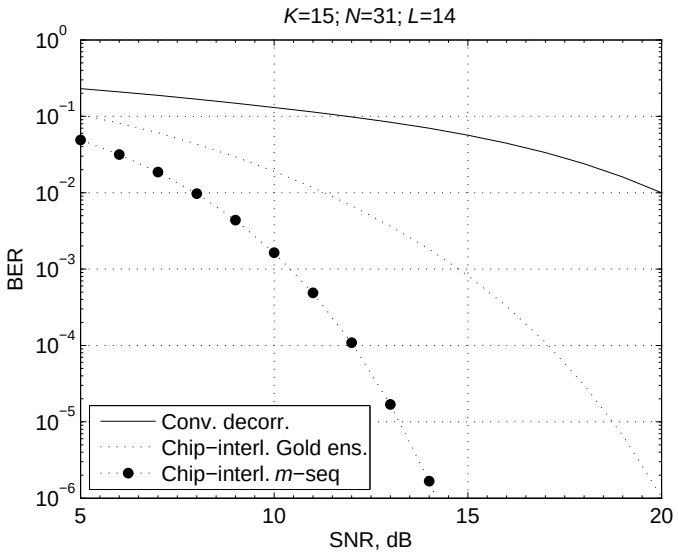

Figure 3.5: Maximal BER dependence on SNR.

comes much higher (up to 3 dB), when the signature ensemble is adjusted to entirely utilize merits of interleaving (shifts of the same m-sequence in the simulated scenario).

Another instructive comparison is presented by Figure 3.5 showing dependencies of maximal BER corresponding to the least favorable users' delay profile on SNR. In this case during the computer simulation a search was per-

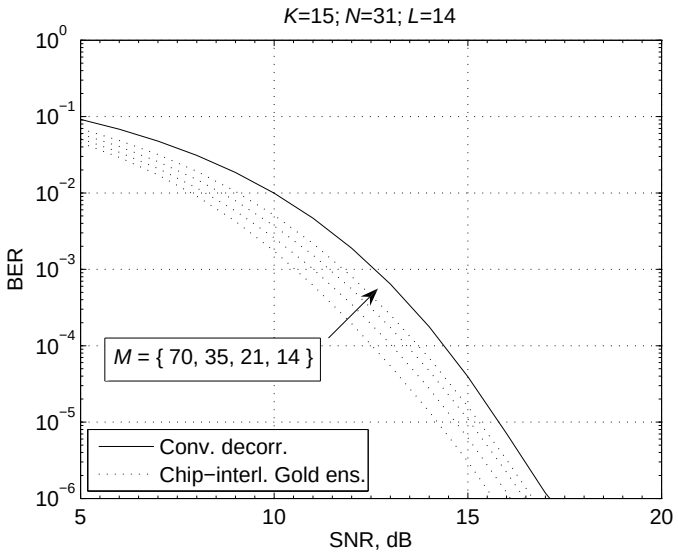

Figure 3.6: Average BER dependance for different M-block size

formed over all iterations in order to find a user delay profile which results in the biggest BER. As is seen, in applications where the worst situation BER is equally (or more) important with an average one the gains of interleaving decorrelation become all the more impressive. At the BER level 10^{-2}, for example, chip-interleaving with Gold ensemble provides about 9 dB gain, and for m-sequence this gain becomes 12 dB.

The above predicted effect of M-block size on interleaving decorrelator performance is supported by Figure 3.6, where curves of average BER are given for the same Gold signatures and $M = 14$, 21, 35 and 70. It may be noted that when M grows from 14 to 70 additional SNR gain up to 1 dB is attainable.

3.3 Chip Interleaving in Oversaturated Systems

Let us recall that in synchronous DS CDMA, where all signatures are strictly time synchronized at the receiver input, the best choice for signatures is an orthogonal set, provided that the number of users K does not exceed the signal space dimension N. As was discussed previously, in such a scenario orthogonal signatures secure total removal of MAI with a single-user (matched-filter) receiver guaranteeing optimal performance in the additive white Gaussian noise channel regardless of the presence of any foreign users' signals.

When the number of users is larger than the signal space dimension the system becomes oversaturated (overloaded). In these circumstances a

method called group orthogonal CDMA (GO-CDMA) [27,91] can be implemented, allowing to increase the number of users K when compared to a conventional orthogonal system, which has the space dimension N as a limit for K. This system yields remarkably good results utilizing at the same time quite simple receiver structure, providing flexible trade-off between receiver complexity and error performance.

Unfortunately, GO-CDMA system is by design limited to synchronous channels only, whereas many practical channels are asynchronous. The receiving algorithm of GO-CDMA relies on the fact that the user signatures are group orthogonal, which can be maintained only when all user signals are synchronous. Any asynchronism between them is catastrophic, leading to unacceptable system performance.

In this Section we consider usage of a modified idea of chip interleaving, chip interleaving with zero padding, in oversaturated systems. It is shown that this approach makes user signals at the receiving end bit-synchronous *independently* of the user delay profile, making thus chip-interleaved GO-CDMA applicable in asynchronous transmission conditions as well. Theoretical calculations and computer simulations demonstrate that at high SNR values the performance of the system is equivalent to the one operating in synchronous channels [36]. More than that, at low SNR values asynchronous GO-CDMA provides $1 \ldots 2$ dB advantage in terms of bit error rate. This result is obtained at the cost of rate reduction, which, however, can be made as small as necessary.

3.3.1 Group Orthogonal CDMA

In Section 2.3 it was shown that for a multiuser system output of a single-user matched filter besides useful information and a noise component contains also MAI, i.e. interference from other users' signals (2.35). This component directly affects the system performance (see Section 3.4.3), and in order to enhance it, it is crucial to keep MAI as small as possible, ideally equal to zero.

As equation (2.35) indicates, a necessary condition to ensure zero MAI is zero cross-correlation of any distinct pair of signatures:

$$R_{kl}(0) = 0, \quad 1 \leqslant k, l \leqslant K, \quad l \neq k. \tag{3.24}$$

Two distinct user signatures for which synchronous CCF is zero, $R_{kl}(0) = 0$, are called *orthogonal*, and an ensemble of user signatures for which any distinct pair of signatures is orthogonal (in other words, (3.24) is true) is called an orthogonal signature ensemble. Certainly, orthogonal ensembles are the best possible in total MAI criterion for a single-user receiver. However, the size of an orthogonal ensemble is strictly limited by its dimension, $K \leqslant N$.

Orthogonal signature ensembles are widely used in telecommunication standards, for example, for user separation in the cdmaOne downlink channel [127], for user separation and separation of different user channels in WCDMA [128] and in many others. On the other hand, in modern telecommunication standards there is a strong trend to increase system capacity as much as possible. Since number of orthogonal signatures is strictly limited by a signal space dimension (spreading factor) N, which is in turn limited by the system bandwidth for the given transmission rate, a natural question arises whether it is possible to construct signature ensemble of bigger size, having at the same time small value of MAI. Ensembles for which number of signatures is greater than the spreading factor $K > N$ are called *oversaturated*, and ratio of number of users to the spreading factor $e_{ov} = K/N > 1$ is called *oversaturation efficiency*.

For a single-user receiver the optimal oversaturated signature ensembles are the ones satisfying the Welch bound (2.61), provided that they are received with equal energies. Signature ensembles satisfying (2.61) are correspondingly called *Welch-bound ensembles*. General methods to produce such ensembles are given for example in [102, 123, 131]. Binary saturated or non-saturated WBE ensembles may exist for only N divisible by four; in this case $K = N$ signatures are just K rows of an $N \times N$ Hadamard matrix, if the latter exists [61, 69].

At the same time even for the Welch-bound ensembles performance of a single-user receiver degrades quite rapidly as the number of user increases. The only possible solution in this case is to use a *multi-user receiver*, which, on the contrary to a single-user receiver, takes into account signatures of other (foreign) users rather than treating them as just additional background noise. Unfortunately, the complexity of such a receivers increases exponentially with the number of users [125], making them hardly possible practically.

There exists quite an elegant solution called group orthogonal CDMA [27, 90, 91], offering a trade-off between receiver complexity and performance. Since for $K > N$ orthogonal signature ensemble does not exist, let us divide all signatures into groups and provide orthogonality between different groups only rather than between every pair of signatures. Consider an oversaturated system with the spreading factor N and the number of users $K > N$, and let us divide N-dimensional signal space into N/D orthogonal subspaces (groups) of dimension D. Then suppose that each of such subspaces accommodates $D + 1$ signatures, so that the oversaturation efficiency becomes $e_{ov} = K/N = 1 + 1/D$. Signature ensembles according to this approach were designed in [91] for oversaturation efficiencies 1.50, 1.33 and 1.25 as linear combinations of orthogonal signatures $\mathbf{h}_j$, $1 \leqslant j \leqslant N$, which can be for example rows of an Hadamard matrix $\mathbf{H}$ of size N. The signature ensemble design criterion was to maximize minimum distance between all possible

group signals in order to minimize the error probability in the maximum likelihood receiver.

Signature ensemble matrices $\mathbf{S}_i$ of size $N \times (D+1)$, containing $D+1$ user signatures as columns are constructed as follows, where subscript i indicates number of subspace, $i = 1, 2, \ldots, N/D$:

$$\mathbf{S}_i = \left(\mathbf{h}_{D_i-D+1}^T \;\; \mathbf{h}_{D_i-D+2}^T \;\; \ldots \;\; \mathbf{h}_{D_i}^T\right) \mathbf{S}_{ov}, \tag{3.25}$$

where $D \times (D+1)$ matrices $\mathbf{S}_{ov}$ for the cases $D = 2$, 3 and 4 are given by (3.26), (3.27) and (3.28), respectively [91]:

$$\mathbf{S}_{ov}^T = \frac{1}{\sqrt{2(1+\alpha^2)}} \begin{pmatrix} \sqrt{2} & \alpha\sqrt{2} \\ \alpha\sqrt{2} & \sqrt{2} \\ \sqrt{1+\alpha^2} & \sqrt{1+\alpha^2} \end{pmatrix}, \tag{3.26}$$
$$\text{where } \alpha = \frac{4 - \sqrt{10+2\sqrt{5}}}{\sqrt{5}-1};$$

$$\mathbf{S}_{ov}^T = \frac{1}{\sqrt{3(1+2\beta^2)}} \times$$
$$\begin{pmatrix} \sqrt{3} & \beta\sqrt{3} & \beta\sqrt{3} \\ \beta\sqrt{3} & \sqrt{3} & \beta\sqrt{3} \\ \beta\sqrt{3} & \beta\sqrt{3} & \sqrt{3} \\ \sqrt{1+2\beta^2} & \sqrt{1+2\beta^2} & \sqrt{1+2\beta^2} \end{pmatrix}, \tag{3.27}$$
$$\text{where } \beta = \frac{-12 + (1+\sqrt{7})\sqrt{14-\sqrt{7}}}{16 - 2\sqrt{7}};$$

$$\mathbf{S}_{ov}^T = \begin{pmatrix} 1 & 0 & 0 & 0 \\ 0 & 1 & 0 & 0 \\ 0 & 0 & 1 & 0 \\ 0 & 0 & 0 & 1 \\ 0.5 & 0.5 & 0.5 & 0.5 \end{pmatrix}. \tag{3.28}$$

The profit of using group orthogonal signaling scheme is that the complexity of the receivers is reduced from the exponential complexity of optimal multiuser detection to linear complexity in the number of users. The multiuser detector in this case is decomposed into N/D parallel independent multiuser subdetectors, each one being quite simple due to subspace orthogonality and low subspace dimension D.

Let us now briefly consider receiver structure for GO-CDMA (Figure 3.7). Using $(D+1) \times 1$ vector $\mathbf{b}_i$ to denote transmitted information bits in the

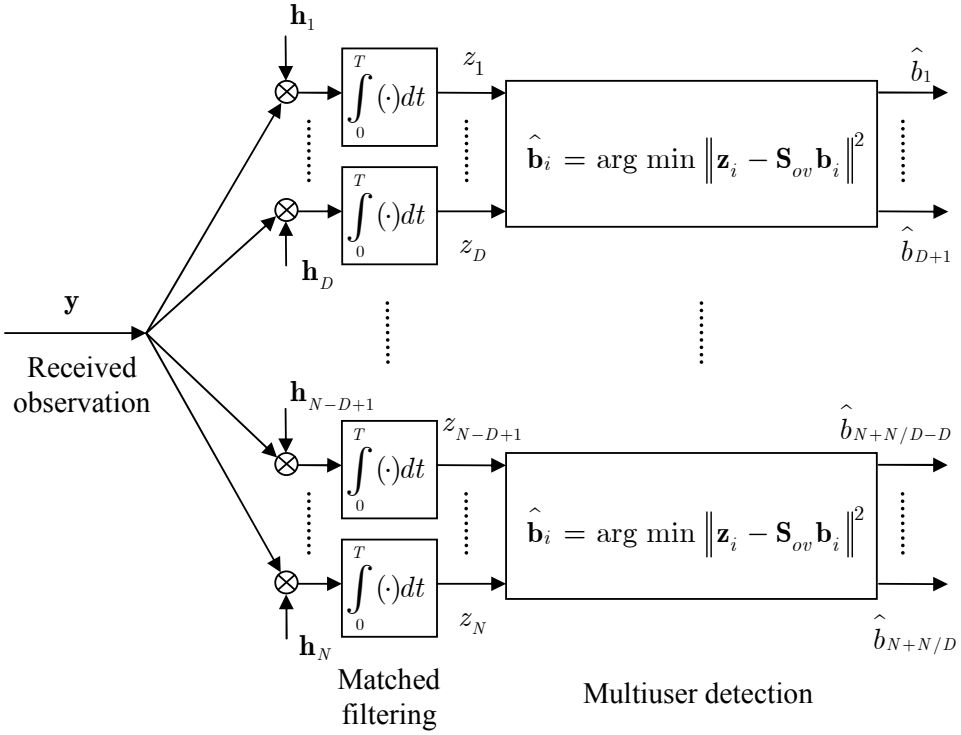

Figure 3.7: Receiver structure for GO-CDMA

i-th group, the received observation $N \times 1$ vector $\mathbf{y}$ for the *synchronous* GO-CDMA system can be expressed as

$$\mathbf{y} = \sum_{i=1}^{N/D} \mathbf{S}_i \mathbf{b}_i + \mathbf{n}, \tag{3.29}$$

where $\mathbf{n}$ is the noise vector. As it was done before, subindex i in all vector-matrix entities is used to stress that they are defined for an isolated i-th subspace, as though only its users are present, $i = 1, 2, \ldots, N/D$.

At the receiving side the obtained observation $\mathbf{y}$ is processed by the bank of matched filters, tuned to the orthogonal signatures $\mathbf{H} = \{\mathbf{h}_j\}$, $1 \leqslant j \leqslant N$: $\mathbf{z} = \mathbf{H}\mathbf{y}$. Finally, the output $N \times 1$ vector $\mathbf{z}$ is divided into N/D groups and in every group i the optimal multiuser receiver [125] is implemented, producing decisions on the transmitted bits $\hat{\mathbf{b}}_i$ [91]:

$$\hat{\mathbf{b}}_i = \arg \min_{\mathbf{b}_i \in \{-1,1\}^{D+1}} \|\mathbf{z}_i - \mathbf{S}_{ov}\mathbf{b}_i\|^2. \tag{3.30}$$

Let us underline again that the described system (and all other oversaturated systems in general) is designed to operate in synchronous channels

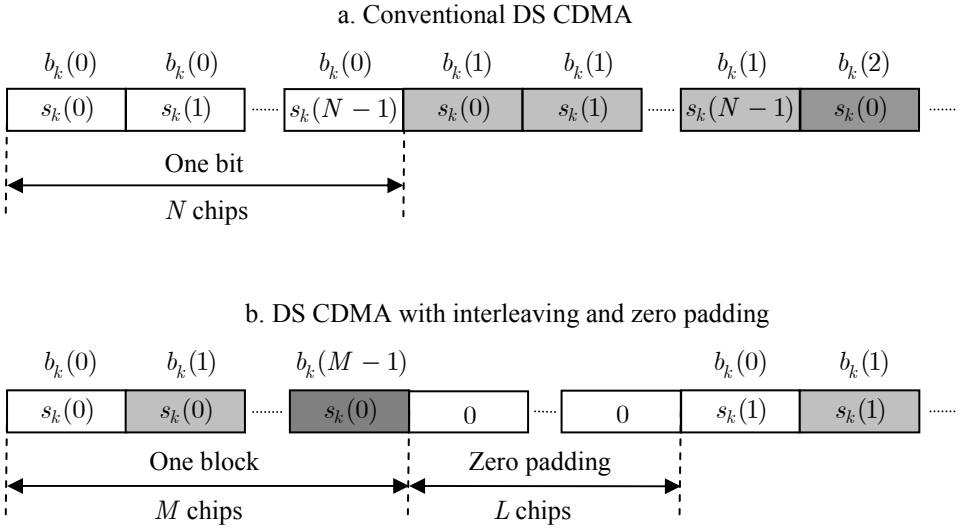

Figure 3.8: Interleaving and zero padding illustration

only. The orthogonality is destroyed even with a smallest time shift between user signatures, making the system completely unusable. However, using a slightly modified idea of chip-interleaving described in the next section it becomes possible to use GO-CDMA systems in channels with arbitrary asynchronism and in multipath channels.

3.3.2 Chip Interleaving with Zero Padding

Let us implement at the transmitting end the chip interleaving with zero padding [132], which can be described as follows. Suppose that the transmitted bitstream of the k-th user, $1 \leqslant k \leqslant K$ is split into blocks of M bits exactly as it was done in Section 3.1. Then a modified procedure of chip-interleaving is applied, by writing a user signal into $M \times N$ matrix row-wise and reading it column-wise, and appending L zeros after reading each column. Here L, as before, is the maximal delay, $L = \max\{m_k\}$, $1 \leq k \leq K$.

After such a procedure the resultant chip pattern for the k-th user will consist of the first chip of the user signature $s_k(0)$ modulated by M consecutive information bits $b_k(0), b_k(1), \ldots, b_k(M-1)$, followed by L zeros, then second chip of the user signature $s_k(1)$ again modulated by the same information bits and followed by L zeros and up to the N-th chip of the user signature $s_k(N-1)$ modulated by the same information bits and followed by L zeros (Figure 3.8, chips of different bits are marked with different density).

The receiving processing is organized as follows. For every user k, $1 \leq k \leq K$ samples of every bit i, $0 \leq i \leq M-1$ (distanced from each other now by $M+L$ chips) are picked out from $\mathbf{y}$ and fed to the matched filter.

Finally, outputs of the matched filters of all users are processed according to (3.30).

3.3.3 GO-CDMA in Asynchronous Channels

The described procedure of interleaving with zero padding guarantees that at the receiving end user signatures for every bit will remain bit-synchronous *independently* of the user delay profile $\{m_k\}$. All the reasoning behind obtaining (3.9) remains in force, but now, due to the zero insertion, within any bit interval all user signatures will be strictly synchronous, whereas for conventional chip interleaving some user signatures could be cyclicly shifted by one chip (which caused appearance of correlations of the shift one).

In other words, interleaving along with zero padding transforms delay m_k chips to Nm_k chips, since after the deinterleaving signal of the k-th user will consist of Nm_k zeros, M consecutive information bits and followed by $N(L - m_k)$ zeros. Bit processing window is now expanded to $0 \leq i \leq M + L - 1$; for every user k i-th bit interval will either contain user's bit $b_k(i - m_k)$ if $m_k \leq i \leq M + m_k - 1$ or vector of N zeros, otherwise, so that the observation for the i-th bit interval takes the form

$$\mathbf{y}_i = \sum_{k=1}^{K} \boldsymbol{\mu}_{i,k} + \mathbf{n}, \tag{3.31}$$

where

$$\boldsymbol{\mu}_{i,k} = \begin{cases} b_k(i - m_k)\mathbf{s}_k, & m_k \leq i \leq M + m_k - 1, \\ \mathbf{0}_{N\times 1}, & \text{otherwise}, \end{cases} \tag{3.32}$$

where $\mathbf{0}_{N\times P}$ is the zero matrix of size $N \times P$.

An illustration of an asynchronous system employing interleaving with zero padding is shown in Figure 3.9, where the maximal delay (and correspondingly the size of the zero padding) is $L = 2$, and delay of the k-th user is also $m_k = 2$.

In the figure a time interval of the zeroth bit is shown ($i = 0$). It is seen that during this bit interval the signal of the k-th user consists of only zeros from zero padding zones, thereby not causing any interference at all. This is in full accordance with (3.32), since for the bit numbers $i = 0, 1$ the condition in the second line is satisfied.

On the other hand, for the bit number $i = 2(= m_k = 2)$ the first condition in (3.32) becomes true, and the signal of the k-th user that falls within the time interval of the bit number two will be $b_k(i - m_k)\mathbf{s}_k = b_k(0)\mathbf{s}_k$.

Since all user signatures are now bit-synchronous, it is possible to implement receiving algorithm for conventional *synchronous* oversaturated CDMA (3.30) despite the asynchronous nature of the system. Note, however, that this algorithm strictly requires that number of users should be equal to the

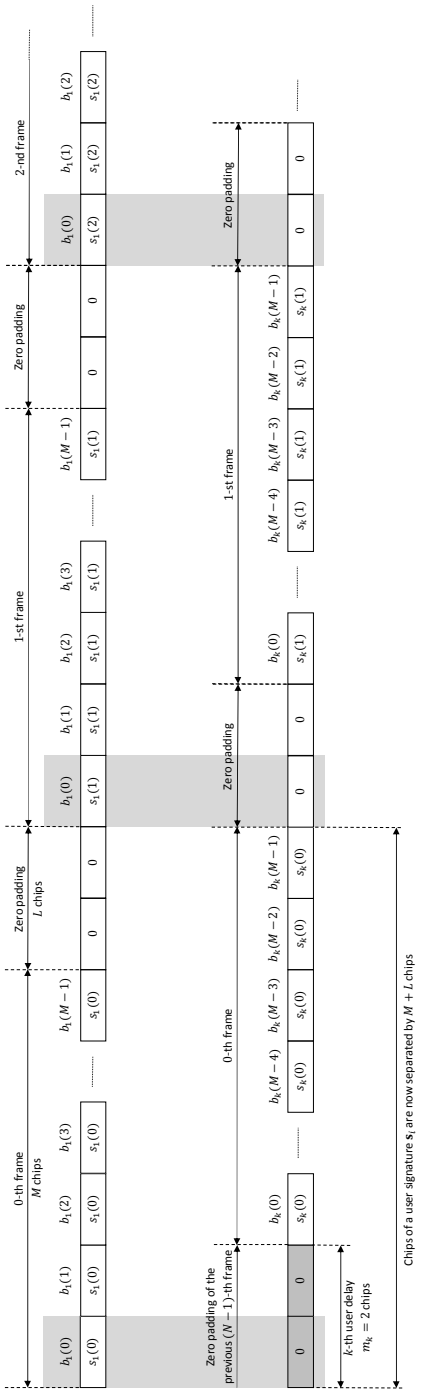

Figure 3.9: Illustration of chip interleaving with zero padding in asynchronous CDMA ($L = 2$); time interval for the zeroth bit ($i = 0$) is shown

number, specified by the signature ensemble design in order to maintain group orthogonality. To fulfill this requirement, at the receiving end we introduce pseudo-users, whose signatures are added to the observation in order to keep the total user number constant. In other words, if according to (3.32) some user signal is absent, a pseudo-user with the same signature is added to the observation (3.31). After this procedure is repeated for all users, (3.31) will contain all user signatures which are synchronous, so that conventional receiving algorithm (3.30) can be readily implemented.

It is also worth noticing that not only the average number of active users in every bit interval is smaller than the total number of users K, but also that this difference increases with maximal delay L. This suggests that receiver structure can be optimized to take this fact into account.

The price for conversion of asynchronous channel into synchronous is rate reduction, since now due to zero insertion number of chips per M bits is $(M + L)N$, whereas for conventional GO-CDMA it is MN. However, choosing block length M big enough their ratio $1 + L/M$ can be made as close to one as one wishes.

3.3.4 Simulation Results

In order to test performance of the described approach, a computer simulation in MATLAB was carried out for the system with spreading factor $N = 256$. Orthogonal subspace dimensions were chosen to be $D = 2$, resulting in $K = 384$ users (oversaturation efficiency $e_{ov} = 1.5$) and $D = 4$, resulting in $K = 320$ users ($e_{ov} = 1.25$) [92]. Maximal asynchronous delay was chosen to be $L = 250$ chips; user delays were random with uniform distribution for every simulation trial. The results were averaged over delays, users and user information bits, assuming their independence.

The results of the simulation are presented in Figure 3.10 for $K = 384$ users and in Figure 3.11 for $K = 320$ users [36]. In both figures the performance of synchronous conventional (not oversaturated) system using orthogonal signatures ($K = 256$ Walsh functions) is shown for comparison.

The results demonstrate that the deteriorative effect of asynchronous delays between users is *completely* eliminated, as it was predicted theoretically. For high SNR values results for asynchronous GO-CDMA systems coincide with results for synchronous ones, whereas for small SNR values performances of asynchronous GO-CDMA are $1 \ldots 2$ dB better. This can be explained by the fact that during a bit interval the average number of active users (not including the pseudo-users) for asynchronous GO-CDMA is smaller than that of conventional synchronous GO-CDMA, which provides advantage at low values of SNR, when performance of the system is mostly determined by the noise component. The comparisons are summarized in Table 3.1 and Table 3.2.

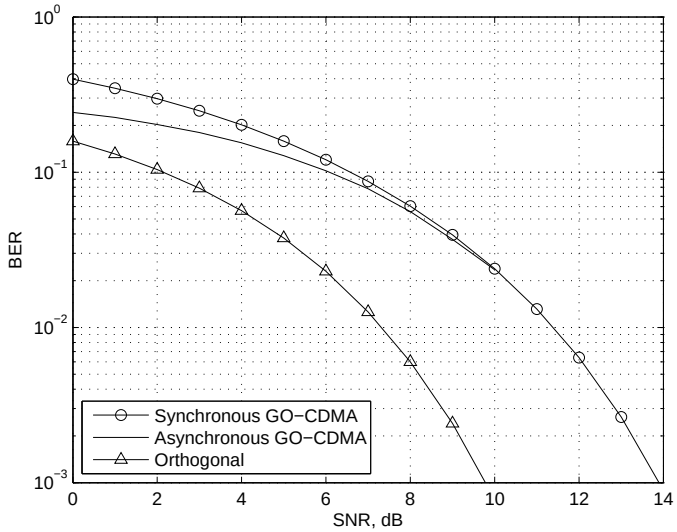

Figure 3.10: Simulation results, $K = 384$ users, $e_{ov} = 1.5$

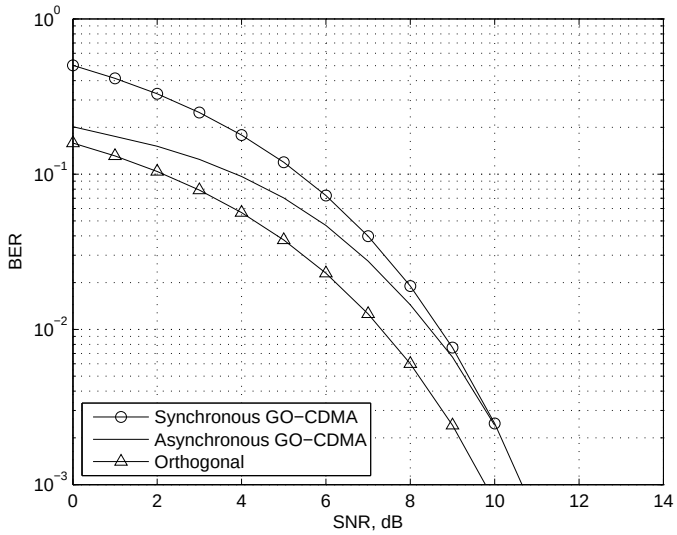

Figure 3.11: Simulation results, $K = 320$ users, $e_{ov} = 1.25$

3.4 Eliminating Odd Correlations in Asynchronous DS CDMA Employing Cyclic Prefix

Finally, in this section we describe and analyze one more method based on the *cyclic prefix* redundancy which can help neutralizing harmful effects of odd CCFs due to asynchronism. Typical of OFDM [47], cyclic prefix technique may appear promising in the traditional single carrier DS CDMA

Table 3.1: Comparison summary, $K = 384$ users, $e_{ov} = 1.5$

BER	Gain
$3 \cdot 10^{-1}$	4 dB
$2 \cdot 10^{-1}$	2 dB
10^{-1}	0.5 dB
$< 10^{-2}$	0 dB

Table 3.2: Comparison summary, $K = 320$ users, $e_{ov} = 1.25$

BER	Gain
$2 \cdot 10^{-1}$	4 dB
10^{-1}	1.3 dB
$7 \cdot 10^{-2}$	1 dB
$2 \cdot 10^{-2}$	0.3 dB
$< 10^{-3}$	0 dB

applications to instrument simple frequency-domain equalization [11]. Here we draw attention to another potential merit of the cyclic prefix related to the removal of odd correlations of signatures.

3.4.1 Conventional Asynchronous DS CDMA

Once again let us consider an asynchronous DS CDMA system with K users, each employing signature of length N, and supposing in addition that every multipath replica has its own phase, which was omitted in the previous sections for simplicity. Assume as before that the maximal asynchronous delay between users is bounded from above by the constant L, that is, $\max\{m_k\} \leq L$.

Generalizing (2.47) to K users, denoting the k-th signal amplitude and phase by A_k and φ_k respectively, the k-th user correlator output corresponding to the data bit $b_k(0)$ may be written as

$$z_k = A_k b_k(0) + \sum_{\substack{l=1 \\ l \neq k}}^{K} A_l \zeta_{kl} \cos \varphi_l \tag{3.33}$$

where $b_k(i) = \pm 1$, $i = \ldots -1, 0, 1, \ldots$ is the i-th data bit of the k-th user and the second addend represents MAI, with ζ_{kl} defined as

$$\zeta_{kl} = b_l(-1)R_{a,kl}(m_{kl} - N) + b_l(0)R_{a,kl}(m_{kl}) + b_l(1)R_{a,kl}(m_{kl} + N), \\ -L \leqslant m_{kl} \leqslant L.$$

The aperiodic CCF $R_{a,kl}(m)$ vanishes whenever $|m| \geq N$, and as is seen, mutual time shift between user signals results in affecting the k-th receiver

output z_k by the pairs of consecutive bits $b_l(-1)$, $b_l(0)$ or $b_l(0)$, $b_l(1)$ of an l-th foreign user ($l \neq k$).

Let us find an expectation of MAI power averaging the latter over random amplitudes, phases, delays and data bits. Assume, as it is done traditionally [99], independence of all random amplitudes, phases, delays and equiprobable data bits and uniformity of phase probability distribution over $[0, 2\pi]$. In addition to the above, suppose that delays m_k, $k = 1, 2, \ldots, K$ take on values within $\{0, 1, \ldots, L\}$ equiprobably, mutual delay m_{kl} thus having probability density function

$$p(m_{kl} = m) = \frac{L + 1 - |m|}{(L+1)^2}, \quad |m| \leq L. \tag{3.34}$$

Let mean square amplitude of all signals be normalized as $\overline{A_k^2} = 1$. Then the average MAI power for the k-th user $\overline{P_{\mathrm{MAI},k}}$ is found as

$$\overline{P_{\mathrm{MAI},k}} = \frac{1}{2} \sum_{\substack{l=1 \\ l \neq k}}^{K} \sum_{m=-L}^{L} \frac{L + 1 - |m|}{(L+1)^2} \Big[R_{a,kl}^2(m) + R_{a,kl}^2(N - m) + R_{a,kl}^2(m + N) \Big]. \tag{3.35}$$

3.4.2 Cyclic Prefix Asynchronous DS CDMA

As (3.35) shows, high level of signature aperiodic CCFs results in high average power of MAI. It is possible, however, to design the system so that only *even* periodic CCFs rather than much harder controllable aperiodic ones affect the average MAI power. Let one bit segment of any signature has L initial chips the same as L last chips implementing thereby a cyclic prefix [11]. In other words, every user's bit now modulates one period segment of the signature of a shorter length $N_1 = N - L$ and is then transmitted with prefixing by L last bit-modulated signature chips (see Figure 3.12). One bit duration for the k-th user can then be described as

$$\mathbf{s}_k(t) = \sum_{i=0}^{L-1} s_k(i + N_1 - L) c_0(t - i\Delta) + \sum_{i=0}^{N_1 - 1} s_k(i) c_0(t - i\Delta - L\Delta). \tag{3.36}$$

To recover a current bit at the receiving end an arriving group signal is correlated with the k-th short signature, discarding prefix, and as a result at the correlator output of the k-th user only *periodic* CCFs $R_{p,kl}(m)$ (corresponding to the short signature period N_1) contribute to MAI independently of the mutual delays:

$$z_k = A_k \frac{N_1}{N} b_k(0) + \sum_{\substack{l=1 \\ l \neq k}}^{K} A_l b_l(0) R_{p,kl}(m_{kl}) \cos \varphi_{kl}, \tag{3.37}$$

where $\varphi_{kl} = \varphi_k - \varphi_l$.

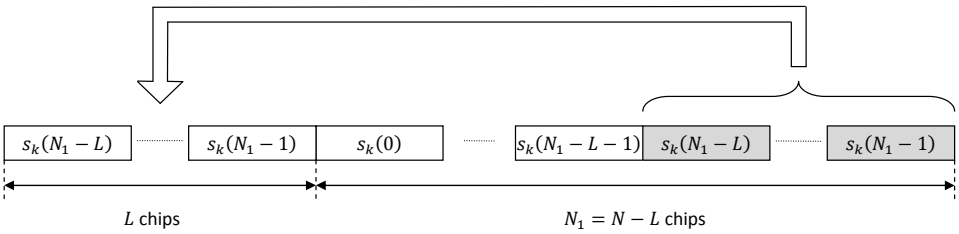

Figure 3.12: Illustration of the one bit segment in CP CDMA for the k-th user

For this case averaging MAI power in A_l, φ_l and m_{kl} gives

$$\overline{P_{\mathrm{MAI},k}} = \frac{1}{2} \sum_{\substack{l=1 \\ l \neq k}}^{K} \sum_{m=-L}^{L} \frac{L + 1 - |m|}{(L+1)^2} R_{p,kl}^2(m), \tag{3.38}$$

which shows that only even periodic CCFs are present in $\overline{P_{\mathrm{MAI},k}}$ with no effect of aperiodic (and consequently odd) CCFs.

As an important particular example consider the situation where $K(L+1) \leq N_1$. Then signature ensemble formed by the K replicas of the same binary minimax sequence from Section 2.7 (i.e. m-sequence, Legendre sequence, etc. [62]) of length N_1 cyclically shifted to each other by $L+1$ chips has equal values $R_{p,kl}^2(m) = 1/N^2$ for any $l \neq k$ all over the delay range $|m| \leq L$. Substituting this into (3.38) produces the average MAI power

$$\overline{P_{\mathrm{MAI},k}} = \frac{K-1}{2N^2}. \tag{3.39}$$

3.4.3 System Comparison and Performance Simulation

Starting with a conventional asynchronous DS CDMA let us express signal-to-noise-plus-interference ratio for the k-th user, its amplitude A_k given, in terms of the average MAI power

$$q_k(A_k) = \frac{A_k}{\sqrt{\overline{P_{\mathrm{MAI},k}} + 1/q^2}} = A_k q_k, \tag{3.40}$$

where $q^2 = 1/\sigma^2$ and q_k^2 are power SNR and SINR at the k-th correlator output respectively corresponding to $A_k = 1$. For the system performance comparison we will use bit error probability estimated analytically by the Gaussian approximation [100] providing fair accuracy up to the probabilities 10^{-3} or smaller [73]. Denote as $p_k(A_k)$ the conditional bit error probability

of the k-th receiver for a fixed amplitude of k-th signal A_k. Then according to the Gaussian approximation [100]

$$p_k(A_k) = Q\left(A_k q_k\right). \tag{3.41}$$

Consider as an example a conventional asynchronous DS CDMA system with spreading factor $N = 127$, $K = 5$ users and maximal delay $L = 20$. Since $K(L+1) < N$, the signature ensemble can be arranged of the cyclic shifts of an m-sequence of the same length as the spreading factor $N = 127$. This choice guarantees low level of MAI in at least one-half occurrences, when consecutive data bits of the l-th foreign user remain the same within the integration interval of the k-th receiver, and thus odd CCFs do not appear at the k-th correlator output. Assume users' amplitudes independent and Rayleigh-distributed, and phases independent and uniform over $[0, 2\pi]$. Gaussian approximation (3.41) then after averaging in A_k gives unconditional bit error probability p_k for the k-th receiver [62]

$$p_k = \frac{1}{2}\left(1 - \frac{q_k}{\sqrt{q_k^2 + 2}}\right). \tag{3.42}$$

The curve calculated from (3.42), (3.40) and (3.35) for the conventional DS CDMA employing the ensemble under discussion is shown in Figure 3.13 by a solid line. The computer simulation estimates of the bit error probability on bit SNR for such a conventional (without CP) system are also presented in the figure.

As an alternative, consider the system with a similar signature ensemble but implementing CP. To make a comparison fair, i.e. preserve the same number of users and data transmission rate we should take for a CP system number of chips per bit including prefix equal to the spreading factor N of a reference conventional CDMA system, meaning that after dropping the CP in the receiver actual spreading factor N_1 of the CP system appears to be $N_1 = N - L = 107$. Keeping the procedure of an ensemble design the same, sequence of length N_1 having low level of periodic *auto-correlation* function sidelobes has to be found, K replicas of which shifted by $L + 1$ chips will be used as spreading sequences. For the considered example a minimax Legendre sequence of the necessary length $N_1 = 107$ exists [62], meeting the above requirement. Note that, since $K(L+1) = 105 < N_1 = 107$, it remains possible to collect necessary number of signatures despite the reduction of the actual spreading factor, so that squared periodic CCFs entering (3.38) will take only values $R_{kl}^2(m) = 1/N^2$. Then (3.40) may be used for the new system, too, after replacing N by N_1, q^2 by $N_1 q^2/N$ (allowing for utilizing only N_1/N fraction of the transmitted bit energy),

and substitution of (3.39):

$$q_k = \frac{1}{\sqrt{\dfrac{(K-1)}{2N^2} + \dfrac{N}{N_1 q^2}}}. \tag{3.43}$$

Now (3.42) and (3.43) give analytical approximation of the bit error probability for the CP system. The dependence obtained is shown in Figure 3.13 by a solid line along with the marks produced by the computer simulation.

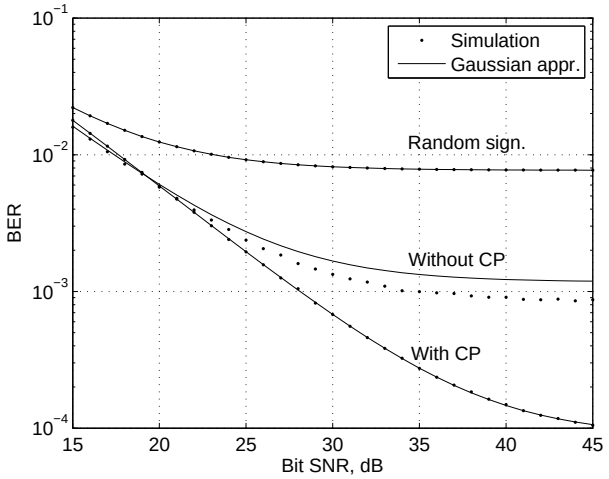

Figure 3.13: Bit error probability versus SNR, N=127, L=20, K=5

As an additional reference Figure 3.13 contains the data (solid line is again for Gaussian approximation) showing the performance of DS CDMA with the same parameters $K = 5$, $L = 20$, $N = 127$ random signatures, which is a typical option of many modern applications. The aim of this is to stress that scenarios are likely where deterministic signature ensembles are visibly more appropriate than the random ones.

As is seen, at low values of SNR CP CDMA system yields to the conventional one, which is well expected, since in this region noise component of an overall interference dominates and bit energy loss due to discarding L CP chips prevails over MAI suppression. At the same time, as SNR grows MAI contribution becomes basic and its reduction in CP CDMA leads to a considerable performance gain.

It is important to stress that the gain could be even greater, if cyclic shifts of a sequence with the *perfect* periodic auto-correlation (e.g. polyphase or ternary sequence [62, 63]) were employed as signatures, since in this case MAI might be eliminated totally.

Chapter 4

Signature-Interleaved DS CDMA

In this Chapter the main focus is shifted to the asynchronism caused by multipath propagation. It is shown that although chip-interleaved DS CDMA and its modifications can successfully mitigate the harmful effect of asynchronism between user signals in AWGN channel, in multipath channels, where every signal is received accompanied by its time-shifted replicas, chip interleaving leads to catastrophic MAI increase.

In Section 4.1 a model for downlink multipath propagation is presented, which will be used in the following chapters, too. Section 4.2 contains analysis of a conventional DS CDMA under multipath propagation.

Section 4.3 presents the main contribution of this Thesis, the idea called signature-interleaved (SI) DS CDMA. In this approach chip interleaving is combined with utilizing more than one signature for every user. It will be shown that this method allows to keep CCFs under predictable bound thus limiting MAI and potentially increasing the system performance. A similar idea of utilizing several signatures and chip interleaving is also used in [78], but it is appended by zero padding, which decreases the system rate.

Section 4.4 is dedicated to obtaining average MAI power for a single-user receiver in conventional DS CDMA, and in Section 4.5 average MAI power is obtained for SI DS CDMA.

4.1 Multipath Propagation

Let us now consider another reason that can cause asynchronism between user signals – multipath propagation. We will concentrate on a downlink transmission scenario, where all user signals are strictly synchronized before the transmission forming the group signal. However, despite this strict synchronism user signals are always received accompanied by the group signal

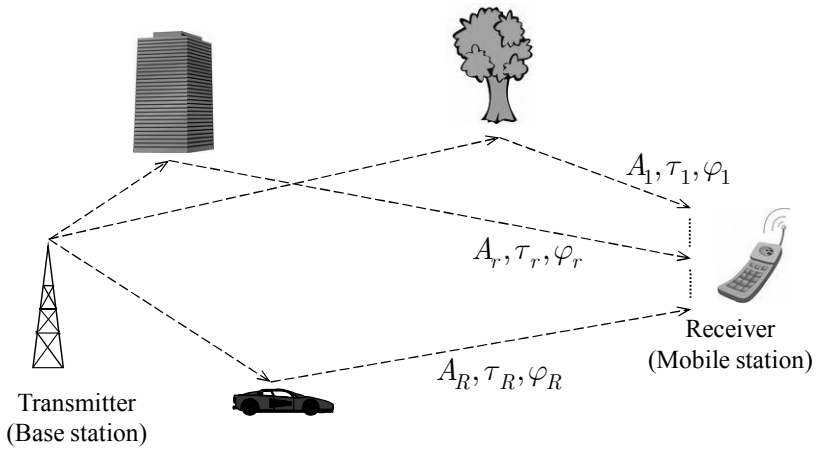

Figure 4.1: Downlink multipath channel

replicas due to multipath propagation [16, 72, 93].

Let us denote the total number or multipath replicas as R. Each replica is delayed by τ_r and corrupted with its own amplitude A_r and phase φ_r, $1 \le r \le R$ (Figure 4.1). We will assume that multipath delays τ_r are nonnegative multiples of the chip duration, $\tau_r = m_r\Delta$, limited from above by the constant L. Such a simplification somewhat overestimates effect of MAI ignoring its reduction related to the chip autocorrelation [99]. Suppose also that multipath rays are sorted in non-decreased order of their delays: $0 = m_1 \le \ldots \le m_r \le \ldots \le m_R \le L$, where delay of the first ray is assumed to be zero, $m_1 = 0$.

4.2 Conventional DS CDMA

Consider first what effect multipath propagation will cause to a conventional DS CDMA. One bit duration signal of the k-th user for the bit $b_k(0)$ can be, as it was done previously, described as

$$\mathbf{s}_k(t) = b_k(0) \sum_{i=0}^{N-1} s_k(i) c_0(t - i\Delta). \tag{4.1}$$

One bit duration of the group signal is then

$$\mathbf{s}(\mathbf{b}; t) = \sum_{k=1}^{K} \mathbf{s}_k(t) = \sum_{k=1}^{K} b_k(0) \sum_{i=0}^{N-1} s_k(i) c_0(t - i\Delta), \tag{4.2}$$

and the group signal for continuous bit stream is

$$\mathtt{S}(t) = \sum_{j=-\infty}^{\infty} \sum_{k=1}^{K} b_k(j) \sum_{i=0}^{N-1} s_k(i) c_0(t - i\Delta - jN\Delta). \tag{4.3}$$

At this state of analysis we will neglect multipath amplitudes and phases, returning to more general case in Section 4.4. Then the received observation (neglecting the background noise) can be written as

$$\mathtt{y}(t) = \sum_{r=1}^{R} \mathtt{S}(t - rm_r). \tag{4.4}$$

Suppose that we want to demodulate the k-th user information bit $b_k(0)$ that was transmitted during the first multipath component $r = 1$. Then part of (4.4) that falls within the time frame $[0, N\Delta]$ of the bit $b(0)$ can be written as

$$\begin{aligned}\mathtt{y}(t) = b_k(0) \sum_{i=0}^{N-1} s_k(t - i\Delta) c_0(t - i\Delta) + \sum_{\substack{l=1 \\ l \neq k}}^{K} b_l(0) \sum_{i=0}^{N-1} s_l(t - i\Delta) c_0(t - i\Delta) \\ + \sum_{r=2}^{R} \sum_{l=1}^{K} \Bigg[b_l(-1) \sum_{i=0}^{m_r - 1} s_l(N - m_r + i) c_0(t - i\Delta) \\ + b_l(0) \sum_{i=m_r}^{N-1} s_l(i - m_r) c_0(t - i\Delta) \Bigg].\end{aligned} \tag{4.5}$$

Calculating the correlation of (4.5) and the k-th user signature we obtain

$$\begin{aligned}z_k(0) = b_k(0) + \sum_{\substack{l=1 \\ l \neq k}}^{K} b_l(0) R_{kl}(0) \\ + \sum_{r=2}^{R} \sum_{l=1}^{K} \big[b_l(-1) R_{a,kl}(m_r - N) + b_l(0) R_{a,kl}(m_r) \big].\end{aligned} \tag{4.6}$$

Second and third term in (4.6) represent MAI, which now includes interference from multipath propagation; it is seen that now not only cross-correlation functions contribute to MAI, but also *auto*-correlation functions.

Equation (4.6) also demonstrates that MAI is affected by CCFs of shifts up to $\max\{m_r\} = L$. In the next section we introduce an approach which allows to eliminate influence of all CCFs except for the shifts $0, \pm 1$.

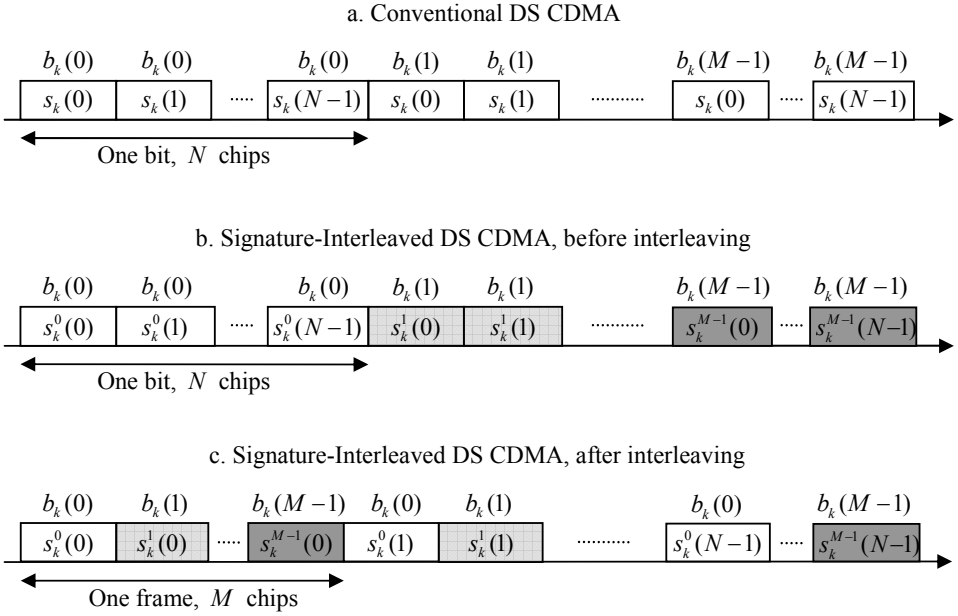

Figure 4.2: Illustration of the interleaving in SI DS CDMA

4.3 Signature-Interleaved DS CDMA

The main distinctive feature of Signature-Interleaved DS CDMA is that every user utilizes not just one signature, as it is the case for the conventional DS CDMA, but M different signatures. Let us denote these M signatures of length N as $s_k^u(t)$, $u = 0, 1, \ldots, M-1$ being number of the signature among all of them assigned to the k-th user, $1 \leq k \leq K$. Assume that all signatures are binary and are normalized to unity energy.

Supposing that a data bit as earlier covers N signature chips, let the data bit $b_k(0) = \{\pm 1\}$ of the k-th user modulate $\mathbf{s}_k^0$, the next one $b_k(1)$ modulate $\mathbf{s}_k^1$, and so on up to the bit $b_k(M-1)$ modulating $\mathbf{s}_k^{M-1}$; bit $b_k(M)$ modulating again $\mathbf{s}_k^0$, etc (Figure 4.2.b, chips of different signatures are shown by shade density).

This way the data-manipulated chip stream is split to blocks of M bits, each block spanning MN chips. Let us write every such block row-wise as entries of the $M \times N$ matrix. The u-th row of this matrix is just bit-manipulated one period segment of the signature $s_k^u(t)$. Let us now read out the entries of the matrix column-wise. After this procedure, chips of the signature $s_k^u(t)$ will be separated from each other by the space $M\Delta$ and accompanied by chips of the signature $s_k^{u+1}(t)$ (Figure 4.2.c), where $s_k^u(i)$, $i = 0, 1, \ldots, N-1$ is the i-th code symbol of $\mathbf{s}_k^u$.

Designating as $c_k^u(t)$ a one-period segment of the signature $s_k^u(t)$ modified

by the interleaving we have

$$c_k^u(t) = \sum_{i=0}^{N-1} s_k^u(i) c_0(t - iM\Delta - u\Delta). \tag{4.7}$$

Being modulated by the bit stream $b_k(jM+u)$, $j = \ldots, -1, 0, 1, \ldots$, $u = 0, 1, \ldots, M-1$, the sequence $d_k^u(t)$ of such one-period segments takes the form

$$d_k^u(t) = \sum_{j=-\infty}^{\infty} b_k(jM+u) c_k^u(t - jMN\Delta). \tag{4.8}$$

Consider now a conventional receiver of the k-th user correlating the observed waveform with the reference (4.7) in order to retrieve bit $b_k(u)$, $u = 0, 1, \ldots, M-1$. Then data-modulated and interleaved signature $d_l^v(t)$ of the l-th user time-shifted by integer number $m_{kl} = m_l - m_k$ chips with respect to $d_k^u(t)$ will create MAI z_{kl} whose absolute value is

$$\begin{aligned} |z_{kl}| &= \left| \int_0^{MN\Delta} c_k^u(t) d_l^v(t - m_{kl}\Delta) dt \right| \\ &= \left| \sum_{j=-\infty}^{\infty} b_l(jM+v) \int_0^{MN\Delta} c_k^u(t) c_l^v(t - jMN\Delta - m_{kl}\Delta) dt \right|, \end{aligned} \tag{4.9}$$

where (4.8) is used to substitute for $d_l^v(t)$. Since one-period segment (4.7) zeroes beyond the interval $[0, MN\Delta]$, only two summands in (4.9) may be nonzero, corresponding to j meeting the inequality $|jMN + m_{kl}| < MN$. Recall that we consider scenarios where all mutual delays are limited by the constant L, $|m_{kl}| < L$, and length of the block M is chosen so that $M \geqslant L$. Then only terms with $j = 0$ and $j = 1$ ($m_{kl} < 0$) or $j = -1$ ($m_{kl} > 0$) contribute to the sum of (4.9):

$$|z_{kl}| = \left| \int_0^{MN\Delta} c_k^u(t) c_l^v(t - m_{kl}\Delta) dt \pm \int_0^{MN\Delta} c_k^u(t) c_l^v[t \pm \theta\Delta] dt \right| \tag{4.10}$$

where $\theta = MN - |m_{kl}|$, sign before θ is the same as the sign of m_{kl}, and signs "+" or "−" between integrals correspond to the cases of two identical or different consecutive l-th user's bits $b_l(v)$, $b_l(v \pm 1)$ inside the window $[0, MN]$. Our goal now is to show that the sum of the integrals under the admitted limitations on m_{kl} is determined by even and odd CCFs of the initial signatures at the shifts of no more than one symbol. Substituting

(4.7) into the first integral results in

$$\sum_{i=0}^{N-1}\sum_{j=0}^{N-1} s_k^u(i)s_l^v(j)\int_0^{MN\Delta} c_0(t-iM\Delta-u\Delta)c_0(t-jM\Delta-v\Delta-m_{kl}\Delta)dt, \tag{4.11}$$

or after changing integration variable t to $t-iM\Delta-u\Delta$

$$\sum_{i=0}^{N-1}\sum_{j=0}^{N-1} s_k^u(i)s_l^v(j)\int_0^{\Delta} c_0(t)c_0\left[t-(j+i)M\Delta-(v+m_{kl}-u)\Delta\right]dt. \tag{4.12}$$

Due to non-overlapping of chips shifted to each other by integer number of durations Δ, the addends of the sum (4.12) are nonzero if and only if $(i-j)M = v-u+m_{kl}$. Since the range of $v-u+m_{kl}$ is $[-2M+2, 2M-2]$, there are only three opportunities of observing this equality: $v-u+m_{kl} = 0, \pm M \Rightarrow i = j, j\pm 1$. Correspondingly, the sum (4.12) has only three possible forms:

$$\sum_{i=0}^{N-1} s_k^u(i)s_l^{u-m_{kl}}(i), \quad \sum_{i=1}^{N-1} s_k^u(i)s_l^{u-m_{kl}+M}(i-1),$$
$$\text{or} \quad \sum_{i=0}^{N-2} s_k^u(i)s_l^{u-m_{kl}-M}(i+1). \tag{4.13}$$

From the borders $0 \le v$, $|m_{kl}| \le M-1$ nonintersecting areas of (m_{kl}, u)-plane follow where first integral of (4.10) equals each of the sums in (4.13), respectively: $u-M+1 \le m_{kl} \le u$, $0 \le u \le M-1$; $u+1 \le m_{kl} \le M-1$, $0 \le u \le M-2$ and $-M+1 \le m_{kl} \le u-M$, $1 \le u \le M-1$. As is seen now the first sum is just (even) periodic CCF of the basic signatures $s_k^u(t)$ (u-th signature of the k-th user) and $s_l^{u-m_{kl}}(t)$ (signature number $u-m_{kl}$ of the l-th user) at zero shift. Similarly, two other sums are aperiodic CCFs of $s_k^u(t)$ either with $s_l^{u-m_{kl}+M}(t)$ shifted by one symbol to the right or with $s_l^{u-m_{kl}-M}(t)$ shifted by one symbol to the left.

Handling analogously the second integral in (4.10) produces the sum

$$\sum_{i=0}^{N-1}\sum_{j=0}^{N-1} s_k^u(i)s_l^v(j)\int_0^{\Delta} c_0(t)c_0\left[t-(j-i)M\Delta-(v\mp\theta-u)\Delta\right]dt \tag{4.14}$$

where sign before θ should be taken opposite to that of m_{kl}. For $m_{kl} > 0$, since $v-\theta-u$ is an integer belonging to $[-MN-M+2, -MN+2M-2]$, there are only two sorts of potentially nonzero terms in (4.14) corresponding to $v-\theta-u = -MN \Rightarrow j = i+N$ and $v-\theta-u = -M(N-1) \Rightarrow j = i+N-1$.

First of them comprises the case $v = u - m_{kl}$ and, having j falling outside the allowed range, adds up to zero. For the second $v = u - m_{kl} + M$ and (4.13) turns into $s_k^u(0)s_l^{u-m_{kl}+M}(N-1)$. With the same reasoning we calculate the sum for the case $m_{kl} < 0$ equaling $s_k^u(N-1)s_l^{u-m_{kl}-M}(0)$.

Thus, combining the last results with (4.13) we arrive at the following equation for MAI (4.10)

$$|z_{kl}| = \begin{cases} \left|\sum_{i=0}^{N-1} s_k^u(i)s_l^{u-m_{kl}}(i)\right|, \\ \qquad u - M + 1 \leqslant m_{kl} \leqslant u,\ 0 \leqslant u \leqslant M-1, \\ \left|\sum_{i=1}^{N-1} s_k^u(i)s_l^{u-m_{kl}+M}(i-1) \pm s_k^u(0)s_l^{u-m_{kl}+M}(N-1)\right|, \\ \qquad u + 1 \leqslant m_{kl} \leqslant M-1,\ 0 \leqslant u \leqslant M-2, \\ \left|\sum_{i=0}^{N-2} s_k^u(i)s_l^{u-m_{kl}-M}(i+1) \pm s_k^u(N-1)s_l^{u-m_{kl}-M}(0)\right|, \\ \qquad -M + 1 \leqslant m_{kl} \leqslant u - M,\ 1 \leqslant u \leqslant M-1. \end{cases} \tag{4.15}$$

Let us denote an aperiodic CCF between signatures $\mathbf{s}_k^i$ and $\mathbf{s}_l^j$ of shift m as

$$R_{(k,i),(l,j)}(m) = \begin{cases} \sum_{n=m}^{N-1} s_k^i(n)s_l^j(n-m), & m \geq 0, \\ \sum_{n=0}^{N+m-1} s_k^i(n)s_l^j(n-m), & m < 0. \end{cases} \tag{4.16}$$

Then (4.15) can be simplified to

$$|z_{kl}| = \begin{cases} \left|R_{(k,u),(l,u-m_{kl})}(0)\right|, \\ \qquad u - M + 1 \leqslant m_{kl} \leqslant u,\ 0 \leqslant u \leqslant M-1, \\ \left|R_{(k,u),(l,u-m_{kl}+M)}(1) \pm s_k^u(0)s_l^{u-m_{kl}+M}(N-1)\right|, \\ \qquad u + 1 \leqslant m_{kl} \leqslant M-1,\ 0 \leqslant u \leqslant M-2, \\ \left|R_{(k,u),(l,u-m_{kl}-M)}(-1) \pm s_k^u(N-1)s_l^{u-m_{kl}-M}(0)\right|, \\ \qquad -M + 1 \leqslant m_{kl} \leqslant u - M,\ 1 \leqslant u \leqslant M-1. \end{cases} \tag{4.17}$$

Equation (4.17) demonstrates that all possible magnitudes of MAI are just even or odd CCFs of basic signatures $s_k^u(t)$ at the shifts of 0, 1, or -1 symbols. It is worthy to note that no autocorrelations contribute to the MAI despite possible presence of multipath signal replicas. This is due to the fact that multiple interleaved signatures are implemented per one user,

and at the MF output not correlation of a signature with its delayed replica is calculated, but correlation of two different signatures.

But the main implication of (4.17) is that, since the second addend of two last rows equals ± 1, any involved odd CCF differs from the associated even CCF by no more than two. This in turn means that if all signatures of all users are taken properly from the ensemble with "good" even CCFs, data modulation will distort the latter ones minimally.

4.4 MAI Power for Conventional DS CDMA

Let us now proceed to a more general model of multipath propagation and include multipath rays' amplitudes and phases into consideration. Multipath ray amplitudes A_r are assumed as random variables with mean square amplitudes $\overline{A_r^2} = \alpha_r^2$, and phases φ_r are random variables with uniform distribution over $[0, 2\pi]$. We will also assume that the fading pattern remains stable during the bit interval $T = N\Delta$, that is, A_r and φ_r are treated as constants during the bit interval and change independently from bit to bit [16,93]. Taking all this into account, the complex envelope of the received observation for a conventional DS CDMA can be written as

$$\mathrm{y}(t) = \sum_{r=1}^{R} A_r \mathbf{s}(\mathbf{b}; t - \Delta m_r) \exp(j\varphi_r) + n(t). \tag{4.18}$$

Let us now consider output of the matched filter for conventional DS CDMA in the described multipath channel, which for the k-th user data bit $b_k(0)$ may be written as

$$\begin{aligned} z_k = {} & A_1 b_k(0) + A_1 \sum_{\substack{l=1 \\ l \neq k}}^{K} b_l(0) R_{kl}(0) \\ & + \sum_{r=2}^{R} A_r \cos\varphi_r \sum_{l=1}^{K} \left[b_l(-1) R_{a,kl}(m_r - N) + b_l(0) R_{a,kl}(m_r) \right] + n_k. \end{aligned} \tag{4.19}$$

Second and third term in (4.19) represent MAI. Let us find an expectation of MAI power, which for the k-th user is written as

$$\begin{aligned} \overline{P_{\mathrm{MAI},k}} = {} & \alpha_1^2 \sum_{\substack{l=1 \\ l \neq k}}^{K} R_{kl}^2(0) \\ & + \frac{1}{2} \sum_{r=2}^{R} \alpha_r^2 \sum_{l=1}^{K} \left[R_{a,kl}^2(m_r - N) + R_{a,kl}^2(m_r) \right]. \end{aligned} \tag{4.20}$$

4.5 MAI Power for SI DS CDMA

Let us now turn to SI DS CDMA. The transmitted group signal now is

$$\mathbf{s}(t) = \sum_{k=1}^{K} \sum_{i=0}^{M-1} b_k(i) \sum_{j=0}^{N-1} s_k^i(j) c_0(t - i\Delta - jM\Delta), \tag{4.21}$$

and for a multipath ray with non-zero delay, part of the previous M-block will fall within the observation window $0 \le t \le MN\Delta$ of the current one. Specifically, for the path with delay m this part takes the form

$$s_m(t) = \sum_{k=1}^{K} \sum_{i=M-m}^{M-1} b_k^{\text{prev}}(i) s_k^i(N-1) c_0(t - (i - M + m)\Delta), \tag{4.22}$$

where $b_k^{\text{prev}}(i)$ is the k-th user i-th information bit of the previous M-block. Its mismatch with the k-th user's i-th information bit of the current M-block $b_k(i)$ will cause appearance of *odd* correlation at the l-th correlator output, $1 \le l \le K$. However, if the maximal multipath delay L is no greater than M, part of the previous M-block (4.22), consisting of m chips, can influence only the first chip of a user signature in the M-block, since elements of a user signature are now distanced by $M \ge \max(m) = L$ chips. Therefore a "fracture" of an odd correlation can occur after the first chip only *independently* of the multipath delay, as compared to conventional DS CDMA, where "fracture" can occur at any position of the signature up to L chips.

Consider as an example receive processing of the k-th user bit $b_k(0)$, which is shown in Figure 4.3. In order to demodulate it, chips of the k-th user signature $\mathbf{s}_k^0$ should be picked out from the observation. The selected samples will also contain chips of a foreign l-th user signature from a delayed multipath signal, specifically, $\mathbf{s}_l^{M-m}$ for the multipath delay m shifted by one chip to the right: $[s_l^{M-m}(N-1), s_l^{M-m}(0), \ldots, s_l^{M-m}(N-2)]$ (other users' signatures from the original and delayed signals are excluded from the consideration to simplify the analysis). Last $N-1$ chips of this signature will be modulated by the information bit $b_l(M-m)$, whereas the first chip $s_l^{M-m}(N-1)$ will be modulated by the bit of the previous block $b_l^{\text{prev}}(M-m)$, whose different polarity will cause appearance of odd cross-correlation with a "fracture" after the first chip. The aforesaid remains true for any pair of user signatures $1 \le k, l \le K$.

It is also worth noticing that if we consider signature of the same user $l = k$ from a delayed multipath signal, at the output of the user correlator there will occur *cross*-correlation between the signatures $\mathbf{s}_k^0$ and $\mathbf{s}_k^{M-m}$ for delays $m < M$, rather than *auto*-correlation of a user signature $\mathbf{s}_k$, as it would be the case in chip-interleaved DS CDMA system.

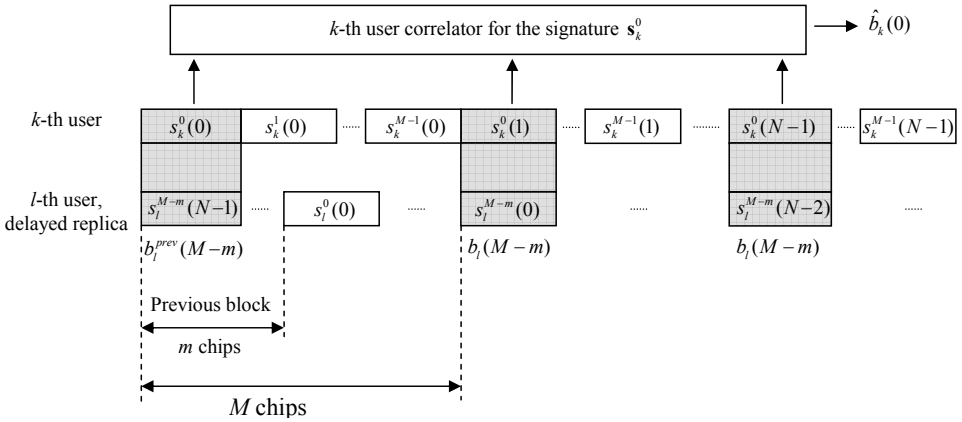

Figure 4.3: Receive processing of the bit $b_k(0)$ of the k-th user

To support abovementioned formally, consider an output of the conventional receiver of the k-th user correlating the observed waveform with the signature $\mathbf{s}_k^i$ in order to retrieve bit $b_k(i)$, $i = 0, 1, \ldots, M-1$:

$$z_k^i = A_1 b_k(i) + A_1 \sum_{\substack{l=1 \\ l \neq k}}^{K} b_l(i) R_{(k,i),(l,i)}(0) + \sum_{r=2}^{R} A_r \cos\varphi_r \sum_{l=1}^{K} \varsigma_{k,l}(i,r) + n_k \tag{4.23}$$

where

$$\varsigma_{k,l}(i,r) = \begin{cases} b_l(i') R_{(k,i),(l,i')}(0), & i \geq m_r, \\ b_l^{\text{prev}}(i') R_{(k,i),(l,i')}(1-N) & \\ \quad + b_l(i') R_{(k,i),(l,i')}(1), & i < m_r, \end{cases} \tag{4.24}$$

and $i' = (i - m_r) \mod M$, $1 \leq k, l \leq K$, $0 \leq i, j \leq M-1$. Then averaging MAI power in amplitudes, data bits and phases as it was done in the previous Section results in

$$\overline{P_{\text{MAI},k}^i} = \alpha_1^2 \sum_{\substack{l=1 \\ l \neq k}}^{K} R_{(k,i),(l,i)}^2(0) + \frac{1}{2} \sum_{r=2}^{R} \alpha_r^2 \sum_{l=1}^{K} \chi_{k,l}(i,r) \tag{4.25}$$

where

$$\chi_{k,l}(i,r) = \begin{cases} R_{(k,i),(l,i')}^2(0), & i \geq m_r, \\ 1/N^2 + R_{(k,i),(l,i')}^2(1), & i < m_r. \end{cases} \tag{4.26}$$

This result demonstrates that the average MAI power depends now on correlations of non-shifted $R_{(k,i),(l,i')}(0)$ or just one-chip-shifted signatures

$R_{(k,i),(l,i')}(1)$ only, *independently* of the maximal multipath delay value L. Potentially, these correlations are significantly easier to control and thereby may result in lower value of the average MAI power. Compare this to the average MAI power for conventional DS CDMA (4.20), where it is affected by CCFs of shifts up to L.

At the same time (4.26) elucidates the necessity of using multiple signatures per user. Indeed, in case of implementation only one signature per user, as it is the case in chip-interleaved DS CDMA, for $k = l$ correlations $R^2_{(k,i),(k,i')}(0)$ in (4.26) turn into auto-correlations $R^2_{k,k}(0) = 1$ of significantly greater value, increasing thus the average MAI power drastically. It is a considerable advantage of SI DS CDMA that no auto-correlations of zero shift contribute to the average MAI power despite presence of multipath signal replicas.

Chapter 5

Signature Ensembles for Signature-Interleaved DS CDMA

As was shown in the previous Chapter, SI DS CDMA allows to mitigate harmful effects of multipath propagation, since it greatly reduces dependance of MAI on badly controllable odd correlations. However, this benefit is obtained at the expense of signature ensemble size increase, which rises the question of ensembles construction methods. In the Chapter various signature ensembles are synthesized based on different demands to correlation properties, and performances of systems using such ensembles are compared in terms of bit error rate.

Section 5.1 concentrates on the ensemble selection criteria, provides several bounds on the maximal number of signatures depending on the maximal CCF value and describes the construction procedure of SI DS CDMA signature ensembles. Section 5.2 provides a comparison of MAI power for DS CDMA and SI DS CDMA as well as comparison of higher MAI moments. Finally, in Section 5.3 ensembles are compared in terms of bit error rate.

5.1 Signature Ensembles for SI DS CDMA

In Section 4.5 the average MAI power for a single-user receiver for SI DS CDMA was found, which is reproduced here for convenience:

$$\overline{P^i_{\mathrm{MAI},k}} = \alpha_1^2 \sum_{\substack{l=1 \\ l\neq k}}^{K} R^2_{(k,i),(l,i)}(0) + \frac{1}{2}\sum_{r=2}^{R} \alpha_r^2 \sum_{l=1}^{K} \chi_{k,l}(i,r) \tag{5.1}$$

where

$$\chi_{k,l}(i,r) = \begin{cases} R^2_{(k,i),(l,i')}(0), & i \geqslant m_r, \\ 1/N^2 + R^2_{(k,i),(l,i')}(1), & i < m_r, \end{cases} \tag{5.2}$$

and $i' = (i - m_r) \mod M$, $1 \leq k, l \leq K$, $0 \leq i, j \leq M-1$.

As was shown in Section 3.4.3 and is widely known from literature [98–100], performance of a single-user receiver depends greatly on MAI level, so the main effort in this chapter will be aimed to construct a set of signatures which minimizes (5.1).

Let us start with obtaining a limit of the number of signatures using the Welch bound (2.61)

$$\rho^2_{\max} \geqslant \frac{K-N}{N(K-1)}, \tag{5.3}$$

where $\rho_{\max} = \max\{|R_{(k,i),(l,j)}(m)|\}$ is a maximal absolute value of correlations for $\forall m \in \{0,1\}$, $1 \leqslant k, l \leqslant K$, $0 \leqslant i, j \leqslant M-1$ except $(m=0) \cup (k=l) \cup (i=j)$. Since in SI DS CDMA every of K users utilizes M signatures, two shifts of which should have small values, K in (5.3) should be replaced with $2KM$, and after solving for $2KM$ (5.3) becomes

$$2KM \leqslant \frac{N - \rho^2_{\max} N}{1 - \rho^2_{\max} N}. \tag{5.4}$$

Based on possible values of $\rho_{\max}$ we will consider three cases.

5.1.1 Zero Correlation Zone Signatures

MAI power (5.1) is minimized when maximal correlation is zero, $\rho_{\max} = 0$, meaning that the maximal number of signatures after substituting $\rho_{\max} = 0$ in (5.4) becomes

$$2KM \leqslant N. \tag{5.5}$$

Suitable candidates in this case are *zero-correlation zone signatures* (ZCZ) [23, 120], especially their binary version [46]. A ZCZ set of P signatures of length N provides zero cross-correlation for any pair of signatures within a zone of Z chips:

$$R_{p,kl}(m) = 0, \quad 1 \leqslant k, l \leqslant P, \quad k \neq l, \quad 0 \leqslant m \leqslant Z, \tag{5.6}$$

and is denoted as $\mathrm{ZCZ}(P, Z, N)$.

Consider now the procedure of constructing a signature ensemble for SI DS CDMA from an arbitrary ZCZ ensemble, which is called the "raw" ensemble. For every of P signatures from the raw ZCZ ensemble, $\left\lfloor \frac{Z+1}{2} \right\rfloor$ its even cyclic shifts are taken as signatures for the SI DS CDMA ensemble, altogether forming $P \left\lfloor \frac{Z+1}{2} \right\rfloor$ signatures. They can be distributed between K

users arbitrary, assigning every of them M signatures from the created set. Certainly, this is possible only if

$$P\left\lfloor\frac{Z+1}{2}\right\rfloor \geq KM. \tag{5.7}$$

More specifically, denote as $((\mathbf{s},i))$ the i-th cyclic shift to the right of the signature $\mathbf{s}$, and suppose that the raw ZCZ set consists of P signatures $\mathbf{u}_j$, $1 \leq j \leq P$. Then signature $\mathbf{u}_1$ will form $\left\lfloor\frac{Z+1}{2}\right\rfloor$ its even cyclic shifts, and these cyclic shifts will serve as signatures for SI DS CDMA ensemble denoted as $\mathbf{s}_n$, $1 \leq n \leq \left\lfloor\frac{Z+1}{2}\right\rfloor$:

$$\begin{aligned}
\mathbf{s}_1 &= ((\mathbf{u}_1,0)) = \mathbf{u}_1,\\
\mathbf{s}_2 &= ((\mathbf{u}_1,2)),\\
&\vdots\\
\mathbf{s}_{\left\lfloor\frac{Z+1}{2}\right\rfloor} &= ((\mathbf{u}_1, 2\left\{\left\lfloor\frac{Z+1}{2}\right\rfloor - 1\right\})).
\end{aligned}$$

Signatures $\mathbf{u}_j$, $2 \leq j \leq P$ are modified analogously. Proof that this set provides zero correlations for shifts zero and one is of no difficulty and directly follows from the ZCZ ensemble definition (5.6).

Note that so far only ZCZ sets with quite limited number of parameters P, Z and N are known [46], which might limit their usage in conventional DS CDMA. Indeed, ZCZ sets are effective only if maximal multipath delay is no greater than the size of zero correlation zone $L \leqslant Z$, which means strong dependance on the multipath propagation channel profile. More than that, even if this condition is satisfied, only even cross-correlations are equal to zeros, while odd ones are still uncontrollable and can take quite significant values for big delays L.

Neither of these issues poses a problem for SI DS CDMA. Following the construction procedure presented above, any set ZCZ(P,Z,N) can be easily transformed into set ZCZ$(P\left\lfloor\frac{Z+1}{2}\right\rfloor,2,N)$ with the necessary zero correlation zone of size two, which is directly suitable for SI DS CDMA.

As for the limitation of the odd correlations for such a ZCZ set, let us recall from (2.23) that any periodic correlation can always be represented as a sum of two aperiodic ones, $R^p_{(k,i),(l,j)}(1) = R_{(k,i),(l,j)}(1) + R_{(k,i),(l,j)}(1-N)$. Since for the binary alphabet of normalized signature ensemble $R_{(k,i),(l,j)}(1-N) = s^i_k(0)s^j_l(N-1) = \pm 1/N$, it is seen that squared aperiodic correlations of the first shift determining average MAI power (5.2) can take on only values $R^2_{(k,i),(l,j)}(1) = \left\{0, 1/N^2\right\}$.

Another possible way to obtain signature ensemble satisfying (5.6) is usage of even cyclic shifts of a signature with *perfect* periodic auto-correlation function $R(m) = 0$, $1 \leqslant m \leqslant N-1$. Such a signature can be

denoted as ZCZ$(1, N-1, N)$, and, using the described construction procedure, will provide the set ZCZ$(\lfloor N/2 \rfloor, 2, N)$, which for the even lengths N transforms (5.5) into equality. This will create a SI DS CDMA signature set of $N/2$ signatures, and is possible only if

$$\left\lfloor \frac{N}{2} \right\rfloor \geq KM. \tag{5.8}$$

Unfortunately, as was mentioned in Section 2.7, no binary signatures exist with perfect PACF except for the trivial case with length $N = 4$.

If demands to the signature alphabet can be relaxed to the *ternary* case, it is possible to use as a signature ensemble even cyclic shifts of a ternary sequence [62,63] with perfect PACF, which exist for a big variety of lengths (see Section 2.7). For the case of *polyphase* signature alphabet even more signatures with perfect PACF exist (Frank, Chu signatures [45,62]).

5.1.2 Low Correlation Zone Signatures

Next possible scenario covers the case when the maximal correlation is $\rho_{\max} = 1/N$, which changes (5.4) into

$$2KM \leqslant N + 1. \tag{5.9}$$

In this case a possible way of constructing signatures for SI DS CDMA is using even cyclic shifts of a *minimax* binary sequence whose PACF $|R(m)| = 1$ ($\rho_{\max} = 1/N$), $1 \leqslant m \leqslant N-1$. The set of signatures thus obtained is called *low correlation zone* (LCZ) one [71]. We will denote a LCZ ensemble as LCZ(P, Z, N):

$$|R_{kl}(m)| = 1, \quad 1 \leqslant k, l \leqslant P, \quad k \neq l, \quad 0 \leqslant m \leqslant Z. \tag{5.10}$$

There exist many minimax binary signatures (see Section 2.7). On the grounds analogous to the previous Section, for such signatures squared aperiodic correlations of the first shift take on values $R^2_{(k,i),(l,j)}(1) = \{0, 4/N^2\}$.

Consider as an example a system with $K = 6$ users, and suppose that maximal multipath delay is $L = 10$ and the spreading factor is $N = 127$. In this case the signature set for SI DS CDMA can be constructed from an m-sequence of length 127 which has a minimax PACF. Since $\lfloor N/2 \rfloor = 63 > KM = 60$, it is possible to use 60 even cyclic shifts of the m-sequence to create the necessary ensemble LCZ$(60, 2, 127)$. For conventional DS CDMA, on the other hand, the necessary signature set can be formed as K cyclic shifts of the same m-sequence.

Figure 5.1 demonstrates dependence of odd CCF peak (multiplied by N for convenience) on spread L for the both created ensembles. It is seen that for SI DS CDMA (dotted line) maximal value of odd CCF is fixed and

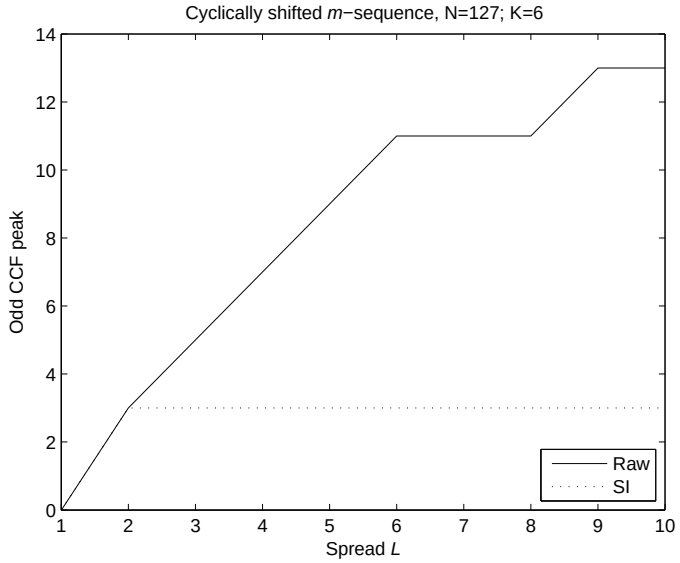

Figure 5.1: Dependence of odd CCF peak on spread L. Ensemble of cyclically shifted m-sequences, $N = 127$, $K = 6$.

is independent of the maximal delay L, as was theoretically predicted. On the contrary, for the "raw" ensemble of conventional DS CDMA (solid line) maximal value of odd CCF rapidly increases with L, becoming more than four times bigger than that of SI DS CDMA for the spread $L = 10$.

5.1.3 Signatures with Bigger Maximal Correlation

Finally, consider the case when $\rho_{\max} \geqslant 2/N$. Let length N, number of users K and spread L be given; let us choose the number of signatures per user $M = L$. Take a minimax ensemble of size P and length N meeting the requirement $KM \leq PN/2$ (Gold, Kasami, Kamaletdinov [67] etc). Take cyclic shifts of any of P minimax sequences shifted to each other by 2 symbols or more. Then we have a total of $\lfloor PN/2 \rfloor$ sequences at the most and all of them are relevant as basic signatures. Their distribution between K users may be done in an arbitrary fashion.

To illustrate the procedure let us take a scenario of the CDMA system with $K = 30$ users operating on the channel with $L = 60$ and lets again choose $M = L = 60$. Let the spreading factor, dictated by necessary rate and available bandwidth be $N = 127$. Then a good option of the raw ensemble is the Gold set with parameters $N = 127$, $P = N + 2 = 129$, producing $\lfloor PN/2 \rfloor = 8191$ candidate signatures, which is much greater than the required number $KM = 1800$, therefore we may easily assign to every of 30 users $M = 60$ basic signatures. According to (2.67), periodic correlations

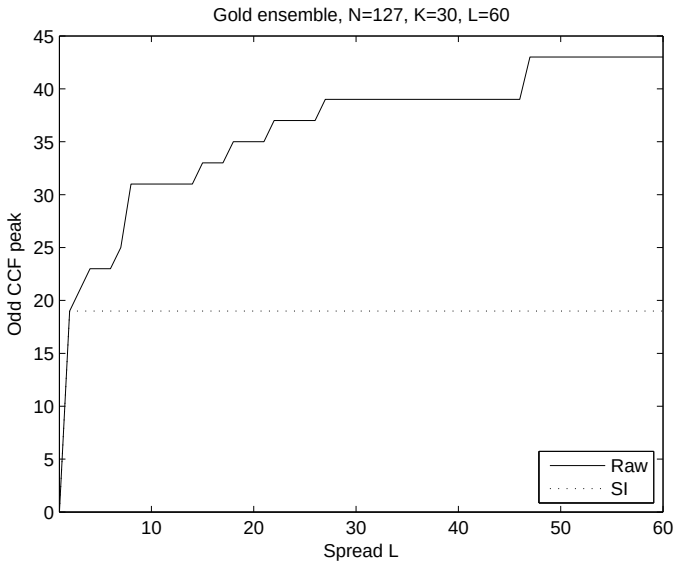

Figure 5.2: Dependence of odd CCF peak on spread L. Gold ensemble, $N = 127$, $K = 30$.

of the Gold set in question do not surpass $N\rho_{\max} = \sqrt{2(N+1)} + 1 = 17$, so that MAI level created by any side signature is never greater than 19 (Figure 5.2). On the contrary, for the raw Gold set the odd CCF peak increases with the spread achieving finally the level 43, i.e. 2.26 times higher.

In the majority of scenarios the number of candidate signatures is significantly bigger than the necessary number of signatures, $\lfloor PN/2 \rfloor \gg 2KM$. Distribution of the candidate signatures between K users may be done in an arbitrary fashion, but naturally, we are interested in a distribution which minimizes MAI power (5.1). A promising way to obtain such a distribution is a random search, described in Section 5.3.1.

5.2 MAI Power Comparison of DS CDMA and SI DS CDMA

Let us now concentrate on comparison of MAI power for DS CDMA and SI DS CDMA. We will assume that delay spread is no greater than one half of the spreading factor, $L \leqslant N/2$, or, in other words, cyclic shifts of the same "raw" signature can be used, so that

$$s_k^u(i) = g_k(i + 2u), \tag{5.11}$$

where $g_k(i)$ is a "raw" signature (taken from Gold set, Kasami set or any other as described in the previous section).

As before, we will assume that $0 \leqslant m_{kl} \leqslant L-1$, so that the third row in (4.15) is not active. For the first row of (4.15) we have $0 \leqslant m_{kl} \leqslant u$, $0 \leqslant u \leqslant M-1$, and its contribution to the MAI power, denoted as TSC_1^1 is

$$\mathrm{TSC}_1^1 = \sum_{u=0}^{M-1} \sum_{m_{kl}=0}^{u} \sum_{k=1}^{K} \sum_{l=1}^{K} \left| \sum_{i=0}^{N-1} s_k^u(i) s_l^{u-m_{kl}}(i) \right|^2 \tag{5.12}$$

$$= \sum_{u=0}^{M-1} \sum_{m_{kl}=0}^{u} \sum_{k=1}^{K} \sum_{l=1}^{K} \left| \sum_{i=0}^{N-1} g_k(i+2u) g_l(i+2u-2m_{kl}) \right|^2, \tag{5.13}$$

where (5.11) is substituted for $s_k^u(i)$. Then

$$\mathrm{TSC}_1^1 = \sum_{u=}^{M-1} \sum_{m_{kl}=0}^{u} \sum_{k=1}^{K} \sum_{l=1}^{K} R_{kl}^2(2m_{kl}), \tag{5.14}$$

$R_{kl}^2(m)$ being even squared cross-correlation of $g_k(i)$ and $g_l(i)$.

Since (5.14) contains mainlobes for all bits of all users (KM in total), it is logical to subtract this contribution, obtaining the negative effect of foreign users only:

$$\mathrm{TSC}_1 = \mathrm{TSC}_1^1 - KM = \sum_{u=0}^{M-1} \sum_{m_{kl}=0}^{u} \sum_{k=1}^{K} \sum_{l=1}^{K} R_{kl}^2(2m_{kl}) - KM. \tag{5.15}$$

Independence of $R_{kl}^2(2m_{kl})$ of u allows to simplify computations, since summation in u, m_{kl} may be done differently:

$$\mathrm{TSC}_1 = \sum_{m_{kl}=0}^{M-1} \sum_{u=m_{kl}}^{M-1} \sum_{k=1}^{K} \sum_{l=1}^{K} R_{kl}^2(2m_{kl}) - KM$$

$$= \sum_{m_{kl}=0}^{M-1} (M - m_{kl}) \sum_{k=1}^{K} \sum_{l=1}^{K} R_{kl}^2(2m_{kl}) - KM. \tag{5.16}$$

Consider now contribution of the second row of (4.15), for which $u+1 \leqslant m_{kl} \leqslant M-1$, $0 \leqslant u \leqslant M-2$:

$$\mathrm{TSC}_2 = \sum_{u=0}^{M-2} \sum_{m_{kl}=u+1}^{M-1} \sum_{k=1}^{K} \sum_{l=1}^{K} \left| \sum_{i=1}^{N-1} s_k^u(i) s_l^{u-m_{kl}+M}(i-1) \right.$$

$$\left. + b s_k^u(0) s_l^{u-m_{kl}+M}(N-1) \right|^2 \tag{5.17}$$

where coefficient b takes on values ± 1 equiprobably. Substituting again (5.11) for $s_k^u(i)$ results in

$$\mathrm{TSC}_2 = \sum_{u=0}^{M-2} \sum_{m_{kl}=u+1}^{M-1} \sum_{k=1}^{K} \sum_{l=1}^{K} \left| \sum_{i=1}^{N-1} g_k(i+2u) g_l(i-1+2u-2m_{kl}+2M) + b g_k(2u) g_l(N-1+2u-2m_{kl}+2M) \right|^2 . \tag{5.18}$$

Using the fact that $g_l(i) = g_l(i+N)$ we have

$$\begin{aligned} \mathrm{TSC}_2 &= \sum_{u=0}^{M-2} \sum_{m_{kl}=u+1}^{M-1} \sum_{k=1}^{K} \sum_{l=1}^{K} \left| \sum_{i=0}^{N-1} g_k(i+2u) g_l(i-1+2u-2m_{kl}+2M) \right. \\ &\qquad \left. + (b-1) g_k(2u) g_l(N-1+2u-2m_{kl}+2M) \right|^2 \\ &= \sum_{u=0}^{M-2} \sum_{m_{kl}=u+1}^{M-1} \sum_{k=1}^{K} \sum_{l=1}^{K} \left| \sum_{i=0}^{N-1} R_{kl}\left(2(m_{kl}-M)+1\right) \right. \\ &\qquad \left. + (b-1) g_k(2u) g_l(N-1+2u-2m_{kl}+2M) \right|^2 . \end{aligned} \tag{5.19}$$

Averaging (5.19) in b gives

$$\begin{aligned} \overline{\mathrm{TSC}}_2 &= \frac{1}{2} \sum_{u=0}^{M-2} \sum_{m_{kl}=u+1}^{M-1} \sum_{k=1}^{K} \sum_{l=1}^{K} R_{kl}^2\left(2(m_{kl}-M)+1\right) \\ &\quad + \frac{1}{2} \sum_{u=0}^{M-2} \sum_{m_{kl}=u+1}^{M-1} \sum_{k=1}^{K} \sum_{l=1}^{K} \left| R_{kl}\left(2(m_{kl}-M)+1\right) \right. \\ &\qquad \left. - 2 g_k(2u) g_l(N-1+2u-2m_{kl}+2M) \right|^2 . \end{aligned} \tag{5.20}$$

Changing the order of summation in u and m_{kl} leads to

$$\begin{aligned} \overline{\mathrm{TSC}}_2 &= \frac{1}{2} \sum_{m_{kl}=1}^{M-1} \sum_{u=0}^{m_{kl}-1} \sum_{k=1}^{K} \sum_{l=1}^{K} R_{kl}^2\left(2(m_{kl}-M)+1\right) \\ &\quad + \frac{1}{2} \sum_{m_{kl}=1}^{M-1} \sum_{u=0}^{m_{kl}-1} \sum_{k=1}^{K} \sum_{l=1}^{K} \left| R_{kl}\left(2(m_{kl}-M)+1\right) \right. \\ &\qquad \left. - 2 g_k(2u) g_l(N-1+2u-2m_{kl}+2M) \right|^2 . \end{aligned} \tag{5.21}$$

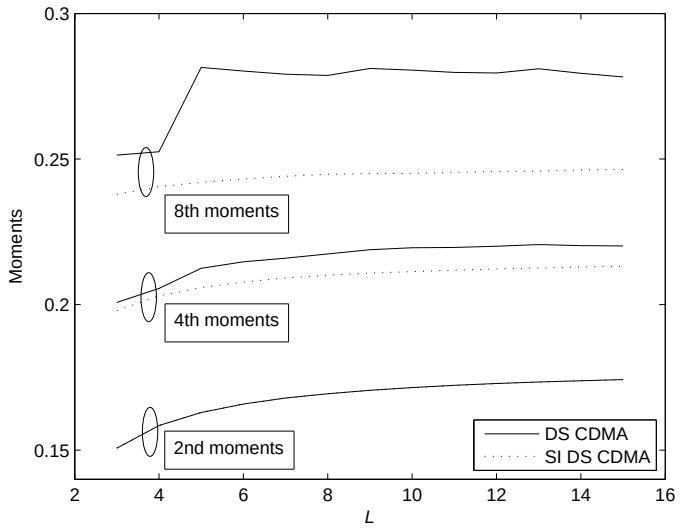

Figure 5.3: MAI moments for Gold ensemble, $K = 32$, $N = 31$

Finally, we have

$$\begin{aligned}\overline{\mathrm{TSC}}_2 = \frac{1}{2}\sum_{m_{kl}=1}^{M-1} m_{kl} \sum_{k=1}^{K}\sum_{l=1}^{K} R_{kl}^2\left(2(m_{kl}-M)+1\right) \\ + \frac{1}{2}\sum_{m_{kl}=1}^{M-1}\sum_{u=0}^{m_{kl}-1}\sum_{k=1}^{K}\sum_{l=1}^{K}\Big| R_{kl}\left(2(m_{kl}-M)+1\right) \\ - 2g_k(2u)g_l(N-1+2u-2m_{kl}+2M)\Big|^2 . \end{aligned} \tag{5.22}$$

Total squared correlation is then a summation of (5.16) and (5.22):

$$\mathrm{TSC} = \mathrm{TSC}_1 + \overline{\mathrm{TSC}}_2, \tag{5.23}$$

and an average squared correlation is (5.23) divided by the total number of addends (MAI contributors):

$$\overline{R^2} = \frac{\mathrm{TSC}}{KM(KM-1)} = \frac{\mathrm{TSC}_1 + \overline{\mathrm{TSC}}_2}{KM(KM-1)}. \tag{5.24}$$

Repeating (5.16), (5.22) and (5.24) for a bigger integer than 2, higher moments [83] can be obtained.

Consider now some illustrative comparisons of MAI power of DS CDMA and SI DS CDMA. Figure 5.3 shows difference in 2, 4 and 8-th moments for Gold ensemble of length $N = 31$ implementing $K = 32$ users; Figure 5.4 for

Gold ensemble of length $N = 127$ implementing $K = 63$ users. It is seen that all the moments are bigger for DS CDMA, and the difference increases with the moment order.

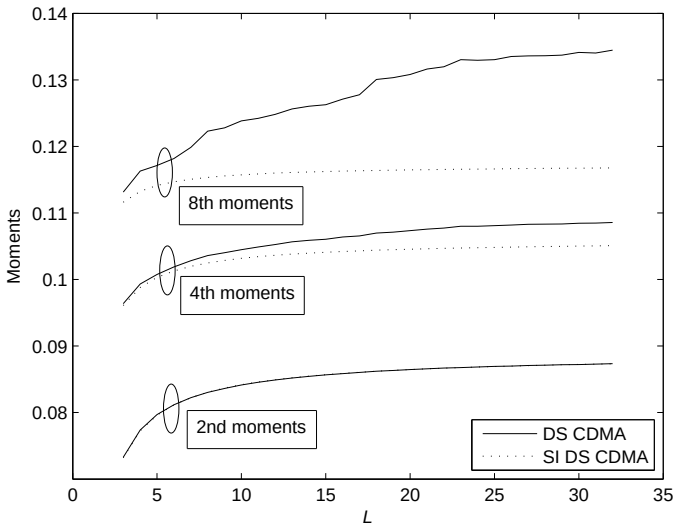

Figure 5.4: MAI moments for Gold ensemble, $K = 63$, $N = 127$

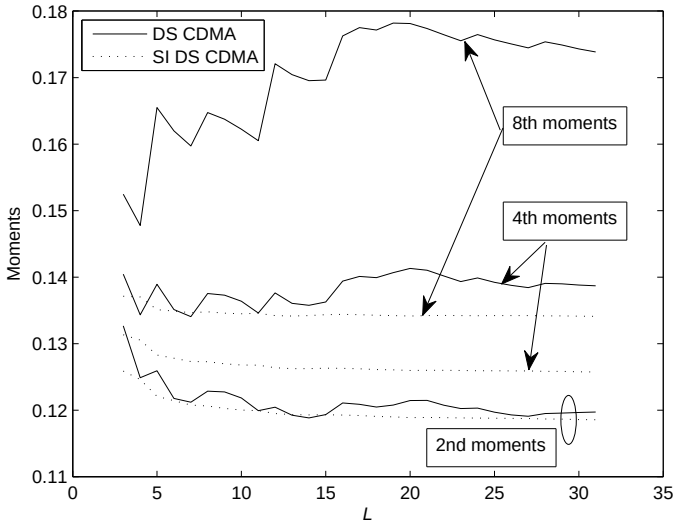

Figure 5.5: MAI moments for Kasami ensemble, $K = 8$, $N = 63$

In this Thesis the Gaussian approximation was used in order to obtain BER from the average power of MAI. However, MAI statistics are not Gaussian, as will be demonstrated, for example, in the next section in Figure 5.6. To obtain a more precise approximation, the usage of higher moments of

MAI is necessary, and since for DS CDMA all these moments are bigger, it is reasonable to expect that BER for DS CDMA will be bigger, too.

Figure 5.4 also demonstrates that for the 8-th moment difference in moment value also increases with the maximal delay L. This suggests that the advantage of SI DS CDMA system will be also increasing with L.

Figure 5.5 for Kasami ensemble of length $N = 63$ implementing $K = 8$ users. All notes for the Gold ensemble moments apply; the difference for the moments for DS CDMA and SI DS CDMA is even bigger.

5.3 BER Comparison of DS CDMA and SI DS CDMA

Consider as an example conventional DS CDMA system with the spreading factor $N = 127$ and $K = 10$ users. Suppose that the system is under 4-rays Rayleigh multipath propagation with average ray energies $\alpha_r^2 = \overline{A_k^2} = [0, -3, -4, -5]$ dB, random ray phases with uniform probability distribution over $[0, 2\pi]$ and delays $m_r = [0, 1, 3, 5]$ chips, which is a typical example of an exponentially decaying multipath channel [16, 42]. Since $K(L + 1) < N$, the signature ensemble can be constructed of K cyclic shifts of a binary m-sequence of the same length as the spreading factor $N = 127$, offset from each other by $L + 1$ chips. This choice guarantees low level of MAI in at least one-half of occurrences, when consecutive data bits of an l-th foreign user in a delayed multipath signal remain the same within the integration interval of the k-th receiver, and thus odd CCFs do not appear at the k-th correlator output.

As in Section 3.4.3, for the system performance comparison we will use bit error probability estimated analytically by the Gaussian approximation. The curve calculated from (3.42), (3.40) and (4.20) for conventional DS CDMA employing the signature ensemble in question is shown in Figure 5.6 (solid line). The results of computer simulation for the same dependence of the bit error probability on SNR are also presented (dotted line). All results are averaged over users, ray phases and amplitudes assuming their independence.

As an alternative, consider the system employing $KM = KL$ even cyclic shifts of the same m-sequence, which is possible since $2KM < N$. Every of K users is then assigned M different signatures of the obtained set. As described in Section 5.1.2, the obtained signature ensemble is LCZ one, with squared periodic correlations of zero and first shift $R^2_{(k,i),(l,j)}(m) = 1/N^2$, $m = \{0, 1\}$, for any variable values except $(m = 0) \cup (k = l) \cup (i = j)$.

As the second alternative consider a system where demand to the signature alphabet is relaxed to the ternary case, making it possible to use as a signature ensemble even cyclic shifts of a sequence with perfect PACF.

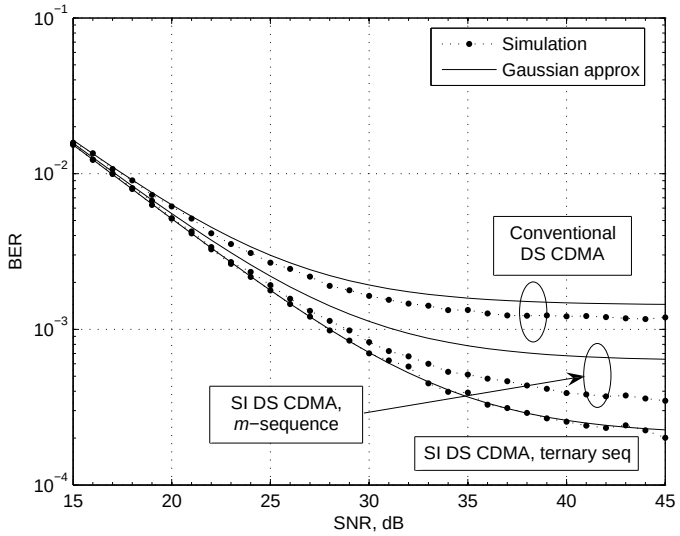

Figure 5.6: Rayleigh channel, $K = 10$ users with spreading factor $N = 127$, m-sequence and ternary sequence

Suitable for the situation in question, a ternary sequence of length $N_1 = 124$ exists [63, 64]. Since inequality $2KM < N_1$ is satisfied, it is possible to assign every user M different cyclic shifts of the ternary sequence. For such an ensemble for $m = \{0, 1\}$ and all combinations of k, l, i and j except $(m = 0) \cup (k = l) \cup (i = j)$ periodic correlations are zero, $R^2_{(k,i),(l,j)}(m) = 0$, making the obtained ensemble ZCZ.

Results for the Gaussian approximations, averaged over users and calculated from (3.42), (3.40) and (5.1) for the considered alternatives are also presented in Figure 5.6, as well as the results of computer simulation as dependencies of the bit error rate on SNR. As is seen, at low values of SNR all considered systems provide almost the same performance, which is to be expected, since in this region BER is mostly defined by the noise component of an overall interference. At the same time, as SNR grows, the MAI contribution increases in importance and therefore reduction of MAI in SI CDMA leads to a considerable performance gain. The graphs convincingly demonstrate that both considered alternatives provide markedly lower probability of error than the conventional DS CDMA system; SI DS CDMA using cyclic shifts of the ternary sequence having the best performance. Irreducible BER (error floor) is lowered for the both alternatives. Divergence of the simulation results from Gaussian approximation occurs due to the fact that MAI for both cases have statistics, differing from the Gaussian ones.

Another system comparison is provided by Figure 5.7, where for conventional system $K = 10$ signatures of Gold set of length $N = 63$ are implemented, while for SI DS CDMA their cyclic shifts are used as signatures.

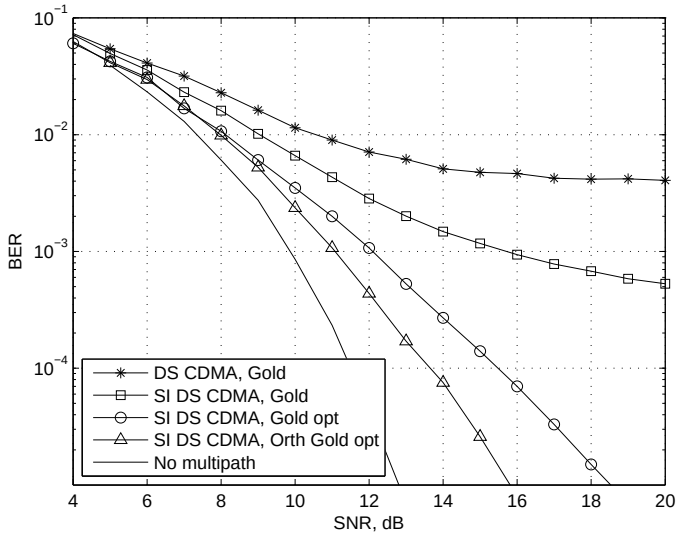

Figure 5.7: AWGN channel, $K = 10$ users with spreading factor $N = 63$, Gold codes

The channel is AWGN, otherwise identical to the previous scenario.

Simulation results for conventional DS CDMA are presented by the line with stars, and for SI DS CDMA by the line with squares. It is clearly seen that SI DS CDMA provides significant gain and reduces the error floor. It is possible, however, to achieve even bigger gain, as described in the next Section.

5.3.1 Optimization of Signature Ensembles Using Random Search

As was mentioned in Section 5.1.3, for a "raw" ensemble of P sequences of length N distribution of their even cyclic shifts among the K users for SI DS CDMA can be done in arbitrary fashion, since for the most ensembles number of candidate sequences is much greater than the number of necessary ensembles for SI DS CDMA: $\lfloor PN/2 \rfloor \gg KM$. However, a set of sequences which minimizes the average MAI power (5.1) would be, naturally, preferable.

Such a set can be found by a random search procedure, which can be illustrated by the following example. A computer simulation was performed in MATLAB environment over 10^6 iterations. At each iteration KM signatures were randomly chosen from the even cyclic shifts of the original Gold set and the average MAI power (5.1) was calculated. Finally, all the calculated MAI powers were compared and the set with the minimum one was taken.

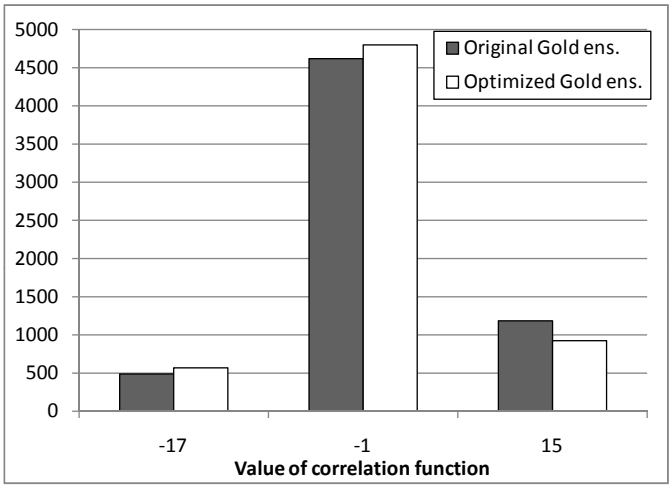

Figure 5.8: Distribution of the CCF values for original and optimized Gold ensemble, $K = 10$, $N = 63$

A comparison of the obtained set (denoted as the optimized Gold ensemble) with the original Gold ensemble is presented in Figure 5.8, where distributions of the CCF values are shown for the both ensembles. Note that according to (4.16) only the limitation of the *maximal* value of CCF is guaranteed for SI DS CDMA, while for the error rate it is also important how often this value is met. It is seen from the figure that the number of CCFs with maximal value 15 is decreased in the optimized ensemble, while CCFs with value -1 are met more often.

Bit error rate for the obtained optimized ensemble is also presented in Figure 5.7 (line with circles). It is seen that the optimization procedure provides significant advantage in terms of BER, resulting in 4 dB gain at the BER level 10^{-3} and removing the error floor.

There exists an approach how BER can be minimized even further. It is known that for the most multipath propagation profiles met in practice, amplitude of the first multipath ray is the biggest [16, 93, 105]: $\alpha_1^2 \geq \alpha_r^2$, $2 \leq r \leq R$. Return again to the expression of the average MAI (5.1), this fact means that the biggest contribution to the average MAI power belongs to the first term, since its scaling coefficient is the biggest:

$$\alpha_1^2 > 0.5\alpha_r^2, \quad 2 \leq r \leq R. \tag{5.25}$$

This term is defined by the correlations at zero shift $R_{(k,i),(l,i)}(0)$, so a signature ensemble for which these CCFs turn into zeros would be desirable for SI DS CDMA.

Such an ensemble does exist; it is called an orthogonal Gold ensemble [96] and can be easily constructed from a "usual" Gold ensemble. Denote the

signatures of a binary nonnormalized Gold set of length N as $\mathbf{s}_k$, $1 \le k \le N+2$. Then signatures of the orthogonal Gold set are constructed by adding a unity in the beginning of the each Gold sequence:

$$\mathbf{s}'_k = [1 \ \mathbf{s}_k], \quad 1 \le k \le N+2. \tag{5.26}$$

Recalling from Section 2.8.1 that for the $N+1$ Gold signatures their CCF at zero shift equals -1, $R_{kl}(0) = -1$, $k \ne l$, it is easy to see that for the orthogonal Gold ensemble these CCFs are zeros:

$$R'_{kl}(0) = \mathbf{s}'_k(\mathbf{s}'_l)^T = 1 + R_{kl}(0) = 0, \tag{5.27}$$

and the average MAI power (5.1) is turned into

$$\overline{P^i_{\mathrm{MAI},k}} = \frac{1}{2}\sum_{r=2}^{R}\alpha_r^2\sum_{l=1}^{K}\chi_{k,l}(i,r), \tag{5.28}$$

so that the influence of the first multipath ray is completely eliminated.

Bit error rate for the optimized orthogonal Gold ensemble is shown in the Figure 5.7 (line with triangles). Its advantage over the conventional Gold ensemble is clearly seen; there is 1 dB gain at the BER level 10^{-3} and about 2 dB gain at the BER level 10^{-4}. Note that despite the multipath channel, performance of the SI DS CDMA with the optimized orthogonal Gold ensemble is only 1 dB worse at BER 10^{-3} than the one in AWGN channel *without* multipath propagation (solid line).

Chapter 6

RAKE Reception for SI DS CDMA in a Multipath Channel

Previous chapters were dedicated to a single-user receiver (matched filter) for SI DS CDMA, and it was shown that it allows to mitigate negative consequences of the multipath propagating to the system performance. However, performance degradation due to multipath fading may be also overcome by employing diversity. A popular way to do so is an implementation of a RAKE receiver, which performs combining of the received multipath components. However, in this case system performance may be limited by increased MAI, which is combined as well.

In this Chapter we analyze efficiency of an equal gain combining (EGC) RAKE receiver for SI DS CDMA in synchronous multipath Rayleigh channel in comparison with that of conventional DS CDMA. It is shown that for a RAKE receiver SI DS CDMA system remains advantages over conventional DS CDMA in terms of bit error rate. Theoretical computations are confirmed by results of the conducted computer simulation, which demonstrated superiority of SI DS CDMA in terms of BER. It is also demonstrated that performance can be further improved by using specifically tailored user signatures.

In Section 6.1 EGC RAKE is described with respect to conventional DS CDMA system, and an expression of its output is obtained. Section 6.2 provides analogous calculations for SI DS CDMA. Finally, in Section 6.3 the performance comparison is presented, with regard to the SNR and the number of users.

6.1 EGC RAKE for Conventional DS CDMA

As before, consider Rayleigh channel with R paths, r-th one having amplitude A_r, phase φ_r and delay τ_r, $1 \le r \le R$. Assume delays of the paths to be nonnegative multiples m_r of the chip duration, $\tau_r = m_r\Delta$, with m_r bounded from above by the constant L: $0 \le m_1 \le \ldots \le m_r \le \ldots \le m_R \le L$, where rays are sorted in non-decreasing order of their delays. We will also assume that fading pattern remains stable during the bit interval, that is, A_r and φ_r are treated as constants. Then complex envelope of the received group signal is of the form

$$y(t) = \sum_{r=1}^{R} A_r s(\mathbf{b}; t - \Delta m_r) \exp(j\varphi_r) + n(t). \tag{6.1}$$

We assume that at the receiving end an equal gain combining RAKE [6,7] is implemented with perfect knowledge of the paths phases, which for the k-th user can be described as calculating correlation of (6.1) and the modified signature

$$s'_k(t) = \sum_{r=1}^{R} s_k(t - \Delta m_r) \exp(-j\varphi_r), \tag{6.2}$$

providing the following result at the output of the receiver:

$$\begin{aligned}
z_k(i) = b_k(i) & \sum_{r=1}^{R} A_r \\
& + \sum_{p=1}^{R} A_p \Bigg[\sum_{\substack{l=1 \\ l \ne k}}^{K} b_l(i) R_{kl}(0) \\
& + \sum_{r=1}^{p-1} \exp\left(j(\varphi_p - \varphi_r)\right) \sum_{l=1}^{K} \Big\{ b_l(i) R_{a,kl}(m_r - m_p) \\
& \qquad + b_l(i+1) R_{a,kl}(N + m_r - m_p) \Big\} \\
& + \sum_{r=p+1}^{R} \exp\left(j(\varphi_p - \varphi_r)\right) \sum_{l=1}^{K} \Big\{ b_l(i-1) R_{a,kl}(m_r - m_p - N) \\
& \qquad + b_l(i) R_{a,kl}(m_r - m_p) \Big\} \Bigg] \\
& + n_k,
\end{aligned} \tag{6.3}$$

where $b_l(i-1)$ and $b_l(i+1)$ are, respectively, information bits of the l-th user preceding and following $b_l(i)$, and $R_{a,kl}(m)$, as before, is an aperiodic

cross-correlation function between signatures $\mathbf{s}_k$ and $\mathbf{s}_l$ of shift m. Finally, a decision on the bit $b_k(i)$ is formed as

$$\hat{b}_k(i) = \mathrm{sgn}\left(\mathrm{Re}\left[\mathrm{z_k(i)}\right]\right). \tag{6.4}$$

The first, second and third terms inside the square brackets in (6.3) represent MAI, from foreign users' signals of the same multipath ray p, $1 \leq p \leq R$; from user signals of the multipath rays with delays no greater than the current one $m_r \leq m_p$, $1 \leq r \leq p-1$; and from user signals of the multipath rays with delays no smaller than the current one, $m_r \geq m_p$, $p+1 \leq r \leq R$, respectively. These equations indicate that MAI level is governed by values of aperiodic CCFs of shifts up to $\max(m_r) = L$. As was shown in the previous chapters, for usually implemented signature ensembles (Gold, Kasami, cyclic shifts of m-sequence etc) values of those are uncontrollable and occur almost at random [99], which may result in high level of MAI and degrade system performance. It is possible, however, to change system design so that only cross-correlations of zero and first shift affect MAI level *independently* of the maximal delay value.

6.2 EGC RAKE for Signature Interleaved DS CDMA

Let us recall from Chapter 4 that the transmitted group signal for SI DS CDMA takes the form

$$s(t) = \sum_{k=1}^{K} \sum_{i=0}^{M-1} b_k(i) \sum_{j=0}^{N-1} s_k^i(j) c_0(t - i\Delta - jM\Delta). \tag{6.5}$$

On the ground analogous to the previous section, output of EGC RAKE receiver of the k-th user processing bit $b_k(i)$, $i = 0, 1, \ldots, M-1$ may then be written as

$$\begin{aligned} z_k^i = b_k(i) \sum_{r=1}^{R} A_r + \sum_{p=1}^{R} A_p \Bigg[& \sum_{\substack{l=1 \\ l \neq k}}^{K} b_l(i) R_{(k,i),(l,i)}(0) \\ & + \sum_{r=1}^{p-1} \exp\left(j(\varphi_p - \varphi_r)\right) \sum_{l=1}^{K} \mu_{kl}(i,r) \\ & + \sum_{r=p+1}^{R} \exp\left(j(\varphi_p - \varphi_r)\right) \sum_{l=1}^{K} \varsigma_{kl}(i,r) \Bigg] + n_k, \end{aligned} \tag{6.6}$$

where

$$\mu_{kl}(i,r) = \begin{cases} b_l(i'') R_{(k,i),(l,i'')}(0), & i < M - m_p + m_r, \\ b_l(i'') R_{(k,i),(l,i'')}(-1) & \\ \quad + b_l^1(i'') R_{(k,i),(l,i'')}(N-1), & i \geq M - m_p + m_r, \end{cases} \tag{6.7}$$

corresponds to the paths with delays no greater than that of the current path $m_r \leq m_p$, $1 \leq r \leq p-1$, where $i'' = (i + m_p - m_r) \bmod M$, and

$$\varsigma_{kl}(i,r) = \begin{cases} b_l(i')R_{(k,i),(l,i')}(0), & i \geq m_r + m_p, \\ b_l^{-1}(i')R_{(k,i),(l,i')}(1-N) & \\ \quad + b_l(i')R_{(k,i),(l,i')}(1), & i < m_r - m_p, \end{cases} \tag{6.8}$$

corresponds to the paths with delays no smaller than that of the current path $m_r \geq m_p$, $p+1 \leq r \leq R$, where $i' = (i - m_r) \bmod M$. $R_{(k,i),(l,j)}(m)$ is aperiodic cross-correlation between signatures $\mathbf{s}_k^i$ and $\mathbf{s}_l^j$; $b_l^1(i)$ and $b_l^{-1}(i)$ are, respectively, the i-th information bits of the M-blocks following and preceding the current one.

Equation (6.6) demonstrates that for SI DS CDMA MAI depends on correlations of non-shifted or just one-chip-shifted signatures only, *independently* of the maximal multipath delay. Values of these correlations can be easily retained under control, making thus level of MAI much smaller than that of conventional DS CDMA.

6.3 Performance Comparison

In order to support abovementioned statement, the performance simulation was carried out for the system with spreading factor $N = 127$, $K = 10$ users under 4-path Rayleigh multipath propagation with average path energies $\overline{A_r^2} = [0, -6, -11.9, -17.9]$ dB, random path phases with uniform probability distribution over $[0, 2\pi]$ and path delays $m_r = [0, 3, 4, 7]$ chips, which corresponds to the Office Channel B propagation model [13].

For conventional DS CDMA $K = 10$ Gold signatures of length $N = 127$ were used as user signature ensemble, which is a reasonable choice used in practice. For SI DS CDMA user signatures were formed as $L = 7$ even cyclic shifts of Gold signatures as described in Section 5.1, since the chosen parameters ($2KL > N$) make usage of ZCZ or low correlation zone ensemble impossible. Similar to Section 5.3.1, a random search was performed to find among all possible cyclic shifts of the Gold ensemble the ones that minimize MAI.

As an additional reference ensemble of orthogonal Gold signatures was used as user signature ensemble for DS CDMA, and its even cyclic shifts as user signature ensemble for SI DS CDMA. In both systems a 4-finger EGC RAKE receiver was implemented [7].

Dependence of bit error rate on signal-to-noise ratio is shown in Figure 6.1. The results are averaged over users, information bits, ray amplitudes and phases, assuming their independence. The graphs demonstrate that RAKE receiver for SI DS CDMA system secures smaller probability of

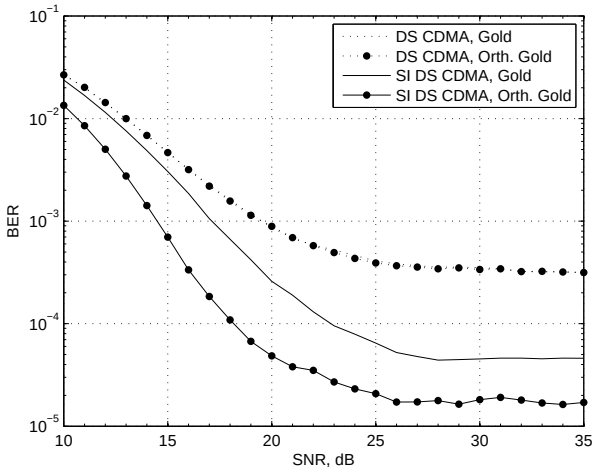

Figure 6.1: 4-finger EGC RAKE, BER vs SNR. $K = 10$, $N = 127$.

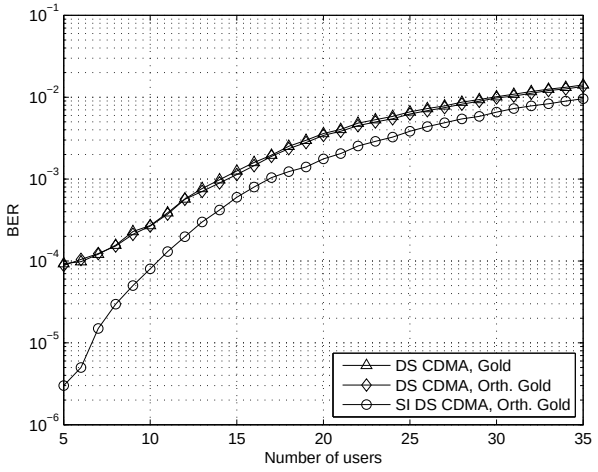

Figure 6.2: 4-finger EGC RAKE, BER vs the number of users. $N = 127$.

error than that of DS CDMA, providing for the Gold ensemble more that 2 dB gain at the BER level 10^{-3} and lowering irreducible BER (error floor).

While for conventional DS CDMA switching to orthogonal Gold signature ensemble does not provide any benefit, for SI DS CDMA it increases gain at the BER level 10^{-3} to 5 dB and lowers irreducible BER further. This can be explained by the fact that for conventional DS CDMA MAI level is defined mostly by aperiodic correlations of user signatures of big shifts, which do not differ much for Gold and orthogonal Gold ensembles. At the same time for SI DS CDMA significant role of defining MAI belongs to user signature correlations of zero shift, which for orthogonal Gold ensemble are zero, $R_{kl}(0) = 0$, $1 \leq k, l \leq K$, $k \neq l$.

Dependence of BER on the number of users is shown in Figure 6.2. It is seen that for the probability of error 10^{-4} SI DS CDMA can accommodate five more users.

Chapter 7

Conclusions

In this Thesis the signature-interleaved DS CDMA was introduced and its efficiency was analyzed in comparison with conventional DS CDMA. It was demonstrated that for SI DS CDMA the average MAI power at the output of a single user correlator and EGC RAKE receiver depends only on correlations of either non-shifted at all or just one-chip-shifted signatures *independently* of the multipath delay value. These correlations can be easily retained under predictably low bound, and as a result, SI DS CDMA provides markedly better performance in terms of bit error rate.

In Chapter 3 an idea of chip interleaving as well as its modifications was considered in application to mitigate harmful effect of asynchronism between users. The chip-interleaving decorrelating detector has been proposed and analyzed. It was demonstrated that the novel algorithm reduces signature asynchronism to no more than one chip interval transforming the decorrelation to a virtually synchronous one. Thereby the chip-interleaved decorrelation secures optimal near-far resistance and provides a visible energy gain, which can be further increased by means of a proper adjustment of signature ensemble as well as increasing interleaving block size.

Then the utilization of group orthogonal CDMA in asynchronous channels was analyzed with the implementation of interleaving and zero padding. It was shown that this approach results in bit-synchronous user signals at the receiving end. Theoretical calculations and computer simulations demonstrated that performance of the system is equivalent to the one operating in synchronous channels, meaning that deteriorative effect of asynchronous delays between users is completely eliminated. More than that, at low SNR values the asynchronous GO-CDMA system can provide $1 \ldots 2$ dB advantage against transmission in synchronous channels in terms of bit error rate. Thus range of oversaturated systems application, by design limited to synchronous channels only, is expanded to asynchronous channels as well.

Finally, implementation of a cyclic prefix in an asynchronous DS CDMA

system has been described and analyzed. Theoretical estimates and computer simulations indicated that removal of odd correlations in DS CDMA thanks to the insertion of a cyclic prefix may in certain scenarios appear beneficial with regard to system performance without compromising system spectral efficiency.

In Chapter 4 the main focus was shifted to the asynchronism caused by multipath propagation. Under these conditions the chip interleaving proves to be inefficient due to appearance of autocorrelations of zero shift, which increases interference level substantially. Instead, it was suggested to combine chip interleaving with utilization of more than one signature per user, the novel idea called signature interleaving. It was shown in details that this approach transforms any asynchronysm to the delay of one chip only.

In Chapter 5 the emphasis was given to signature ensembles for SI DS CDMA. Various signature ensembles were synthesized based on different demands to correlation properties. Expressions for the average MAI power for a single-user receiver were also obtained for conventional DS CDMA and for SI DS CDMA.

Performance of a single-user correlator in SI DS CDMA system utilizing different signature sets was also investigated in this Chapter. A random search was implemented in order to improve correlation properties of signature ensembles. While optimizing ensemble obtained from Kasami set did not lead to any valuable result, optimization of the ensemble obtained form Gold set provided significant gain in BER performance as compared to conventional DS CDMA. Additional gain can be obtained if orthogonal Gold set is implemented.

Finally, in Chapter 6 usage of equal gain combining RAKE receiver for signature-interleaved DS CDMA in Rayleigh multipath channel was analyzed and its performance was compared with that of conventional DS CDMA system. It was demonstrated that for SI DS CDMA MAI level at the output of the RAKE receiver depends on user signature correlations of zero and one shift only, independently of the multipath delay. Theoretical computations were confirmed by results of the conducted computer simulation, which demonstrated superiority of SI DS CDMA in terms of BER. It is also demonstrated that performance can be further improved by using specifically tailored user signatures.

Despite the fact that the Thesis was supposed to serve as a comprehensive study on chip and signature interleaving, the subject for further research can be briefly underlined. First, implementation of chip interleaving with zero padding for oversaturated GO-CDMA in multipath fading requires further research. Although it was shown that in asynchronous AWGN channel usage of such chip-interleaving for GO-CDMA can be very beneficial, the case when asynchronism is created due to multipath propagation was left

out of the picture. Then, the procedure of signature ensemble creation for SI DS CDMA can be investigated further. In this Thesis it was suggested to use random search to find an appropriate ensemble, whereas the regular algorithm to construct signature ensemble would be preferable.

Bibliography

[1] WPAN high rate alternative PHY. Technical report, IEEE 802.15.3a task group.

[2] WPAN low rate alternative PHY. Technical report, IEEE 802.15.4a task group.

[3] A conversation with Claude Shannon. *IEEE Commun. Mag.*, 22(5):123–126, 1984.

[4] F. Adachi, M. Sawahashi, and H. Suda. Wideband DS-CDMA for next-generation mobile communications systems. *IEEE Commun. Mag.*, 36(9):56–69, 1998.

[5] G. R. Aiello and G. D. Rogerson. Ultra-wideband wireless systems. *IEEE Microw. Mag.*, 4(2):36–47, June 2003.

[6] M. S. Alouini, S. W. Kim, and A. Goldsmith. RAKE reception with maximal-ratio and equal-gain combining for DS-CDMA systems in Nakagami fading. In *Proc. of the 6th IEEE Int. Conf. on Universal Personal Commun. Record*, volume 2, 1997.

[7] A. Annamalai, C. Tellambura, and V. K. Bhargava. Equal-gain diversity receiver performance in wireless channels. *IEEE Trans. Commun.*, 48(10):1732–1745, 2000.

[8] H. Arslan, Z. N. Chen, and M.-G. Di Benedetto. *Ultra Wideband Wireless Communication*. Wiley-Interscience, 2006.

[9] R. H. Barker. Group synchronizing of binary digital systems. *Commun. Theory*, pages 273–287, 1953.

[10] P. Baronti, P. Pillai, V. W. C. Chook, S. Chessa, A. Gotta, and Y. F. Hu. Wireless sensor networks: A survey on the state of the art and the 802.15.4 and ZigBee standards. *Comput. Comm.*, 30(7):1655–1695, 2007.

[11] K. L. Baum, T. A. Thomas, F. W. Vook, and V. Nangia. Cyclic-prefix CDMA: an improved transmission method for broadband DS-CDMA cellular systems. In *Proc. Wireless Commun. and Networking Conference, WCNC2002*, volume 1, 2002.

[12] L. D. Baumert. *Cyclic Difference Sets*. Springer-Verlag, 1971.

[13] P. A. Bello. Generic channel simulator. Report BTR 103, final report under contract MDA904-95-C-2078, BELLO, Inc., 1997.

[14] A. Bensky. *Short-range Wireless Communication: Fundamentals of RF System Design and Application*. Elsevier, 2 edition, 2004.

[15] R. E. Blahut. *Algebraic Codes for Data Transmission*. Cambridge: Cambridge University Press, 2003.

[16] N. Blaunstein and J. B. Andersen. *Multipath Phenomena in Cellular Networks*. Artech House, 2002.

[17] A. B. Carlson. *Communication Systems*. McGraw-Hill New York, 1986.

[18] B. Chatschik. An overview of the Bluetooth wireless technology. *IEEE Commun. Mag.*, 39(12):86–94, December 2001.

[19] D. S. Chen and S. Roy. An adaptive multiuser receiver for CDMA systems. *IEEE J. Sel. Areas Commun.*, 12(5):808–816, June 1994.

[20] D. Chu. Polyphase codes with good periodic correlation properties (corresp.). *IEEE Trans. Inf. Theory*, 18(4):531–532, July 1972.

[21] H. A. Cirpan and M. K. Tsatsanis. Chip interleaving in direct sequence CDMA systems. In *Proc. IEEE Int. Conf. Acoustics, Speech, and Signal Processing (ICASSP'97)*, volume 5, 1997.

[22] G. R. Cooper and R. W. Nettleton. A spread-spectrum technique for high-capacity mobile communications. *IEEE Trans. Veh. Technol.*, 27(4):264–275, 1978.

[23] X. Deng and P. Fan. Spreading sequence sets with zero correlation zone. *IEE Electron. Lett.*, 36(11):993–994, May 2000.

[24] E. H. Dinan and B. Jabbari. Spreading codes for direct sequence CDMA and wideband CDMA cellular networks. *IEEE Commun. Mag.*, 36(9):48–54, September 1998.

[25] C. Ding, M. Golin, and T. Kløve. Meeting the Welch and Karystinos-Pados bounds on DS-CDMA binary signature sets. *Designs, Codes and Cryptography*, 30(1):73–84, August 2003.

[26] R. C. Dixon. *Spread Spectrum Systems with Commercial Applications.* John Wiley & Sons, 1994.

[27] D. V. Djonin and V. K. Bhargava. New results on low complexity detectors for over-saturated CDMA systems. In *Proc. IEEE Global Telecommunication Conf. (GLOBECOM'96)*, volume 2, pages 846–850, San Antonio, TX, USA, November 25–29, 2001.

[28] A. Dudkov. Optimization of signature ensembles for SI DS CDMA using random search. In *Proc. IEEE 7th Int. Symp. Electromagnetic Compatibility and Electromagnetic Ecology*, Saint-Petersburg, Russia, June 26–29, 2007.

[29] A. Dudkov. RAKE reception for signature-interleaved DS CDMA in Rayleigh multipath channel. In *Proc. of the 6th International Workshop on Multi-Carrier Spread Spectrum (MC-SS 2007)*, Herrsching, Germany, May 7–9, 2007.

[30] A. Dudkov. Signature ensembles for signature-interleaved DS CDMA. In *Proc. of the Signal Processing for Wireless Commun. Workshop (SPWC 2007)*, London, UK, June 6–8, 2007.

[31] A. Dudkov. Signature-interleaved DS CDMA in Rayleigh multipath channel. In *Proc. of the IEEE Int. Symp. on Wireless Communication Systems (ISWCS'07)*, Trondheim, Norway, October 16–19, 2007.

[32] A. Dudkov and V. Ipatov. Asymptotic optimality of random PSK signature ensembles. In *Proc. of the 6th IEEE Int. Symp. on Electromagnetic Compatibility and Electromagnetic Ecology (EMC'05)*, Saint-Petersburg, Russia, June 26–29, 2005.

[33] A. Dudkov and V. Ipatov. Eliminating odd correlations in asynchronous DS CDMA employing cyclic prefix. In *Proc. of the IEEE Mediterranean Electrotechnical Conf. (MELECON 2006)*, Malaga, Spain, May 3–7, 2006.

[34] A. Dudkov and V. Ipatov. Chip-interleaved decorrelation in asynchronous DS CDMA. In *Proc. of the VIII IEEE Workshop on Signal Processing Advances in Wireless Commun. (SPAWC 2007)*, Helsinki, Finland, June 17–20, 2007.

[35] A. Dudkov and V. P. Ipatov. Signature-interleaved DS CDMA: controlling odd correlation peaks. In *Proc. IEEE 16th Int. Symp. Personal, Indoor and Mobile Radio Commun. (PIMRC'05)*, volume 4, pages 2527–2530, September 11–14, 2005.

[36] A. Dudkov and J. Paavola. Asynchronous oversaturated group orthogonal CDMA using chip interleaving with zero padding. In *Proc. of the IEEE Int. Symp. on Wireless Communication Systems (ISWCS'07)*, Trondheim, Norway, October 16–19, 2007.

[37] A. Dudkov, J. Paavola, and V. Ipatov. Oversaturated group orthogonal CDMA in multipath channels using chip interleaving with zero padding. In *Proc. of the 18th Annual IEEE Int. Symp. on Personal Indoor and Mobile Radio Commun. (PIMRC'07)*, Athens, Greece, September 3–7, 2007.

[38] A. Duel-Hallen, J. Holtzman, and Z. Zvonar. Multiuser detection for CDMA systems. *IEEE Personal Commun. Mag.*, 2(2):46–58, April 1995.

[39] J. Eberspächer, C. Hartmann, C. Bettstetter, and H. Vögel. *GSM – Architecture, Protocols and Services*. Wiley-Blackwell, 2009.

[40] A. El-Rabbani. *Introduction to GPS: The Global Positioning System*. Artech House, 2002.

[41] S. Eliahou and M. Kervaire. Barker sequences and difference sets. *L'Enseignement Mathématique*, 38:345–382, 1992.

[42] T. Eng and L. B. Milstein. Coherent DS-CDMA performance in Nakagami multipath fading. *IEEE Trans. Wireless Commun.*, 43(234):1134–1143, 1995.

[43] M. Ergen. *Mobile Broadband: Including WiMAX and LTE*. Springer, 2009.

[44] M. Etoh. *Next Generation Mobile Systems: 3G & Beyond*. John Wiley and Sons, 2005.

[45] P. Fan and M. Darnell. *Sequence Design for Communications Applications*. John Wiley and Sons, 1996.

[46] P. Z. Fan, N. Suehiro, N. Kuroyanagi, and X. M. Deng. Class of binary sequences with zero correlation zone. *IEE Electron. Lett.*, 35:777–779, 1999.

[47] K. Fazel and S. Kaiser. *Multi-Carrier and Spread Spectrum Systems*. John Wiley and Sons, 2003.

[48] R. Frank. Polyphase codes with good nonperiodic correlation properties. *IEEE Trans. Inf. Theory*, 9(1):43–45, January 1963.

[49] M. Ghavami, L. B. Michael, and R. Kohno. *Ultra Wideband Signals and Systems in Communication Engineering*. John Wiley & Sons, 2004.

[50] D. Gislason. *Zigbee Wireless Networking*. Newnes, 2008.

[51] S. G. Glisic. *Advanced Wireless Communications: 4G Technologies*. John Wiley and Sons, 2004.

[52] R. Gold. Optimal binary sequences for spread spectrum multiplexing. *IEEE Trans. Inf. Theory*, 13(5):619–621, May 1967.

[53] S. W. Golomb. *Shift Register Sequences*. Aegean Park Press, 1992.

[54] S. W. Golomb and G. Gong. *Signal Design for Good Correlation for Wireless Communication, Cryptography, and Radar*. Cambridge University Press, 2005.

[55] G. H. Golub and C. F. Van Loan. *Matrix Computations*. JHU Press, 3 edition, 1996.

[56] X. Gui and T. S. Ng. A novel chip-interleaving DS SS system. *IEEE Trans. Veh. Technol.*, 49(1):21–27, 2000.

[57] T. Halonen, R. G. Romero, J. Romero, and J. Melero. *GSM, GPRS and EDGE Performance: Evolution Towards 3G/UMTS*. John Wiley and Sons, 2003.

[58] E. Hardouin and C. Laot. A chip-interleaving pattern retaining orthogonality in DS-CDMA systems: application to the multicode downlink. In *Proc. IEEE 58th Vehicular Technology Conference (VTC 2003-Fall)*, volume 4, 2003.

[59] S. Haykin. *Communication Systems*. John Wiley & Sons, 2001.

[60] B. Hoffman-Wellenhoff, H. Lichtenegger, and J. Collins. *Global Positioning System: Theory and Practice*. Springer-Verlag, 2001.

[61] V. Ipatov. On the Karystinos-Pados bounds and optimal binary DS-CDMA signature ensembles. *IEEE Commun. Lett.*, 8(2):81–83, February 2004.

[62] V. Ipatov. *Spread Spectrum and CDMA: Principles and Applications*. John Wiley and Sons, 2005.

[63] V. P. Ipatov. Ternary sequences with ideal periodic correlation properties. *Radio Eng. Electron. Phys.*, 24(10):75–79, 1979.

[64] V. P. Ipatov. Contribution to the theory of sequences with perfect periodic autocorrelation properties. *Radio Engineering and Electronic Physics*, 25:31–34, 1980.

[65] M. J. Juntti and B. Aazhang. Finite memory-length linear multiuser detection for asynchronous CDMA communications. *IEEE Trans. Commun.*, 45(5):611–622, 1997.

[66] M. Kaeo. *Designing Network Security: A Practical Guide to Creating a Secure Network Infrastructure*. Cisco Press, 2 edition, 2003.

[67] B. Z. Kamaletdinov. An optimal ensemble of binary sequences based on the union of the ensembles of Kasami and bent-function sequences. *Problemy Peredachi Informatsii*, 24(2):104–107, 1988.

[68] M. R. Karim and M. Sarraf. *W-CDMA and cdma*2000 *for* 3*G Mobile Networks*. McGraw-Hill Professional, 2002.

[69] G. Karystinos and D. Pados. New bounds on the total squared correlation and optimum design of DS-CDMA binary signature sets. *IEEE Trans. Commun.*, 51(1):48–51, January 2003.

[70] T. Kasami. Weight distribution formula for some class of cyclic codes. Technical Report R-265, University of Illinois, Urbana, April 1966.

[71] S.-H. Kim, J.-W. Jang, J.-S. No, and H. Chung. New constructions of quaternary low correlation zone sequences. *IEEE Trans. Inf. Theory*, 51(4):1469–1477, April 2005.

[72] L. Korowajczuk, B. S. A. Xavier, A. M. F. Filho, L. Z. Ribeiro, C. Korowajczuk, and L. A. DaSilva. *Designing cdma*2000 *Systems*. John Wiley and Sons, Chichester, 2004.

[73] J. Lehnert and M. Pursley. Error probabilities for binary direct-sequence spread-spectrum communications with random signature sequences. *IEEE Trans. Commun.*, 35(1):87–98, 1987.

[74] G. Leus and M. Moonen. MUI-free receiver for a shift-orthogonal quasi-synchronous DS-CDMA system based on block spreading in frequency-selective fading. In *Proc. IEEE Int. Conf. Acoustics, Speech, and Signal Processing (ICASSP'00)*, volume 5, 2000.

[75] G. Leus and M. Moonen. MUI-free receiver for a synchronous DS-CDMA system based on blockspreading in the presence of frequency-selective fading. *IEEE Trans. Signal Process.*, 48(11):3175–3188, 2000.

[76] N. Levanon and E. Mozeson. *Radar Signals*. Wiley, 2004.

[77] R. Lidl and H. Niederreiter. *Introduction to Finite Fields and their Applications*. Cambridge University Press, 1994.

[78] Y. N. Lin and D. W. Lin. Multicode chip-interleaved DS-CDMA to effect synchronous correlation of spreading codes in quasi-synchronous transmission over multipath channels. *IEEE Trans. Wireless Commun.*, 5(10):2638–2642, 2006.

[79] R. Lupas and S. Verdú. Near-far resistance of multiuser detectors in asynchronous channels. *IEEE Trans. Commun.*, 38(4):496–508, 1990.

[80] U. Madhow, M. L. Honig, and M. Bellcore. MMSE interference suppression for direct-sequence spread-spectrum CDMA. *IEEE Trans. Commun.*, 42(12):3178–3188, December 1994.

[81] S. Maeng and B. G. Lee. Extended-window decorrelating detector for asynchronous CDMA channels and its performance analysis. *IEEE Trans. Commun.*, 49(1):35–40, 2001.

[82] H. Meikle. *Modern Radar Systems*. Artech House, 2008.

[83] J. M. Mendel. Tutorial on higher-order statistics (spectra) in signal processing and system theory: theoretical results and some applications. *Proc. IEEE*, 79(3):278–305, March 1991.

[84] L. E. Miller and J. S. Lee. *CDMA Systems Engineering Handbook*. Artech House, 1998.

[85] S. Moshavi. Multi-user detection for DS-CDMA communications. *IEEE Commun. Mag.*, 34(10):124–136, October 1996.

[86] N. J. Muller. *Desktop Encyclopedia of Telecommunications*. McGraw-Hill Professional, 3 edition, 2002.

[87] T. Ojanperä and R. Prasad. An overview of air interface multiple access for IMT-2000/UMTS. *IEEE Commun. Mag.*, 36(9):82–86, 1998.

[88] T. Ojanperä and R. Prasad. *Wideband CDMA for Third Generation Mobile Communications*. Artech House, 1998.

[89] S. Olariu and M. C. Weigle. *Vehicular Networks: From Theory to Practice*. CRC Press, 2009.

[90] J. Paavola. *Signature ensembles and receiver structures for oversaturated synchronous DS-CDMA systems*. PhD thesis, University of Turku, Turku, Finland, December 2007.

[91] J. Paavola and V. Ipatov. Oversaturating synchronous CDMA systems on the signature per user basis. In *Proc. 5th European Personal Mobile Commun. Conf. (EPMCC '03)*, pages 427–430, Glasgow, Scotland, April 22–25, 2003.

[92] J. Paavola and V. Ipatov. Performance analysis of oversaturated group orthogonal CDMA system in multipath channel. In *Proc. IEEE 17th Int. Symp. Personal, Indoor and Mobile Radio Commun. (PIMRC'06)*, Helsinki, Finland, September 11–14, 2006.

[93] M. Pätzold. *Mobile Fading Channels: Modelling, Analysis and Simulation*. John Wiley and Sons, 2002.

[94] M. Peng, Y. J. Guo, and S. K. Barton. One-shot linear decorrelating detector for asynchronous CDMA. In *Proc. IEEE Global Telecommunication Conf. (GLOBECOM'96)*, volume 2, pages 1301–1305, London, UK, November 18–22, 1996.

[95] H. V. Poor and S. Verdu. Probability of error in MMSE multiuser detection. *IEEE Trans. Inf. Theory*, 43(3):858–871, 1997.

[96] B. M. Popović. Efficient despreaders for multi-code CDMA systems. In *Proc. Int. Conf. Universal Personal Commun. (ICUPC'97)*, volume 2, pages 516–520, San Diego, CA, October 12–16, 1997.

[97] R. Price and P. E. Green. A communication technique for multipath channels. *Proceedings of the IRE*, 46(3):555–570, 1958.

[98] J. Proakis. *Digital Communications*. McGraw-Hill, August 2000.

[99] M. Pursley and D. Sarwate. Performance evaluation for phase-coded spread-spectrum multiple-access communication – part II: Code sequence analysis communications. *IEEE Trans. Commun.*, 25:800–803, 1977.

[100] M. B. Pursley. Performance evaluation for phase-coded spread-spectrum multiple-access communication–part I: System analysis. *IEEE Trans. Commun.*, 25(8):795–803, 1977.

[101] S. Redl, M. Weber, and M. Oliphant. *An Introduction to GSM*. Artech House, 1995.

[102] C. Rose. CDMA codeword optimization: interference avoidance and convergence via class warfare. *IEEE Trans. Inf. Theory*, 47(6):2368–2382, September 2001.

[103] A. H. M. Ross and K. S. Gilhousen. *The Communications Handbook*, chapter CDMA technology and the IS-95 North American standard, pages 199–212. CRC Press, 1996.

[104] M. Rupf and J. L. Massey. Optimum sequence multisets for synchronous code-division multiple-access channels. *IEEE Trans. Inf. Theory*, 40(4):1261–1266, July 1994.

[105] A. Saleh and R. Valenzuela. A statistical model for indoor multipath propagation. *IEEE J. Sel. Areas Commun.*, SAC-5:128–137, 1987.

[106] D. V. Sarwate and M. B. Pursley. Crosscorrelation properties of pseudorandom and related sequences. *Proc. of the IEEE*, 68(5):593–619, May 1980.

[107] B. Schmidt. Cyclotomic integers and finite geometry. *J. Am. Math. Soc.*, 12:929–952, 1999.

[108] H. Schulze and C. Lüders. *Theory and Applications of OFDM and CDMA: Wideband Wireless Communications*. John Wiley and Sons, 2005.

[109] J. Shen and Z. Ding. Edge decision assisted decorrelators for asynchronous CDMA channels. *IEEE Trans. Commun.*, 47(3):438–445, 1999.

[110] Y. Q. Shi, X. M. Zhang, Z. C. Ni, and N. Ansari. Interleaving for combating bursts of errors. *IEEE Circuits Syst. Mag.*, 4(1):29–42, 2004.

[111] V. M. Sidelnikov. On mutual correlation of sequences. 12(1):197–201, 1971.

[112] M. K. Simon, J. K. Omura, R. A. Scholtz, and B. K. Levitt. *Spread Spectrum Communications Handbook*. McGraw-Hill, Inc., New York, NY, USA, 1994.

[113] K. Siwiak and D. McKeown. *Ultra-wideband Radio Technology*. John Wiley & Sons, 2004.

[114] B. Sklar. *Digital Communications*. Prentice Hall PTR, Upper Saddle River, New Jersey, 2001.

[115] W. Stahnke. Primitive binary polynomials. *Mathematics of Computation*, pages 977–980, 1973.

[116] R. Steele. *Mobile Radio Communications*. Pentech Press, 1992.

[117] S. Tachikawa and G. Marubayashi. Spread time spread spectrum communication systems. In *Proc. IEEE Global Telecommunication Conf. (GLOBECOM'87)*, pages 617–619, 1987.

[118] S. Tachikawa, K. Toda, T. Ishikawa, and G. Marubayashi. Direct sequence/spread spectrum communication systems using chip interleaving and its applications for high-speed data transmission on power line. *IEICE*, pages 343–351, 1991.

[119] P. Tait. *Introduction to Radar Target Recognition*. Institution of Electrical Engineers, 2005.

[120] H. Torii, M. Nakamura, and N. Suehiro. A new class of zero-correlation zone sequences. *IEEE Trans. Inf. Theory*, 50(3):559–565, March 2004.

[121] H. L. Van Trees. *Detection, Estimation, and Modulation Theory, Part I*. Wiley-IEEE, 2003.

[122] R. Turyn and J. Storer. On binary sequences. 12(3):394–399, 1961.

[123] S. Ulukus and R. Yates. Iterative construction of optimum signature sets in synchronous CDMA systems. *IEEE Trans. Inf. Theory*, 47(5):1989–1998, July 2001.

[124] S. Ulukus and R. D. Yates. User capacity of asynchronous CDMA systems with matched filter receivers and optimum signature sequences. *IEEE Trans. Inf. Theory*, 50(5):903–909, May 2004.

[125] S. Verdú. *Multiuser Detection*. Cambridge University Press, 1998.

[126] P. Viswanath and V. Anantharam. Optimal sequences and sum capacity of synchronous CDMA systems. *IEEE Trans. Inf. Theory*, 45(6):1984–1991, September 1999.

[127] A. J. Viterbi. *CDMA – Principles of Spread Spectrum Communication*. Addison-Wesley, 1995.

[128] B. H. Walke. *UMTS: The Fundamentals*. John Wiley and Sons, 2003.

[129] D. S. Watkins. *Fundamentals of Matrix Computations*. John Wiley and Sons, 2 edition, 2002.

[130] L. R. Welch. Lower bound on the maximum cross correlation of signals. *IEEE Trans. Inf. Theory*, 20:397–399, 1974.

[131] P. Xia, S. Zhou, and G. Giannakis. Achieving the Welch bound with difference sets. *IEEE Trans. Inf. Theory*, 51(5):1900–1907, May 2005.

[132] S. Zhou, G. B. Giannakis, and C. Le Martret. Chip-interleaved block-spread code division multiple access. *IEEE Trans. Commun.*, 50(2):235–248, 2002.

[133] S. Zhou, P. Xia, G. Leus, and G. B. Giannakis. Chip-interleaved block-spread CDMA versus DS-CDMA for cellular downlink: a comparative study. *IEEE Trans. Wireless Commun.*, 3(1):176–190, 2004.

[134] R. E. Ziemer, R. L. Peterson, and D. E. Borth. *Introduction to Spread Spectrum Communications*. Prentice-Hall, 1995.

Turku Centre for Computer Science
TUCS Dissertations

84. **Dragoş Truşcan**, Model Driven Development of Programmable Architectures
85. **Eugen Czeizler**, The Inverse Neighborhood Problem and Applications of Welch Sets in Automata Theory
86. **Sanna Ranto**, Identifying and Locating-Dominating Codes in Binary Hamming Spaces
87. **Tuomas Hakkarainen**, On the Computation of the Class Numbers of Real Abelian Fields
88. **Elena Czeizler**, Intricacies of Word Equations
89. **Marcus Alanen**, A Metamodeling Framework for Software Engineering
90. **Filip Ginter**, Towards Information Extraction in the Biomedical Domain: Methods and Resources
91. **Jarkko Paavola**, Signature Ensembles and Receiver Structures for Oversaturated Synchronous DS-CDMA Systems
92. **Arho Virkki**, The Human Respiratory System: Modelling, Analysis and Control
93. **Olli Luoma**, Efficient Methods for Storing and Querying XML Data with Relational Databases
94. **Dubravka Ilić**, Formal Reasoning about Dependability in Model-Driven Development
95. **Kim Solin**, Abstract Algebra of Program Refinement
96. **Tomi Westerlund**, Time Aware Modelling and Analysis of Systems-on-Chip
97. **Kalle Saari**, On the Frequency and Periodicity of Infinite Words
98. **Tomi Kärki**, Similarity Relations on Words: Relational Codes and Periods
99. **Markus M. Mäkelä**, Essays on Software Product Development: A Strategic Management Viewpoint
100. **Roope Vehkalahti**, Class Field Theoretic Methods in the Design of Lattice Signal Constellations
101. **Anne-Maria Ernvall-Hytönen**, On Short Exponential Sums Involving Fourier Coefficients of Holomorphic Cusp Forms
102. **Chang Li**, Parallelism and Complexity in Gene Assembly
103. **Tapio Pahikkala**, New Kernel Functions and Learning Methods for Text and Data Mining
104. **Denis Shestakov**, Search Interfaces on the Web: Querying and Characterizing
105. **Sampo Pyysalo**, A Dependency Parsing Approach to Biomedical Text Mining
106. **Anna Sell**, Mobile Digital Calendars in Knowledge Work
107. **Dorina Marghescu**, Evaluating Multidimensional Visualization Techniques in Data Mining Tasks
108. **Tero Säntti**, A Co-Processor Approach for Efficient Java Execution in Embedded Systems
109. **Kari Salonen**, Setup Optimization in High-Mix Surface Mount PCB Assembly
110. **Pontus Boström**, Formal Design and Verification of Systems Using Domain-Specific Languages
111. **Camilla J. Hollanti**, Order-Theoretic Mehtods for Space-Time Coding: Symmetric and Asymmetric Designs
112. **Heidi Himmanen**, On Transmission System Design for Wireless Broadcasting
113. **Sébastien Lafond**, Simulation of Embedded Systems for Energy Consumption Estimation
114. **Evgeni Tsivtsivadze**, Learning Preferences with Kernel-Based Methods
115. **Petri Salmela**, On Commutation and Conjugacy of Rational Languages and the Fixed Point Method
116. **Siamak Taati**, Conservation Laws in Cellular Automata
117. **Vladimir Rogojin**, Gene Assembly in Stichotrichous Ciliates: Elementary Operations, Parallelism and Computation
118. **Alexey Dudkov**, Chip and Signature Interleaving in DS CDMA Systems

Turku
Centre *for*
Computer
Science

Joukahaisenkatu 3-5 B, 20520 Turku, Finland | www.tucs.fi

University of Turku
- Department of Information Technology
- Department of Mathematics

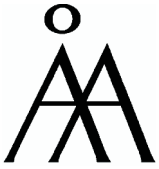

Åbo Akademi University
- Department of Information Technologies

Turku School of Economics
- Institute of Information Systems Sciences

ISBN 978-952-12-2300-6
ISSN 1239-1883

Alexey Dudkov

Chip and Signature Interleaving in DS CDMA Systems

Alexey Dudkov

Chip and Signature Interleaving in DS CDMA Systems

Alexey Dudkov

Chip and Signature Interleaving in DS CDMA Systems